DEVELOPMENT AND TESTING OF A BI-2212 TEXTURED POWDER CONDUCTOR

A Dissertation

by

KYLE CAMERON DAMBORSKY

Submitted to the Office of Graduate and Professional Studies of
Texas A&M University
in partial fulfillment of the requirements for the degree of

DOCTOR OF PHILOSOPHY

Chair of Committee,	Peter McIntyre
Committee Members,	Alfred McInturff
	Chia-Ren Hu
	Karl Ted Hartwig
Head of Department,	George Welch

May 2014

Major Subject: Physics

ABSTRACT

Superconducting wires based on the high field superconductor $Bi_2Sr_2Ca_1Cu_2O_{8+x}$ are an enabling technology for the development of very high field (>18 T) magnets. While these conductors have the potential to serve as the conductors for magnets operating in excess of 45 T, the achieved current carrying capacity of these materials is too low for economical implementation in high field operation. This is in part due to low density of the superconductors within the cores, the presence of current occluding non-superconducting phases, and a non-optimum alignment of the superconducting particles that form the conductor. The body of work reported in this dissertation aims to develop methods to align (texture) the superconducting particles within the conductors, to enhance the density of the superconducting filaments, to examine a heat treatment that does not form parasitic phases, and to demonstrate that long lengths of superconducting wire can be fabricated with these properties.

Three general experimental thrusts are carried out within the work. First, methods for texturing Bi-2212 loose powders were developed and the products of these developments were characterized via x-ray diffraction and microscopy to qualify the degree of imparted texture. The second thrust focused on the development of a monocore wire based on a high density textured Bi-2212 precursor. Multiple wires were extruded and drawn through traditional processes and the products were characterized microscopically to ascertain the quality of the products. The third and final thrust was the development of a non-melt heat treatment that was shown to grow grains of Bi-2212

powder and densify composites. Measurements of the transport critical currents for the heat treated conductors were carried out in boiling liquid helium and background magnetic fields of up to 5 T. These results were correlated to microstructural observations. Ultimately, it was found that the connections between grains in the sintered conductors were insufficient to allow robust transport current and only 1% of the predicted transport currents were reached through the sintering study.

DEDICATION

To my loving and tolerant wife, Dr. Joanne Damborsky and to my son Noah. Without your continued loving presence in my life, this work would have never been completed. Thank you for always giving me a reason and a place to come home.

"If you can do a half-assed job of anything, you're a one-eyed man in the kingdom of the blind." – Kurt Vonnegut, *Player Piano*

ACKNOWLEDGEMENTS

The list of people who have pushed, pulled, driven, or helped me through this processes is immense. Please tolerate me as I do my best to thank everyone who has made the past 6+ years an incredibly journey.

First, I'd like to thank my committee for their guidance and instruction throughout my time at Texas A&M. I owe my understanding of the microscopic theory of superconductivity to Dr. Chia-Ren Hu and will always be grateful for his tutelage. For the myriad of times he has loaned equipment, expertise, and career guidance, I would like to thank Dr. K. T. Hartwig. Of course, my education would have been utterly incomplete without the impromptu lectures and encyclopedic knowledge of applied superconductivity, magnet technology, accelerator physics, and aviation that are embodied by Dr. Alfred McInturff. Finally, I am forever indebted to my graduate advisor, Dr. Peter McIntyre for constantly providing motivation and allowing me the opportunity to find and overcome challenges as a young investigator. In no other environment would I have been able to experience the breadth of science that was offered under Dr. McIntyre's guidance and I am all the better for the experiences he has offered me over these 6 ½ years. For these and the countless other ways that he has influenced me as a scientist, I will always be grateful and proud to call him my advisor.

Without the sage wisdom, dedication to science, and skills of our group's technical staff, this work would have never been initiated, much less completed. For every pearl of wisdom I've garnered about physics and the laws of nature, I've gained

twice as much knowledge in the art of designing and executing a science experiment from our staff. I will forever be grateful and look back fondly on the times that Andrew Jaisle, Tim Elliott, Raymond Garrison, and Nick Diaczenko shared their trenches on the frontline of science. Without their support and friendship, I would have been completely and utterly lost.

My predecessors as graduate students (some of whom turned into postdocs) have been an enjoyable combination of support, distraction, and friends. Nate Pogue will always remind me the idea for this dissertation arose with him over a pint and I am grateful for both his technical support with this work and personal advice while navigating the perils of graduate school. Trey Holik has also been a constant presence and supporter, always bringing his cheerful demeanor and contagious positivity to late night/early morning short-sample tests.

Elizabeth Sooby, Justin Comeaux, Joshua Kellams, Klaus Smit, Karie Melconian, and the other students who are toiling in the group after me all have my deepest thanks for their kinship and for the amount of science they have shown me. I hope that I have been able to help them in their endeavors as much as they have helped me in my own.

I am also greatly appreciative of Dr. Feng Lu's steady hands and expertise with material's characterization. He has been a pleasure to work alongside and a wonderful traveling companion on the long drive to Tallahassee.

Our undergraduates have also been incredibly helpful, particularly David Rahmani who performed some of the work in this study. William Baker also helped with

the roll processing experiments and his efforts are greatly appreciated. Chris Benson was also a pleasure to work and has gone on to represent our lab well. I am also grateful to the other undergraduates who have spent more or less time with the group. Last but not least, Chase Collins has provided a great deal of support to the CAD work that was a part of this project and I am deeply appreciative of all his contributions.

Dior Sattarov has been a mainstay at the lab and it has been a pleasure to work alongside him on so many new and exciting concepts. I will always appreciate his guidance in my brief attempts to enter the world of finite element analysis.

Dr. Saeed Assadi has been a breath of fresh air in the last few years of this process. His early morning coffee sessions have enlightened me to the world of science policy, politics, and the national lab system. His determination and dedication to his craft have set an exceptionally high standard for young scientists to reach and I am thankful for the positive influence he has maintained on my career.

Likewise, Tom Mann has been a welcome addition to the group over the last few years and has helped me immensely to navigate the world of postdoc's and hiring practices. His input and assistance during these turbulent times have been incredibly helpful and are truly appreciated.

Without the expertise and collaboration from the National High Magnetic Field Laboratory and Applied Superconductivity Center in Tallahassee, this work would have been nearly impossible. Special thanks to William Starch for performing our extrusions and to Eric Hellstrom, Jianyi Jiang, Ulf Trociewitz, and Natanette Craig for their discussions and assistance with short sample measurements. Patrick Noyes contributions

to our short sample tests were also greatly appreciated during our time at the NHMFL, as were his stories from his time in our lab.

Mark Rikel's work to provide us with the Bi-2212 powders used in this study and his countless conversations regarding Bi-2212 processing are also greatly appreciated.

Of course, I'm extremely grateful to John Buttles, Steve Ingersoll, and the rest of the team at Bailey Tool and Mfg. for fabricating the die sets that were used to make our wires.

I would also be remiss if Robert Barber, William Merka, Tom Weimar, Mark Platt, James Phillips, and Dan Dattalo were not mentioned and thanked. Each of them has enabled me to carry out the work within this dissertation and have taught me something new.

I must thank the people who are responsible for my arrival at Texas A&M. I am forever grateful to my undergraduate advisor, Lev Kaplan, and the faculty and students within the Physics Department at Tulane University. My graduate career would not have existed without the preparation they gave me in 4 memorable years. Likewise, my high school teachers, particularly Miriam Patton and Linda Allen are responsible for inspiring me to pursue physics as a career and I will always consider myself fortunate for having them as teachers. Tony Williams showed me that my future was in academics rather than athletics and his support through my high school career will always be remembered and appreciated.

I must also thank my brother, Ryan, his wife, Ashley, for never letting me take myself too seriously. Their grounding presence and support have kept me in the real world while my head has tried to float among the clouds.

Last, but certainly not least, my parents, Ronnie and Terri, have been more supportive in all of my endeavors than any son could ever hope for or deserve. Their love and belief in me have made me the man I am today and there is no expression of gratitude that is sufficient to convey the depths of my appreciation for what they have done for me. They have my respect, heartfelt thanks, and my love.

TABLE OF CONTENTS

Page

LIST OF FIGURES

Page

LIST OF TABLES

Page

1. INTRODUCTION

1.1 Superconductors for High Field Magnets

1.1.1 Introduction to Superconducting Wires

Since the discovery of superconductivity [1], the applications of conductors that operate without loss have been a tantalizing prospect for the development of efficient, high field magnets. In fact, Onnes himself envisioned the creation of 10 T magnets with a lead conductor [2]. Unfortunately for Onnes, the only superconductors known in the earliest epoch of superconductivity were elemental, Type I superconductors. These materials are universally plagued by critical fields (the magnetic field which destroys the superconducting state) of less than 90 mT for Ta which fundamentally prevents their use in magnet applications [3].

The use of superconductors for the creation of high magnetic fields experienced a new vigor with the subsequent discovery of Type II superconductors which are primarily alloys, intermetallics, or ceramics although Nb, V, and Tc are elemental Type II superconductors [3-6]. While similar to their predecessors in their ability to carry currents without losses while in the superconducting state, their behavior in magnetic fields is markedly different. Namely, Type II superconductors typically allow magnetic flux to penetrate into the bulk of the material above a certain threshold critical field (H_{c1}). Instead of destroying the superconducting state as in a Type I conductor, these Type II materials isolate the penetrating flux within a small normal region of the conductor as explained by Abrikosov [7]. The remainder of the material is screened from

the penetrating flux by the generation of a vortex of supercurrents that oppose every quantized unit of magnetic flux that penetrates the conductor. While these vortices inherently contain a normal core which does not contribute to lossless current carrying, the remainder of the material remains in the superconducting state. As more and more flux is applied to the material, these vortices arrange themselves into a triangular lattice which is the minimum energy distribution of the vortices. This action continues until a second critical field, known as the upper critical field or H_{c2}, is reached and the superconducting state is finally destroyed. For Type II superconductors, this upper critical field can be extremely high, reaching 14.5 T for NbTi [8] and 30.1 T for Nb3Sn [9], which are the most commonly used conductors for magnet technology. Compared to the Type I conductors, the fundamental limits of Type II materials make them inherently applicable to the generation of > 1 T magnetic fields.

While the upper critical field is an important parameter for Type II superconductors, it is insufficient to qualify a material for service as a magnet conductor. If a current is carried through the conductor, the vortex lattice experiences a force from the self-field of the current and from the interaction of adjacent vortices. This force acts to displace the vortices which then propagate the normal core across the conductor in what is known as vortex flow. This motion dissipates energy within the superconductor which subsequently destroys the superconducting state. To maintain lossless transport current requires the stabilization of the vortex lattice in the presence of a transport current, or pinning the individual vortices. This pinning can be achieved through defects in the superconducting lattice, either occurring naturally as boundaries between

individual regions of perfect superconductor (grains) or artificially through the introduction of dislocations within a grain or inclusion of secondary phases with weak or no superconducting properties. Regardless of the mechanism, these pinning sites produce an energy favorable location for the penetration of magnetic flux. With a uniform distribution of these pinning centers in the superconductor, the lattice is stabilized so long as the force acting on the vortices is insufficient to overcome the potential holding the vortex at the pin. The force acting on an individual vortex is dependent on both the current density within the conductor, J, the magnetic flux density, B, and the temperature of the superconductor [10]. When this force exceeds the strength of a pinning center, the vortex jumps to another site, releasing energy in the process. Provided sufficient cooling is available and the remainder of the lattice is stable, these vortex jumps are transient effects which do not necessarily provide the fundamental limit of the conductor as their effects are reversible. The limit is instead reached when the entire vortex lattice flows or heat may not be effectively removed from the superconductor, causing an irreversible transition out of the superconducting state throughout the material. Due to repulsive interactions between vortices which are solely dependent on the magnetic field, a threshold field for the irreversible vortex flow can be established. This field, known as the irreversibility field, H_{irr}, is the magnetic field at which a superconductor can no longer carry lossless current at a given temperature. While the superconducting state may be maintained magnetically above H_{irr} since the vortex lattice will stabilize itself outside of the presence of a current, the introduction of

any current to the material results in a cascading flow of vortices and destroys the superconducting state [11, 12].

To be useful for current carrying applications in significant magnetic fields, a superconductor must allow penetration of magnetic flux, otherwise all currents are confined to the surface of the material, and this penetrating flux must not dissipate energy in the presence of currents. Therefore, strongly pinning Type II superconductors are the most useful materials for the generation of high magnetic fields [13].

With these basic requirements in mind, practical applications of superconductors typically require one to consider the economics of an application. After all, superconducting materials are typically novel, require exceptional amounts of processing, and their operation requires the implementation of a cryogen or very low temperature (< 77 K) working gas which is an inherently an energy intensive endeavor. The total effect is that a superconducting magnet is a highly technical, expensive device. However, superconductors have two unique advantages. First, they may operate without loss at exceptionally high currents. This is an important consideration for large scale applications such as accelerators which typically use thousands of kilometers of wire operating at several thousand amperes. For a superconducting magnet, the power required to operate this system is effectively the energy bill of the cryogenic system. However if the device were made with a normal conductor, say Cu, power would have to be applied to overcome the resistive losses of the conductor and to remove the heat caused by these resistive losses, increasing the cost per hour of operation. Economy then favors the use of superconductors when long term installations can recoup their

installation costs through more efficient operation [14, 15]. This is the argument which has driven the use of superconductors in MRI magnets [16, 17], particle accelerators, and high field research magnets [18], all of which are long life, high use devices.

A second advantage of superconductors that is pertinent to very high field operations is the exceptional current these materials can carry, even in very small cross section wires. To engineer a magnet, one would like to pack as much current as close as possible to the volume of interest. This places a premium on the current density of the conductor. Since normal conductors are limited by the amount of heat they generate and one must therefore remove, superconductors typically exhibit much greater current densities than normal conductors at modest fields and low temperatures.

As previously mentioned, superconductors typically find applications in magnets for particle accelerators, MRI/NMR magnets, and in research magnets requiring high field operation. Particle accelerators and NMR magnets generally push the development of conductors for the production of higher magnetic fields. These applications both require very precise control of the magnetic field quality, which is primarily achieved by dictating the location of the conductors. While technologically possible, high aspect ratio wires or tapes are difficult to engineer, particularly in accelerator magnets. Instead, round or square wires are highly preferred for these applications as they allow for straightforward fabrication processes and simple tooling [19].

A final requirement for high field magnets, particularly rampable magnets like those found in particle accelerators, is a filamentary wire in which a composite wire is formed. The composite has a high quality normal conductor matrix, such as copper or

aluminum, with multiple filaments of superconducting symmetrically distributed throughout the matrix. The conductors are optimized by decreasing filament sizes which in turn decreases the magnetization of the individual filaments. As screening currents are setup within the superconductor to resist changes in magnetic fields, minimizing the magnetization, or stored energy, within each filament and subsequently maximizing the surface area to volume ratio of the filaments to enable effective heat transport through a normal matrix, produces a stable conductor during changes in current and magnetic field. So long as the power dissipated within the conductor is lower than the effective rate of heat removal, the conductor is stable to transient changes. While this argument was articulated with respect to ramping magnets, minimizing the diameter of filaments helps stabilize the conductor against any disturbance which dissipates heat. Additionally, coupling currents between filaments may be reduced by helically transposing the filaments [11].

In summary, for application as a magnet conductor, a superconducting wire must be based upon a Type II material with an irreversibility field above the desired operational field. Additionally, the highest performing magnets, namely dipole and quadrupole magnets for particle accelerators, require fine, multifilamentary conductors with the highest current density possible at the given operating field and temperature.

1.1.2 The High Field Frontier

Historically, the development of superconducting wires for high field applications has been driven by the High Energy Physics (HEP) community. As previously discussed, accelerator dipoles typically have the most stringent requirements

for superconducting wires in high field operation. The push for higher fields has been motivated by the desire to increase the collision energy of synchrotron accelerator facilities, which roughly scales as:

$$E\ [GeV] = 0.3\ \times B[T] \times R[m]$$

While increasing the radius of a synchrotron is an effective means to increase the collision energy, the cost of increasing the circumference of the device adds to both the capital cost of creating the tunnel and increases the number of magnets, RF cavities, and every other system within the accelerator. While this was a consideration during the development of existing accelerator facilities such as the LHC [20], Tevatron [21, 22], and RHIC [23], pragmatic considerations dictate that new accelerators be installed within the existing infrastructure of the accelerator community. Therefore, maximizing the magnetic field strength of bending dipoles within the ring is the most effective way to increase the threshold for discovery in terrestrial HEP.

To date, every superconducting dipole magnet in a synchrotron accelerator has been fabricated from NbTi wire. With the installation of the LHC, the ultimate performance of NbTi (8.33 T @ 1.9 K) has been achieved, most likely making the LHC the last hadron collider to be based upon NbTi [20]. Increasing the energy frontier will therefore require the adoption of a new superconducting material. At the time of this publication, Nb_3Sn is poised to serve as the immediate replacement to NbTi. However, in an accelerator dipole geometry, Nb_3Sn is limited in application to fields of 18 T [24]. While this allows for a doubling of the LHC's energy, it does not allow for the frontier extending research that will inevitably be desirable in the next generation of HEP

experiments. This next great step forward in the energy frontier will therefore require the maturation of a new conductor for HEP.

Candidate materials for this generational shift in HEP conductors are presently limited to 2 materials: Bi-2212 and YBCO. While YBCO has a higher current density than Bi-2212 [25], it is only available as a high performance conductor in monofilament tape form. As previously described in Section 1.1.1, a monofilamentary tape is the least desirable geometry for an HEP conductor. Meanwhile, Bi-2212 may be fabricated in round wire, multifilament geometries that are scalable to long lengths. This makes Bi-2212 the most promising conductor for the future of HEP [26-30].

1.2 Bi-2212 Basics

Bi-2212 is a high-temperature superconducting ceramic with a transition temperature of up to 90 K [31] and an upper critical field of ~100 T at 4.2 K [32]. Bi-2212 is part of the Bi-Sr-Ca-Cu-O family of superconductors that also includes the Bi-2201 (Raveau, $T_c = 35$ K) [33-35] and Bi-2223 phases ($T_c = 110$ K, $\mu_0 H_{c2} = 39$ T) [36]. Of the three phases within the Bi-Sr-Ca-Cu-O system, the Raveau phase carries little current and has a low upper critical field with $\mu_0 H_{c2}(4.2\text{ K}) = 3$ T, making it unsuitable for the common applications of superconductors [37]. However, the Bi-2212 and Bi-2223 phases exhibit exceptional critical temperatures, tantalizing critical current densities at 4.2 K and 77 K, and remarkable upper critical fields. As such, the Bi-2212 and Bi-2223 phases have been extensively studied in the past two decades at the fundamental level to elicit information about the mechanisms of high-temperature

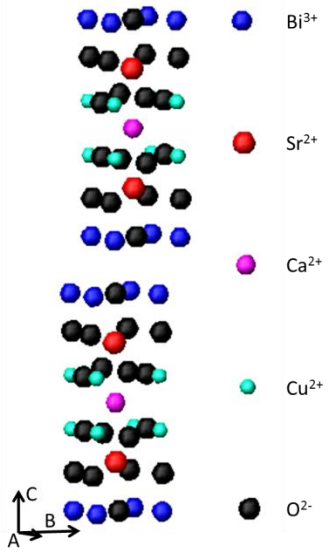

Fig. 1: Bi-2212 unit cell. Atomic radii are scaled by a factor of 2 for clarity.

superconductivity and in the field of applied superconductivity with the fabrication of wires and tapes based upon the materials.

Unlike Type I superconductors and the low temperature superconductors, the bismuth based conductors exhibit a marked anisotropy in their superconducting properties with transport currents primarily flowing within the copper oxide layers, which are shown in the unit cell in Fig. 1. This 2 dimensional structure requires that grains of Bi-2212 and Bi-2223 form links that minimize the out of plane current transport (c-axis transport). This may be accomplished by growing large, plate-like grains with parallel copper oxide planes. Furthermore, the mechanical properties of the material exhibit a similar anisotropy, namely the shear strength between the bismuth oxide layers is markedly lower than that of any other crystalline plane [38] and crystalline growth occurs preferentially in the ab planes [39]. These two complimentary

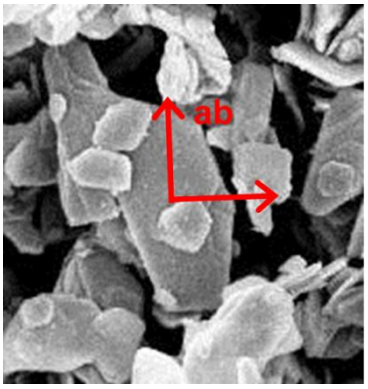

Fig. 2: Micaceous Bi-2212 platelets with ab plane labeled.

effects determine the microscopic behavior of Bi-2212: single crystals tend to grow into a high aspect ratio platelet and upon milling, a micron scale micaceous powder is formed with similarly aspected platelets as shown in Fig. 2 [40].

1.3 The OPIT Conductor

For practical purposes, superconducting wires must be fabricated in continuous lengths at least 1 km to be efficiently used in most high energy physics (HEP) applications. In previous generations of superconducting wires, these lengths have been fabricated by conventional metallurgical processes since the precursor materials (Nb, Sn, Ti, Al, etc.) have all been ductile metals that generally co-reduce well with copper (matrix material) and are readily formed into fine filament wires. However, the bismuth based superconductors are oxides and are inherently brittle materials. The combination of the necessity for texturing and poor deformation properties dictates that for any practical application, BSCCO based conductors must be “grown” in place. For superconducting wires, this requires a wind and react strategy, the process of which differs for the Bi-2212 and Bi-2223 phases. Both wires begin as an Oxide Powder in

Tube (OPIT) conductor in which a matrix material, universally a silver alloy, is formed into a seamless tube and packed with either a phase pure powder or a stoichiometric mixture of precursor oxides [41]. Standard wire fabrication techniques are utilized to form long lengths of multifilament conductor which must then be reacted to create a textured, well connected superconducting core for supercurrent transport. At this point processing Bi-2212 and Bi-2223 conductors diverges. In the Bi-2223 conductors, a thermomechanical processing is required in which the Bi-2223 composite is subjected to an annealing/sintering heat treatment, then undergoes further deformation (typically rolling) to impart a large degree of texture to the grains. The conductor is then subjected to a final heat treatment that results in a highly textured, well connected transport matrix. The end result of this processing is a high aspect ratio wire (generally 2.5:1) or tape capable of carrying appreciable currents at 77 K. However, the anisotropy of the tape creates a conductor that is difficult to utilize in a magnet winding and lacks the current density of YBCO tapes [25, 42]. Given that 2223 is slightly more robust than YBCO in windings and still carries appreciable currents at 77 K, it has found applications in niche areas typically related to superconducting motors or generators, but also in DC high current transfer lines [43].

Meanwhile, the Bi-2212 phase is typically cold drawn into fine wire dimensions with no intermediate sintering or annealing steps. Bi-2212/Ag round wires then require a true wind and react processing in which the round Bi-2212 wire is wound into its final geometry, then subjected to a high temperature (~890 C) heat treatment in a 100% O_2 atmosphere. This heat treatment is typically referred to within the literature as partial

melt processing (PMP). The name implies the Bi-2212 phase decomposes into a Bi rich liquid, alkaline earth cuprates (AEC's), a copper free phase, and the 2201 phase depending on the temperature, oxygen partial pressure, and cation stoichiometry. Here the term partial melt refers to the presence of some solid components, the AEC's, 2201, and copper free phases, as well as the liquid. The solubility of oxygen within the liquid formed during decomposition is lower than that of the solid, and the liquid releases oxygen to the surrounding environment. This is one of the key reasons that Ag is utilized as a matrix material in Bi-2212 conductors: at the reaction temperatures, the diffusion rate of O_2 through Ag is among the highest in nature [44]. Furthermore, this partial melt phase is highly corrosive and tends to leach cations from the surrounding environment, poisoning the final superconducting phase [27]. Fortunately, only about 3 wt% Ag is soluble in the melt and the matrix remains fairly unaffected [45]. However, impurities within the Ag (ie. oils from the tube fabrication or Cu contamination), or even materials contacting the Ag (SiO_2 insulating sleeves and fabrics or mandrel materials for windings) can diffuse into the partial melt or leach cations from the partial melt to poison the reaction and destroy the superconducting phase [46]. Each of these issues has been addressed through empirical studies with varying degrees of success, culminating in the state of the art engineering density of 800 A/mm2 [47]. After as little as 8 minutes above the partial melt temperature, the wire or coil is slowly cooled to allow the liquid to recrystallize into the Bi-2212 phase. The transport properties of the superconducting wire have been found to be sensitive to differences in the peak temperature of 2 C with ~10% decreases in J_c observed for 2 C changes in peak temperature. Similarly, dwelling

too long at max temp also decreases the wire performance, making it very difficult to accurately and reproducibly react a large coil from the conductor [18]. Upon recrystallization, the Bi-2212 appears to be somewhat aligned, matching the contours of the Ag surfaces. However, AEC's, 2201, and other parasitic phases also precipitate out of the melt and become current impediments while void spaces, left over from the initial porosity of the packed powder, appearing due to the dissolution of Ag and breakdown of the matrix, or the result of trapped gases originally adsorbed on the surface of the powder, coalesce and form large empty bubbles within the matrix [48-50]. The net result of these impediments is a drastically reduced and variable cross sectional area of Bi-2212 in the finally reacted conductor resulting in wire transport currents that are drastically lower than the theoretical values one would expect of high density, well aligned Bi-2212 from single crystal studies [51]. To date, this problem has been addressed by altering the partial melting process. Steady but slow progress has been made in enhancing the transport properties of these conductors, yet the HEP goal of a conductor with engineering densities greater than 1000 A/mm^2 in background fields above 20 T remains elusive [25, 26].

1.4 Hypotheses

Limitations of state of the art OPIT conductors appear to arise from a plurality of processing issues including low superconducting core densities, presence of occluding parasitic phases, and un-optimized texture. To address these issues with the intention of increasing core J_c as well as the overall engineering density of Bi-2212 conductors, three distinct hypotheses were conceptualized:

1. Bi-2212 powders may be pre-textured by aligning the high transport current ab planes of the conductor parallel to one another.

2. A wire fabrication process based on a high density, textured Bi-2212 precursor may be realized in a manner that preserves the texture and achieves a near theoretical density superconducting core.

3. A non-melt heat treatment process may be employed to grow and connect a textured Bi-2212 conductor without rapid growth of parasitic phases or the growth of occluding void spaces.

Testing these three basic hypotheses was the foundation of the work in this dissertation and the ultimate goal of this work was the demonstration of a high core density textured powder conductor (TPC) that achieves as good or better J_c and J_e than an OPIT conductor after a non-melt sintering heat treatment.

1.5 Document Outline

This work is divided into distinct chapters that address the individual hypotheses outlined in the previous section. Chapter 2 addresses the development of pre-texturing methods. Chapter 3 focuses on the development of a high core density textured powder conductor through a wire fabrication process. Chapter 4 describes the heat treatments used within this study and compares them to processes found in the literature. Chapter 5 focuses on characterization of the conductors including transport current measurements correlated to microstructural phenomena. Chapter 6 summarizes the conclusions that may be reached from the completed work and provides insight into future directions for the development of a textured powder conductor.

2. TEXTURING

2.1 Bi-2212 Powders

Bi-2212 precursor powders for OPIT wire fabrication have historically been produced by a myriad of vendors [52-54] and independent research groups in their attempts to fabricate Bi-2212 conductors [55-58]. Several powder processing routes have been reported in the expansive literature, however two methods dominate. The first is a carbonate decomposition route in which oxides and carbonates of Bi, Sr, Ca, and Cu are mixed in a stoichiometric ratio of the cations. These precursors are calcined, typically in oxygen or air, then ground to fine scale. Subsequent calcinations and grinding steps are utilized to remove more carbon and to drive the solid phase diffusion process toward a homogeneous equilibrium of near stoichiometric Bi-2212. This method is affordable, may be carried out with relatively high purity, and is achievable in nearly any laboratory environment. Consequently, the carbonate decomposition route is widely used by research groups developing their own conductors. However, the quality of these powders varies drastically among groups with the main difference being the inclusion of impurities (most notably carbon) and the homogeneity of the powders. Due to the extreme variations in stoichiometry and purity of early powders, it is difficult to compare much of the early work on Bi-2212 wires as variations between powder batches contributes to wild swings in wire performance.

Higher purity and more homogeneous powders are prepared via Nexans eutectic melt cast processing [59]. This process utilizes a eutectic point in the Bi-2212 phase

diagram that allows for the formation of a highly homogeneous amorphous mixture of near stoichiometric Bi-2212 to be formed. This melt cast material is then jet milled to fine powder and may be processed in a variety of different manners to form granular, agglomerated, or fine powders comprised of primarily Bi-2212 and low non-metallic impurities. Generally, this powder is superior to home grown varieties, with very reproducible results achieved from batch to batch and year to year. As such, Oxford Superconducting Technologies has adopted Nexans powders for all of their OPIT wire production. For development purposes, the only drawbacks of the Nexans powder are the expense and lack of domestic production.

Table 1: Available Bi-2212 Powders

Manufacturer	Powder Condition	Composition
Praxair	-200 Mesh (75 μm or smaller)	$Bi_{2.29}Sr_2Ca_1Cu_{2.016}$
Nexans	Jet Milled/d_{50} = 1.38 μm	$Bi_{2.17}Sr_{1.96}Ca_{0.87}Cu_{2.00}$
SCI	Ball Milled/Agglomerated	$Bi_{2.06}Sr_{2.04}Ca_{0.87}Cu_{2.03}$

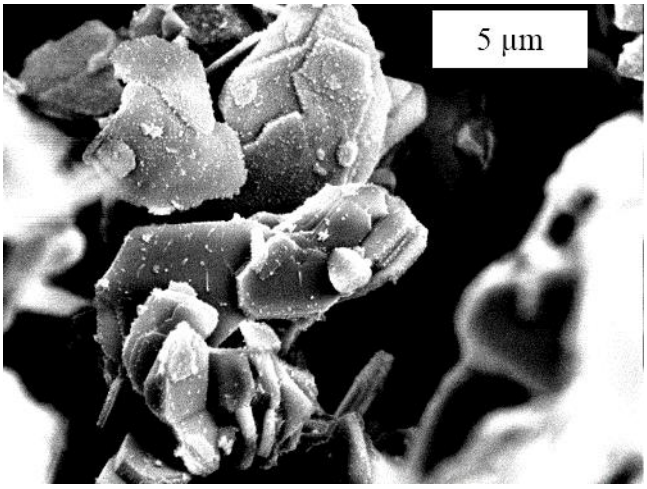

Fig. 3: SEI of micaceous Bi-2212 powder particles showing a platelet morphology with ~100 nm thickness and micron scale widths.

For the body of this work, powders were sourced from a variety of manufacturers and preparations. Table 1 lists the respective vendors, powder type, and particle size. Typically, all powders contained micron scale, micaceous particulates like those shown in Fig. 3. Some Nexans powders were agglomerated into several hundred micron balls like those shown in Fig. 4. In both agglomerated and fine powders, the basic unit of the material are the fine, randomly oriented grains of Bi-2212.

2.2 Texture Definition

For the purpose of this study, texture is defined as the induced alignment of the micaceous grains of Bi-2212. As described previously in Section 1.2, the preferred orientation for high current transport in Bi-2212 conductors is with the c-axis perpendicular (out of plane) to the transport current. The most useful measurements of texture are therefore of the relationship between the c-axis and ab planes of the multitude of Bi-2212 particles in a sample. Two criteria have been established to evaluate the

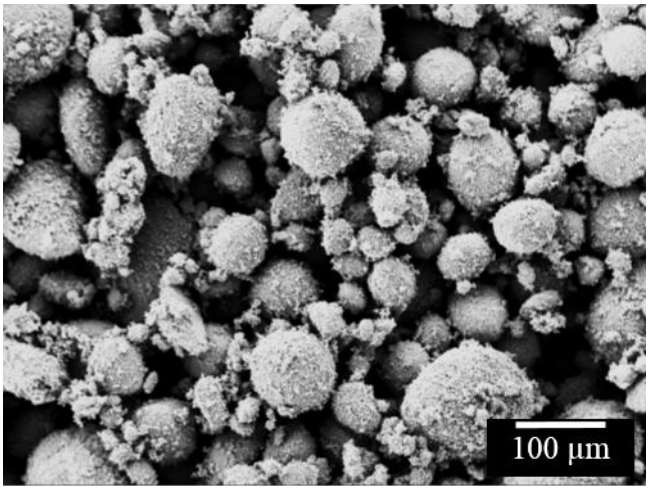

Fig. 4: Secondary electron image of agglomerated Nexans powder. Agglomeration is primarily due to electrostatic charging effects.

degree of texture in a given powder sample. First, samples are examined microscopically using an SEM to determine qualitatively whether the sample primarily has ab planes within the imaged plane. To quantify the degree of texture, albeit somewhat crudely, x-ray diffraction (XRD) techniques were used to examine the out of plane c-axis texture. This was accomplished by comparing the maximum intensity of a c-axis diffraction peak, typically the (00$\underline{1}$0) or (008) peak, to that of an ab peak, typically (200/020), or dominant randomly dispersed peak (115) in a ratio that was subsequently deemed a texture parameter, τ, given by:

$$\tau = \frac{I_{0010} - 0.25 * I_{115}}{I_{0010} + 0.75 * I_{115}}$$

This analysis was modeled after examples found in the literature [52, 60]. As the texture parameter approaches 1, more and more of the ab planes are aligned parallel to one another at the while the parameter returns a value approaching 0 for a truly random

powder alignment. While incredibly useful in determining the behavior of a given powder sample with multiple texturing applications, the parameter fails at providing a comparison between powder samples of different particle size distributions and compositions. This failure is primarily due to differences in particle size distributions which lead to differing dispersions of incident x-rays. This in turn can lead to peak broadening which artificially decreases the apparent value of the texture parameter which uses only a maximum intensity approach rather than the area under the peak. For the ultimate purpose of this study, a single powder was used, so the texture parameter served as a sufficient figure of merit for the imparted texture to samples of this powder and provided significant, meaningful guidance during the development of the various texturing methods.

2.3 Texturing Methods

In the attempt to impart a high degree of pre-texture to Bi-2212 powders for subsequent wire fabrication, several methods were examined in detail and evaluated based upon the degree of achieved texture, relative density of the products from the process, contamination issues, and commercial scalability. While novel in the sense that pre-texturing Bi-2212 powders had not been undertaken, several methods for texturing Bi-2212 conductors have been reported in the literature [61-64]. These methods are predominantly based upon tape like conductors and are therefore limited by anisotropic properties that were intended to be specifically avoided in all wire fabrication techniques of this study as they lead to conductors which are difficult to incorporate in high field, fast ramping magnets. Additionally, texturing methods during melt processing of Bi-

2212/Ag conductors have been reported as well. Specifically, these efforts include magnetic melt processing (MMP), in which conductors are heat treated within a background magnetic field [65-67], institution of thermal gradients to control grain growth [68], and manipulation of the Ag/Bi-2212 interface to control oxygen diffusivity [69]. Universally, these conductor geometries and processing methods led to incremental increases in J_c, typically on the order of 10% over traditionally processed materials, increases in J_e were less forthcoming. Additionally, undesirable side effects were observed, specifically anisotropic conductor properties with respect to applied field and difficulty scaling to coil fabrication process, specifically with MMP.

In order to achieve an enhanced precursor texture while maintaining purity and a high packing density in a Bi-2212/Ag conductor, several methods were directly examined in this study. These included magnetic texturing, die stamping, and roll compaction. The following sections address the details of each texturing method as well as the examination of the imparted texture.

2.3.1 Magnetic Texturing

Due to an anisotropic magnetic susceptibility [70-72] Bi-2212 particles preferentially align their c-axis parallel to applied magnetic fields. Table 2 lists the magnetic susceptibilities of Bi-2212 in both the ab plane and along the c-axis, and Fig. 5 shows the orienting torques acting on a Bi-2212 particle in an applied magnetic field. In a vacuum, this orienting torque would induce a series of oscillations that would keep the particulates of Bi-2212 in harmonic motion indefinitely. In order to achieve a true textured powder, a viscous damping medium was required to dampen this periodic

motion and align the particles with c-axis parallel to the applied field. Two distinct series of experiments were performed with magnetic texturing. The first consisted of mixing Bi-2212 loose powders in epoxy and allowing the epoxy to cure in an applied magnetic field. A second method utilized organic solvents which acted as a viscous, removable carrier for the loose powders.

Table 2: Anisotropic Magnetic Susceptibility of Bi-2212 Single Crystal

Crystalline Axis	Magnetic Susceptibility (cm^3/g) [72]
a/b	-0.8×10^{-7}
c	2×10^{-7}

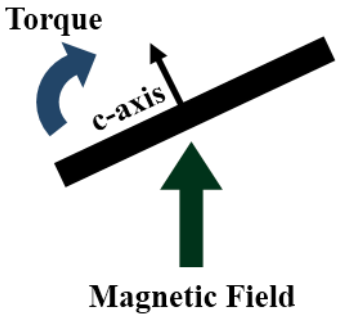

Fig. 5: Orienting torque acting on a single, micaceous Bi-2212 particle in 2 dimensions. The magnetization vector is the vector sum of the diamagnetic susceptibility in the ab plane and the paramagnetic response along the c-axis.

Epoxy Carrier

Epoxies were used as both a viscous damping medium and to preserve powder samples for XRD studies in a series of proof of concept experiments for magnetic texturing. Samples were prepared by mixing loose Bi-2212 powders in epoxy and

allowing the particles to settle in a magnetic field while the epoxy cured in a small, removable cup. In these studies, two different epoxies were sourced. Both epoxies originated from Buehler and carried brand names of Epoxicure (500 cP viscosity) and Epothin (250 cP) [73]. The dependence of induced texture on applied field strength was examined over a series of applied background fields in several different magnets. These included magnets within the Electrical Engineering department at TAMU and at the National High Magnetic Field Laboratory in Tallahassee, FL. Additionally, effects of time in field were examined on textured development during the curing process. Finally, two different powders were explored in the study, one an agglomerated Nexans powder, the other an ancient batch of Praxair powder that had seen multiple months of exposure in the back of a late model BMW as part of a proprietary TAMU accelerator laboratory

Fig. 6: Epoxy sample cup with mixed Bi-2212 powder on non-magnetic sample holder. The magnetic field would be oriented vertically (parallel to the supporting dowels) in this image.

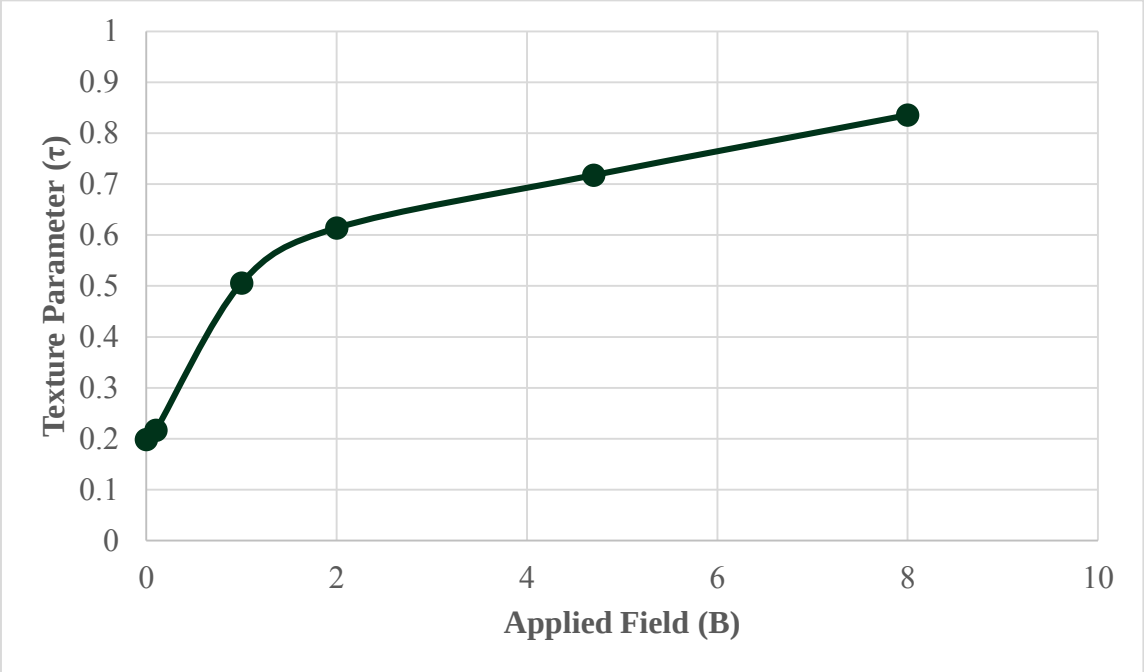

Fig. 7: Texture parameter vs. applied field strength for Praxair powder in a 500 cP epoxy.

aging process. Fig. 6 [40] shows a sample mounted in the test fixture, ready to be loaded into the magnet bore.

Upon curing, the samples were removed from their cups and samples were examined with XRD to ascertain their degree of texture. Due to settling, it was evident that the higher powder concentration was located at the gravitational minimum, which was also the flattest, smoothest surface, making it the ideal face for XRD analysis.

Texture Dependence on Applied Field Strength

To study the effects of applied field strength on the orientation of loose Bi-2212 powders, a volume of 1.25 cm^3 the Praxair powder from Table 1 was uniformly mixed with a 15 cm^3 of Epoxicure in a small cup. Upon mixing, these samples were immediately placed within the bore of a variable field superconducting magnet and

allowed to harden in a fixed background field of up to 8 T. After curing, the samples were removed from the magnet and the bottom surface of the cured samples was subjected to XRD. The results of these experiments are presented in Fig. 7 and indicate that the naïve suspicion that increasing magnetic field strength leads to a monotonically increasing particle alignment is indeed true [53].

Powder, Viscosity, and Time in Field Effects

Due to the fact that a fresh Bi-2212 powder was required for actual conductor fabrication and epoxy would most likely not be the carrier medium of choice for a conductor development, a second round of experiments were carried out at fixed field of 8.9 T. Praxair and Nexans powders as listed in Table 1 were used in this study. Additionally, both the Epothin and Epoxicure epoxies were used to determine the effect of viscosity on the process. Samples were prepared by measuring 1.25 cm^3 of powder and mixing this volume in 15 cm^3 of epoxy. The samples were immediately loaded into the bore of the magnet, then allowed to cure for variable amounts of time ranging from 5 minutes to the full cure time of the epoxy, which was 9 h for the Epothin and 6 h for the Epoxicure. Samples were then removed from the bore and, if necessary, allowed to complete their cure outside of the applied field. Upon completion of the cure, samples were removed from their mounting cups and XRD was performed to determine the texture parameter. The results of these experiments are presented in Fig. 8.

From Fig. 8, several observations may be immediately made. First, there is a distinct difference between the texture observed in the two different powders with the Praxair powder more strongly orienting with the magnetic field. This effect was due to

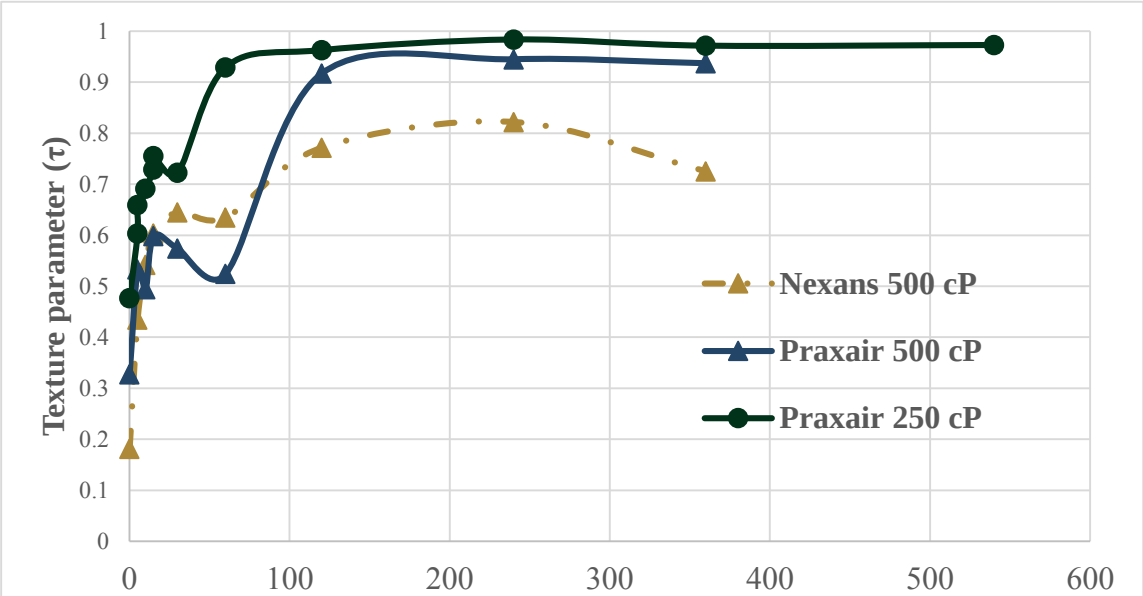

Fig. 8: Texture vs. time for various epoxy and powder combinations. All data from an 8.9 T applied field.

the larger particle size of the Praxair powders whose greater surface in the ab plane increased the magnetic moment of the particles under the applied field. Additionally, the Nexans powder was observed to electrostatically agglomerate, which would prevent the individual particulates from orienting themselves, thereby lowering the imparted texture. Secondly, while a slight difference was seen between the 250 cP and 500 cP epoxies, this effect was small compared to the differences between powders.

Regarding the texture evolution with respect to time, the texture plateau appeared after 2 hours of exposure to the magnetic field. This time roughly correlated to the working time for the epoxy, which markedly increased its viscosity after about 2 hours of pot time [74].

Solvent Carriers

While the epoxy carriers provided a sufficient vehicle to understand the effects of various powders, field strengths, and viscosities of the carrier, the epoxy was irremovable and left no room for application to a wire geometry. At this point, it was necessary to develop a deposition method that would provide a viscous medium for powder deposition that was easily removable, left a negligible amount of contamination, and would not disturb the imparted texture during removal. Early work with Bi-2212 conductors focused on tape casting techniques such as doctor blade manufacturing which deposited a slurry of Bi-2212 suspended in an organic binder onto a moving substrate [61, 75, 76]. These open faced tapes were then heated to burn out the organic binder, presumably leaving little or no contamination behind. Afterward, these tapes could be melt processed to connect the superconducting grains. Despite significant current densities at the time of their fabrications, these tape conductors were highly anisotropic with large AC losses and limiting geometries. However, these previous works demonstrated that certain alcohols left little or no residue on Bi-2212 powders and displayed no net interaction with the material. Furthermore, alcohols are readily available in very high purities at low costs and tend to have very high vapor pressures allowing them to be removed by evaporation with a variety of techniques. Three alcohols with were chosen for the solvent deposition study: isopropanol, methanol, and ethanol. In general, these solvents were mixed with Bi-2212 powders to form a slurry that could be deposited on a substrate followed by removal of the solvent. Ultimately the concept for preparing these slurries was for the fabrication of a modified jelly roll

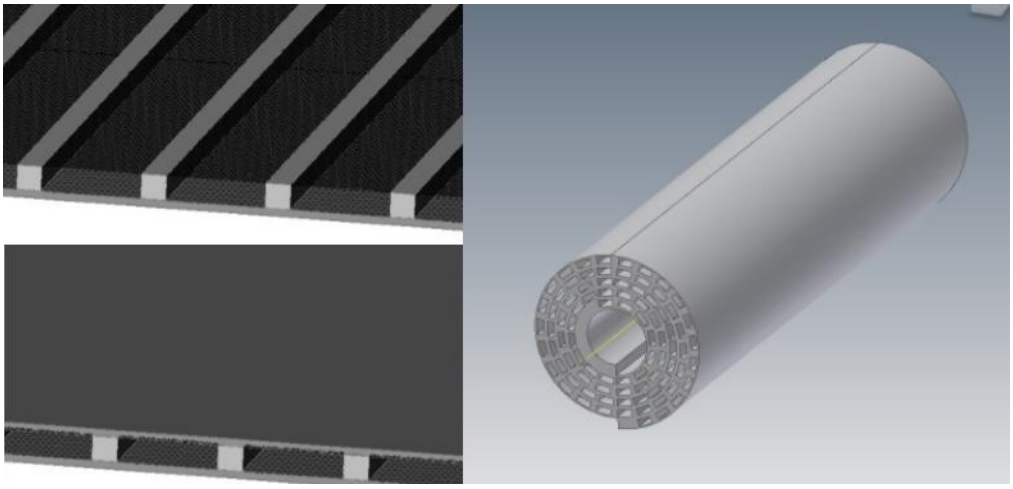

Fig. 9: Jelly roll fabrication process. Textured precursor is placed into a specially prepared substrate (top left), an Ag foil is laid across the top (bottom left) and the composite is rolled to form a billet for subsequent area reduction processes (right).

conductor based upon the highly textured Bi-2212 powder [77]. In this model, a corrugated or troughed silver foil would be filled with a Bi-2212/solvent slurry. A background magnetic field would be applied and the solvent would be evaporated, leaving behind only the Bi-2212. The substrate could then be wound around a central mandrel and drawn into a multifilament wire based upon the textured powder. The process is illustrated in the images of Fig. 9 [52]. As a proof of concept, textured samples were prepared by dispersing a fixed mass of Bi-2212 loose powder in a fixed volume of alcohol. Typically, 1.6 g of powder was dispersed in 20 mL of solvent. Due to aggregation of the dry powders, the very dense Bi-2212 sank in the low viscosity, low density solvents. To combat this effect, samples were agitated ultrasonically for a minimum of 15 minutes. Fig. 10 shows the dispersion achieved through ultrasonic agitation for one such sample.

To apply the background magnetic field, a 7.0 T magnet was used. A fixture was fabricated that consisted of a vacuum tight tube, at the bottom of which was placed an aluminum SEM sample mount in a sealed volume. A schematic of the experimental setup is shown in Fig. 11 [52]. The fixture was placed inside the bore of the magnet and the top 5.0 mL of the agitated slurry was injected into the tube via a syringe. After a settling time of 5 minutes, a vacuum pump was used to evacuate the tube. Instead of rapidly pulling vacuum, a throttling valve was incorporated to prevent rapid boiling of the solvents. Pumping continued until the alcohol was completely removed from the sample, as indicated by a precipitous drop in pressure within the sample chamber. Empirically, samples that were not allowed the full 5 minutes of settling time were missing significant quantities of powder, indicating that the Bi-2212 was being pulled off with the vacuum pump as a fine powder. Additionally, samples that were evaporated too rapidly went into a violent boiling regime that disturbed the texture of the samples. The fixture was then removed from the field and the textured powder samples were carefully removed from the fixture for further study. The tube was flushed with organic

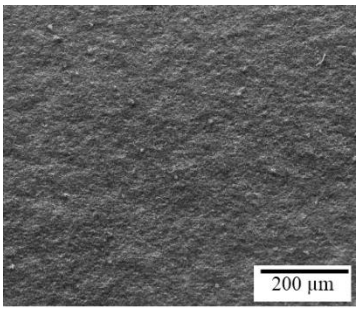

Fig. 10: Coating from an ultrasonically agitated Bi-2212/Ethanol slurry. Solvent was evaporatively removed.

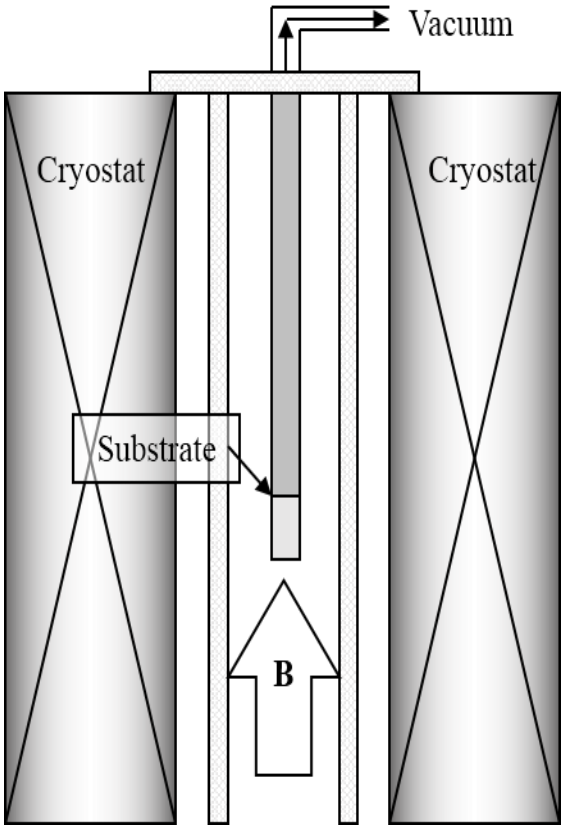

Fig. 11: Solvent deposition experimental layout. Samples were loaded through the vacuum evacuation tube via syringe and allowed to settle in the applied field. After settling, vacuum was pulled on the sample chamber to remove the volatile solvents.

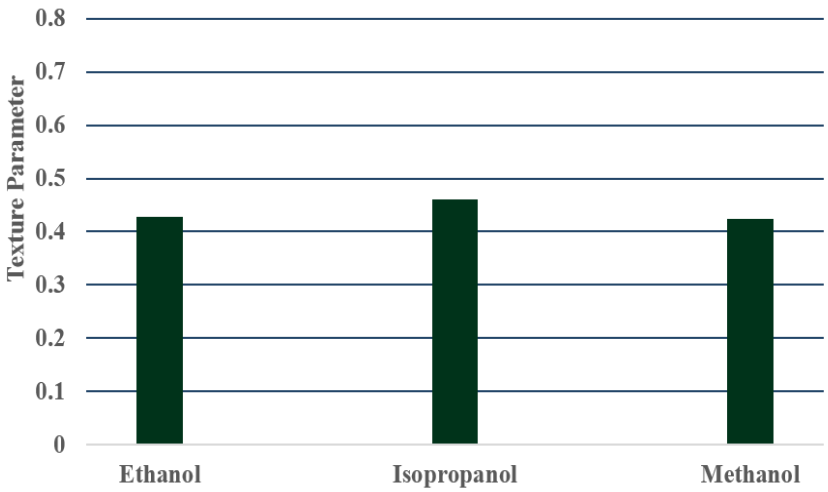

Fig. 12: Texture parameter evaluated at 7.0 T for primary solvents. © 2011 IEEE

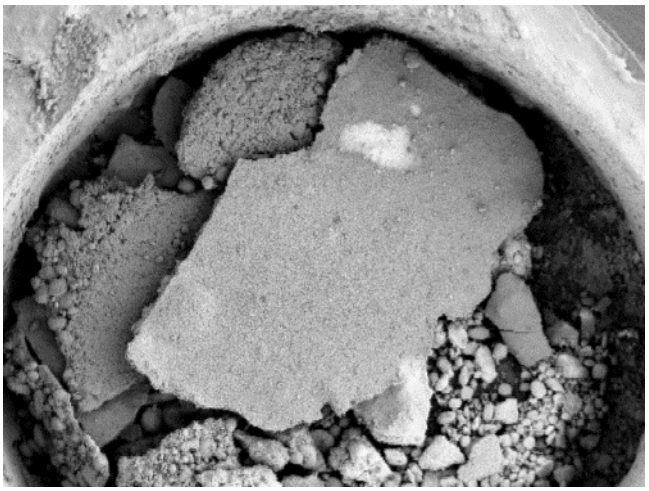

Fig. 13: Destroyed coating due to rapid boiling of the ethanol carrier solvent.

solvent and wiped clean multiple times to remove any residual Bi-2212 along the walls before a run was repeated.

Samples were then taken for XRD analysis to ascertain their texture parameters. Fig. 12 shows the texture parameter of various solvents in a 7.0 T background field. These results indicated that there were no major differences in imparted texture between the three non-interacting solvents investigated.

Microscopy was carried out to determine the quality of the powder coating. As previously discussed, the quality of powder coatings varied with the speed at which the solvent was evacuated. Examples of poor and acceptable powder coatings are shown in Fig. 13 and Fig. 14 respectively. Even in the acceptable coatings, it was evident that a large amount of porosity persisted in the deposited powders.

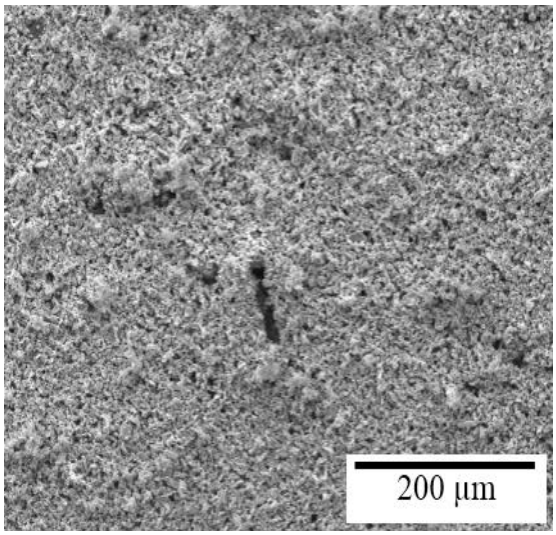

Fig. 14: Deposited coating allowing a sufficient settling time and evaporation rate.

Magnetic Texturing Conclusions

Through both x-ray diffraction and SEM studies, magnetic texturing of Bi-2212 through use of a carrier medium of either epoxy or a removable liquid was confirmed. General trends existed that higher viscosity fluids resulted in a greater degree of texture by dampening the harmonic motion of the Bi-2212 particles in applied field. Additionally, increased applied field strength was also observed to enhance the degree of imparted texture. Ultimately, the solvent deposition method was an acceptable avenue for pre-texturing Bi-2212 powders for a jelly-roll conductor approach [53].

2.3.2 Mechanical Texturing

Aside from the anisotropic magnetic properties utilized to advantage in the previous section, Bi-2212 also demonstrates an anisotropic shear modulus and bulk modulus [38]. In many ways, Bi-2212 behaves very similarly to mica, a mineral with a crystalline structure very close to that of Bi-2212. Both materials exhibit preferential

shear planes that allow particles to slide over one another. Combined with the higher modulus along the c-axis, Bi-2212 preferentially deforms under load by sliding along the ab planes. These anisotropic properties and the general platelet shape of Bi-2212 powders allow them to stack so their c-axes are normal to whatever surface on which they light. However without an orienting force, random effects influence the packing, leading to either a randomly oriented powder, similar to dumping a pile of bricks on the ground, or an electrostatically agglomerated powder, like Styrofoam packing peanuts clinging together.

Given the anisotropic mechanical behavior of the particles, it was hypothesized that texture could be achieved by applying a force normal to the plane in which texture is desired to be achieved. This force would primarily overcome electrostatic effects and enhance the packing density of the particles, locking them in place with one another to form a solid unit. To examine the possibility of achieving texture in this manner, a series of experiments were undertaken. The first consisted of a simple die set to demonstrate that texture could be achieved through uniaxial application of mechanical force. Secondly, a demonstration of the scalability of the texturing method to a continuous process was undertaken. Finally, a series of die sets were commissioned to provide textured samples which would be conducive to short sample testing and ultimately, wire fabrication. A relationship was established between compaction force and density as well as between compaction force and imparted texture of Bi-2212 powders.

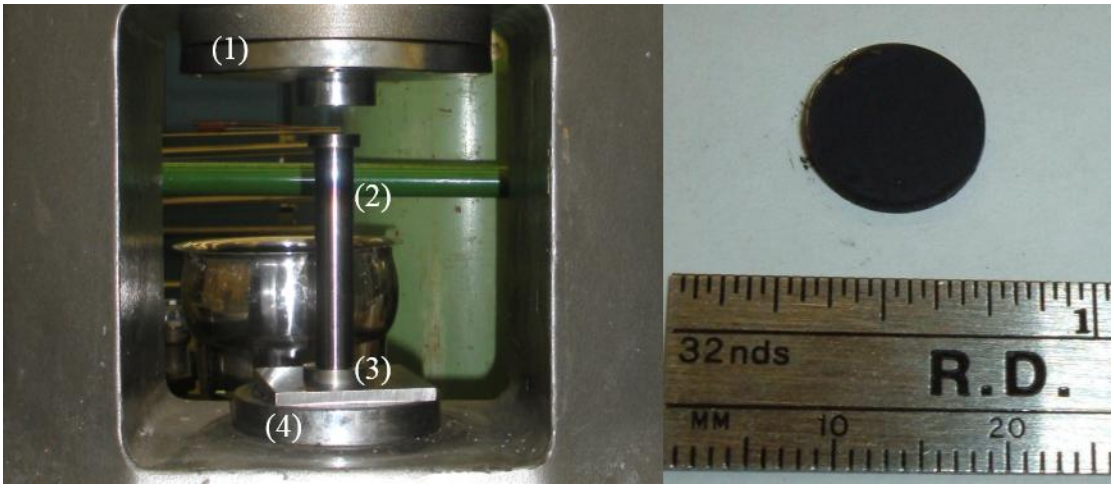

Fig. 15: Die set (left) and coined pellet (right). Die set consists of a hydraulic press (1), hardened tool steel hammer (2), Alloy 1144 Steel mold (3), and hardened O1 tool steel anvil (4).

Pellet Studies

The first and most rudimentary method of examining texture development by mechanical methods was through the fabrication of high density pellets of Bi-2212 through a round die set. These die sets were of varying diameters and consisted of three components: a hardened tool steel anvil, a hardened hammer (a mold ejector pin), and a medium strength (Alloy 1144) sleeve. The sleeve was placed on top of the anvil and loaded with a precise mass of Bi-2212 powder. The hammer was inserted and then a hydraulic press was used to slowly apply a loading force. After allowing the particles to settle under load, which typically required multiple additions of force, the hydraulic load was removed and the pellet was ejected from the sleeve. One example of the die set and a fabricated pellet are shown in Fig. 15.

The amount of pressure applied to the samples was varied to determine the dependence of pellet thickness (and thereby density) and texture on the applied force.

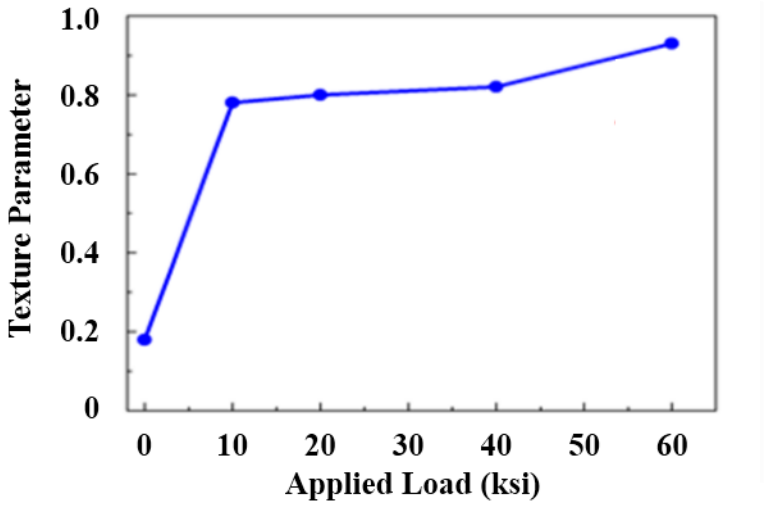

Fig. 16: Texture parameter vs. applied pressure for pellets.

XRD was used to find the texture parameter of the pellets. Results from these experiments are presented in Fig. 16 [52]. It was found that loads as low as 10 ksi were sufficient to compact the powders into a stable configuration. Furthermore, it was evident that increasing applied pressure had the predictable effect of enhancing the pellet density and that texture also increased with applied pressure. Both of these effects saturated with applied pressures exceeding ~40 ksi, while 20 ksi resulted in a drastic increase in both density and texture.

Microstructure examination of the pellets indicated that the surfaces were indeed highly textured and had very little apparent porosity. Importantly, the surface showed no significant signs of contamination from the stamping process, indicating that the hardness of the steels in these die sets was sufficient to hold up against the hard, abrasive Bi-2212 powders [52].

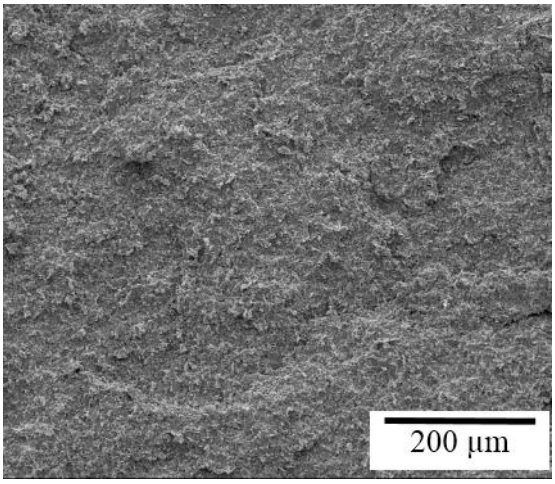

Fig. 17: Surface of pellet cleaved parallel to its face. The bulk appears highly uniform and remains well aligned.

While the surface of the pellets was evidently well textured, questions remained as to the behavior of the bulk of the material. To examine the bulk of the material, a series of pellets were fabricated and subsequently cleaved along their mid-plane. This was accomplished by using a razor blade to halve the pellet, like splitting open an Oreo. The two halves were then characterized with XRD and SEM to establish the texture of the bulk. For a compaction pressure of 20 ksi, an average texture parameter of 0.79 was found on the cleaved surfaces. This result agreed favorably with the results of surface texturing at the same compaction pressure. Furthermore, the texture was confirmed via microscopy and Fig. 17 shows a representative SEM image of the cleaved pellets.

At this point, a conclusion was reached that an optimum density and texture could be obtained by applying a 20 ksi load normal to the desired texturing plane. This value was chosen because texture was at the plateau level with respect to applied pressure, yet the density remained low enough to allow for subsequent deformation.

Round pellets could not readily be fabricated into a geometry desirable for wire fabrication, so a new method for creating conductor ready textured powders was required to be established for incorporation of mechanical pre-texturing in a wire fabrication process [40, 52].

Continuous Roll Processing

Aside from the inhospitable geometry of the pellet studies, batch processes typically limit the applications of superconducting materials as short lengths increase the number of joints in long length applications. As joints are typically the most problematic area in a superconducting application [78], it is imperative to limit their number and precisely control their location. At the present, Bi-2212 production is only limited in length by available sizes in Ag tubing which allows for at least 1 km long production [79]. Given a die stamping process, even in an amenable geometry for wire fabrication, is inherently limited in length by the scale with which the Bi-2212 may be compacted, an alternative to batch processing is necessary to maintain any semblance of economy in Bi-2212 wire fabrication and to produce the several kilometer lengths that are coveted by the HEP community and magnet technologists in general.

The parameters for such a continuous process were clearly that the process must be able to produce a uniformly textured sample by applying a mechanical load of 20 ksi to loose Bi-2212 powders without introducing contaminants. Additionally, it was highly desirable from both a safety point of view and a scientific perspective to control the atmosphere that the process takes place in. This is to prevent the adsorption of carbon dioxide and water onto the surface of the Bi-2212 powders, which would then be trapped

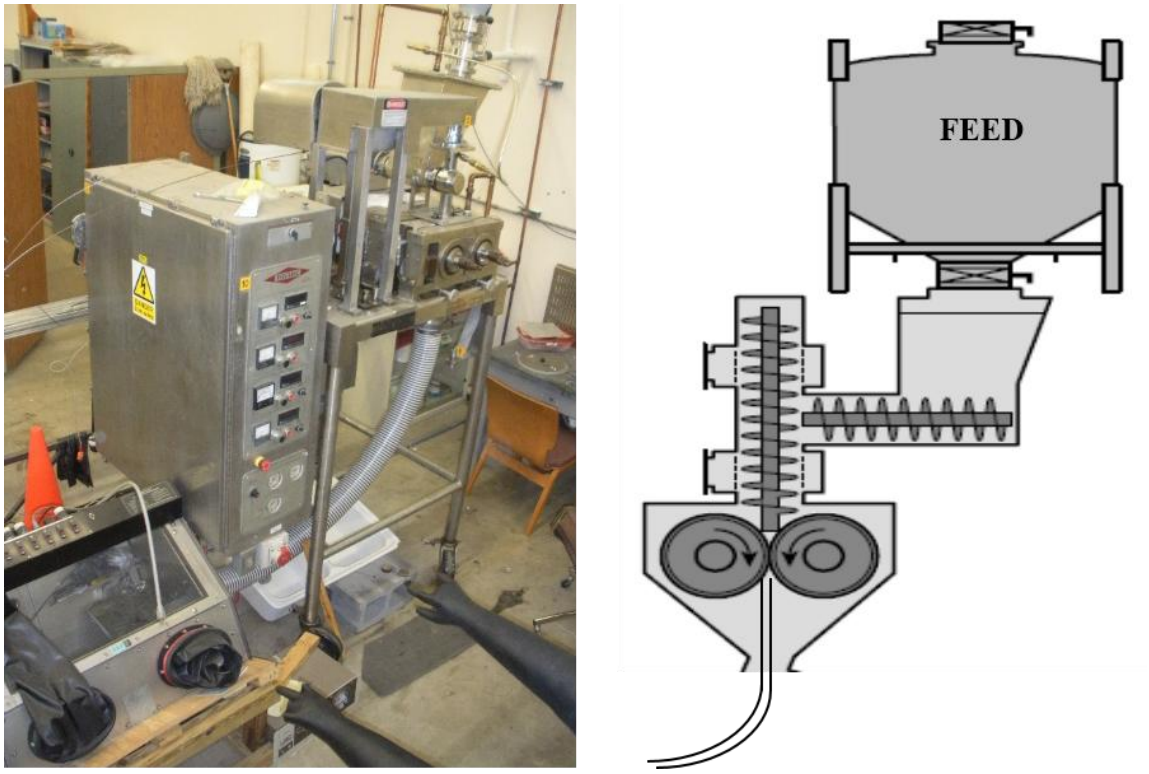

Fig. 18: Installed L-83 Chilsonator (left) and mechanical schematic of the roll processing unit (right). The glovebox in the image (left) enables a positive or negative pressure to be maintained for during operation, maintaining the hermetic seal on the output. © 2011 IEEE

within a conductor to be processed later. Additionally, providing atmosphere control for the powder is the primary engineering safety control that prevents the inhalation of the sharp, ultrafine particles.

Roll processing evinced itself as the leading concept to provide the requisite compaction and texturing in an industrial scale processes. To demonstrate the feasibility of such an approach, a demonstration scale experiment of the effects of roll compacting Bi-2212 powders was undertaken. To enable this endeavor, a piece of equipment from the pharmaceutical industry was adapted for use in the roll processing of Bi-2212 loose

powders. Fig. 18 [40, 52] shows the equipment, an L83 Chilsonator procured from Fitzpatrick Co. The device consists of two hardened steel rollers rotating in opposite direction to one another with a variable gap width between the two rollers. Powder is forced through the rollers by a vertical feed screw and a constant supply of powder is provided through a horizontal auger connected to a hopper containing the loose powder. Variable parameters include the vertical auger's rotational speed, roll gap width controlled by a variable hydraulic pressure, and the powder feed rate from the hopper. By tuning these parameters, a uniform density ribbon of Bi-2212 powders was produced. Since these ribbons were inherently stiff and atmosphere control was still important, an uptake system was employed that allowed the fabrication of 1 m long ribbons of Bi-2212. In practice, lengths in excess of 1 m would be possible with a superior take-up system and the length of ribbon produced would only be limited by the amount of available powder in an industrial scale process.

Table 3: Properties of Roll Processed Ribbons [52]

Sample	Loose Powder	Ribbon Transverse	Ribbon Longitudinal	Ribbon Bulk	20 ksi Pellet
Texture parameter, τ	0.16	0.70	0.70	0.67	0.70
Density g/cm^3	----		4.24		3.9

Confirmation of the texture and evaluation of the imparted density of the ribbons were carried out utilizing the methods described previously. Results of the texture evaluation are shown in Table 3 [40, 52, 80] along with SEM images of the compacted ribbons surface and cross sections in Fig. 19 and Fig. 20 respectively. Density measurements

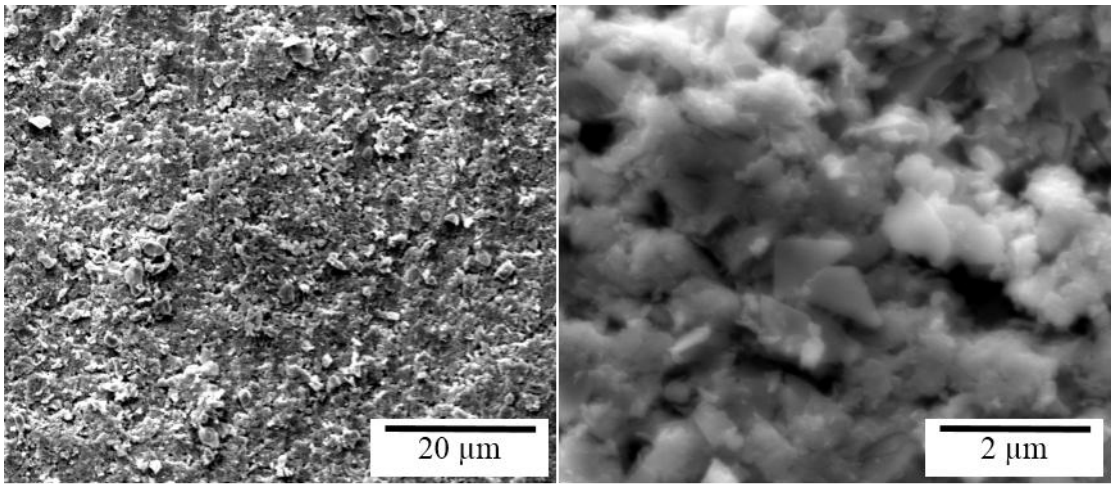

Fig. 19: SEM images of the surface of a continuously compacted ribbon from the Chilsonator. Surface roughness is greater than that of the pellets (left), but the imparted texture is nearly identical (right).

were performed by direct measurement of at the thickness of a given ribbon via micrometers and area fraction calculations were achieved by taking scanned images of the ribbons with a calibrated scale and post processing them in ImageJ. Due to the complicated load structure of a rolling process, the compaction pressure applied to the powder was not well defined. However, upon comparison of the texture and density of the roll compacted ribbons, the roll compaction method was equivalent to applying a load of ~20 ksi to the powder in a die stamping process.

While the roll processing experiments were successful in demonstrating the efficacy of the method for texturing and densifying the loose Bi-2212 powders, the scale of the experiments was not amenable to further process development. First, the wide ribbons were inhospitable for heat treatment and short sample measurement. These highly compacted ribbons were also very difficult to cut or trim after fabrication and

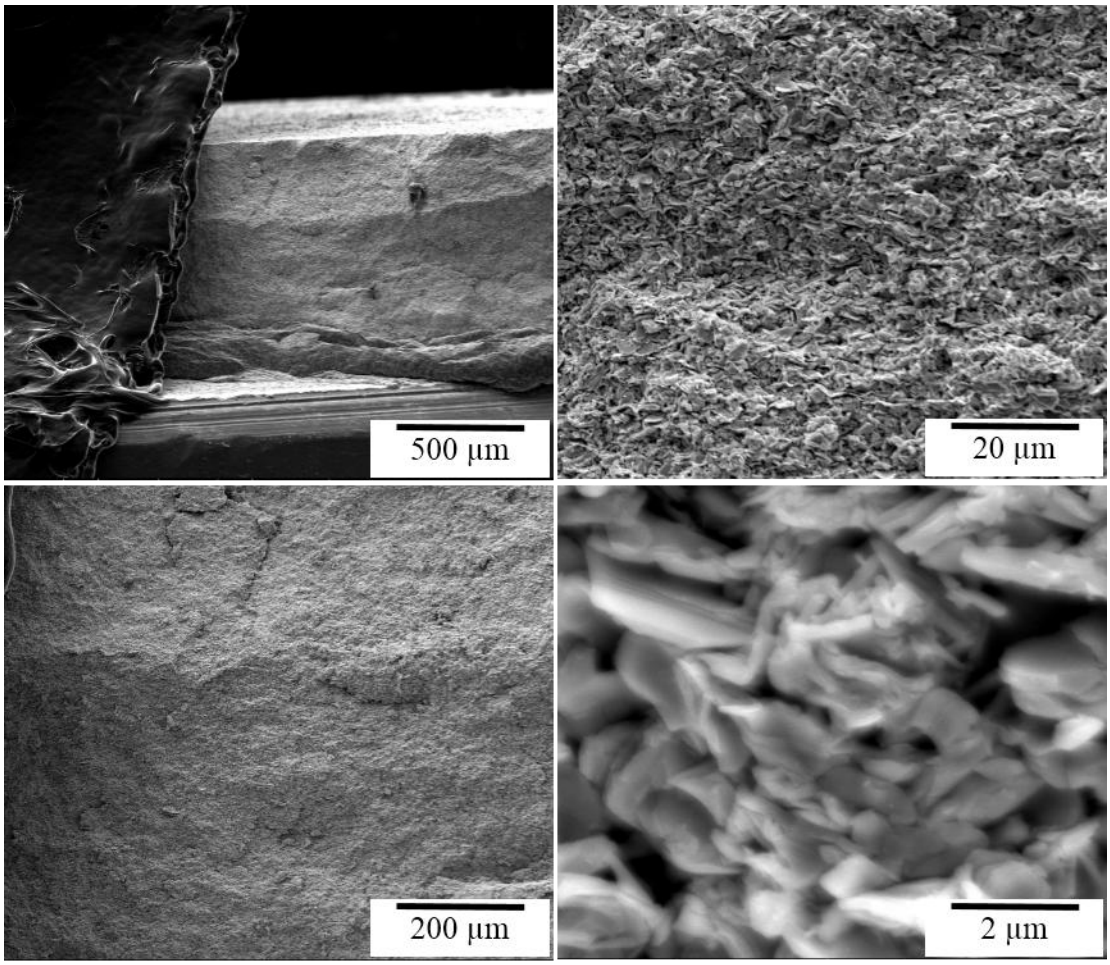

Fig. 20: SEM images (SEI) of a transverse fractured ribbon of Bi-2212 from the chilsonator. Very low void space is prevalent and the narrow aspect ratio grains are apparent in the highest magnification images.

altering the dimensions coming from the Chilsonator presented an engineering challenge whose solution required redesigning the entire compaction process. Additionally, several kilograms of powder were required to operate the Chilsonator for even a minimum run with a significant fraction of that powder resulting as waste in either the leading or trailing feed of the process. While initial commissioning took place with a quantity of inexpensive, low quality powder, running the process with high quality powders for

conductor development would have been prohibitively expensive. As such, the development of a batch scale process for further conductor development became necessary.

Square Rod Compaction

In an effort to economically and efficiently fabricate a conductor that would allow for the development of deformation processes of the high density, textured conductor as well as to embody a conductor which may be heat treated and tested for transport measurements, a series of die sets were commissioned. These die sets worked on the principle of uniaxial compression in much the same manner as the pellet studies and were specified to produce samples of a given dimension for either direct short sample testing of Bi-2212 bulk material or for a wire development project.

Direct Short Sample Measurement

To match available power supplies and to rapidly enable short sample testing, the first die set was fabricated to produce a 1 mm x 1 mm x 150 mm square rod of Bi-2212 at compaction pressures up to 80 ksi, but nominally specified at 20 ksi. The die set is shown in Fig. 21 with a coined bar shown in Fig. 22. As with the pellet studies, compaction took place in air and all components of the die set were cleaned prior to each coining operation. Texture of these bulk materials was confirmed via XRD and microcopy as shown in Fig. 23 and Fig. 24 [80]. No contamination from the die set

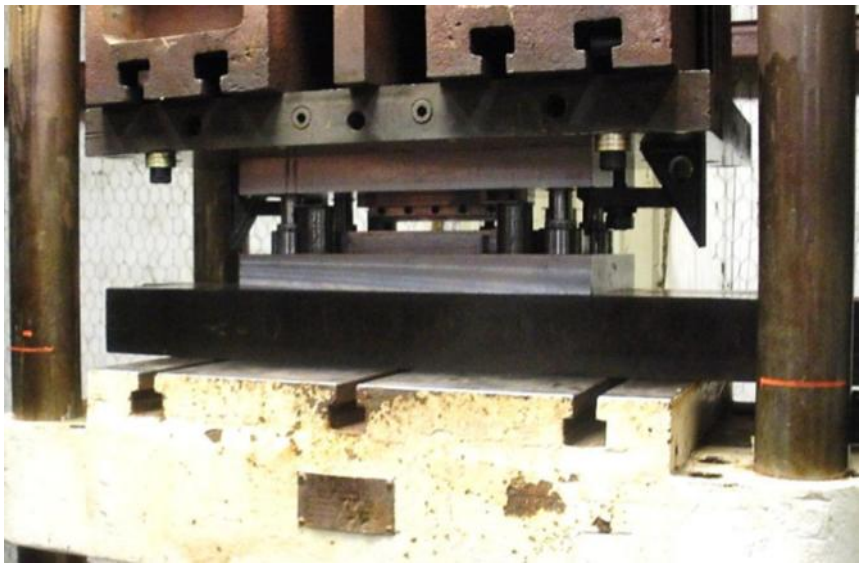

Fig. 21: Die set for compacting square rods mounted in a hydraulic press. Powder is loaded into the lower half (mold) then aligned with the upper half (hammer) for the compacting strikes.

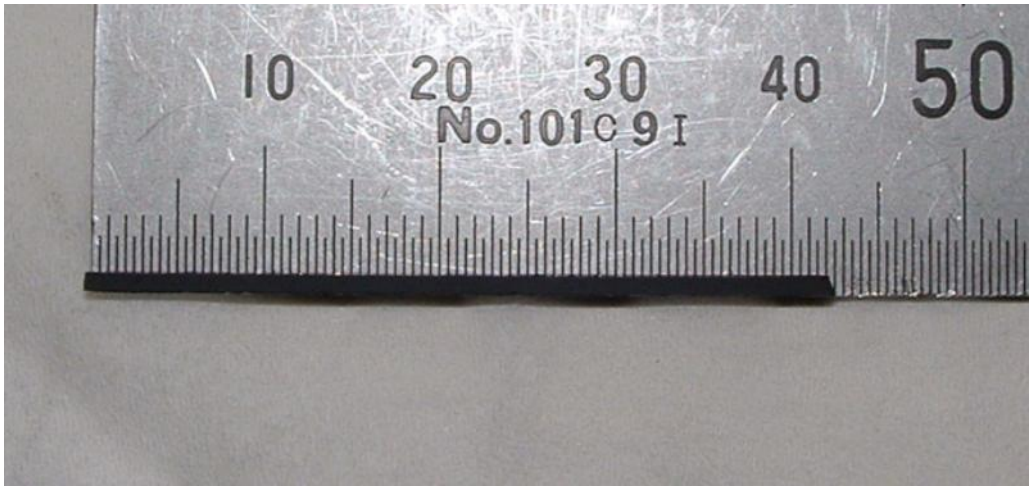

Fig. 22: A 1 mm x 1 mm x 43 mm coined square rod for direct transport measurement.

(comprised of D2 and M2 steels) was found in the resulting bars. After coining, samples were heat treated in contact with Ag foils to provide current transport leads as described in the Heat Treatment section.

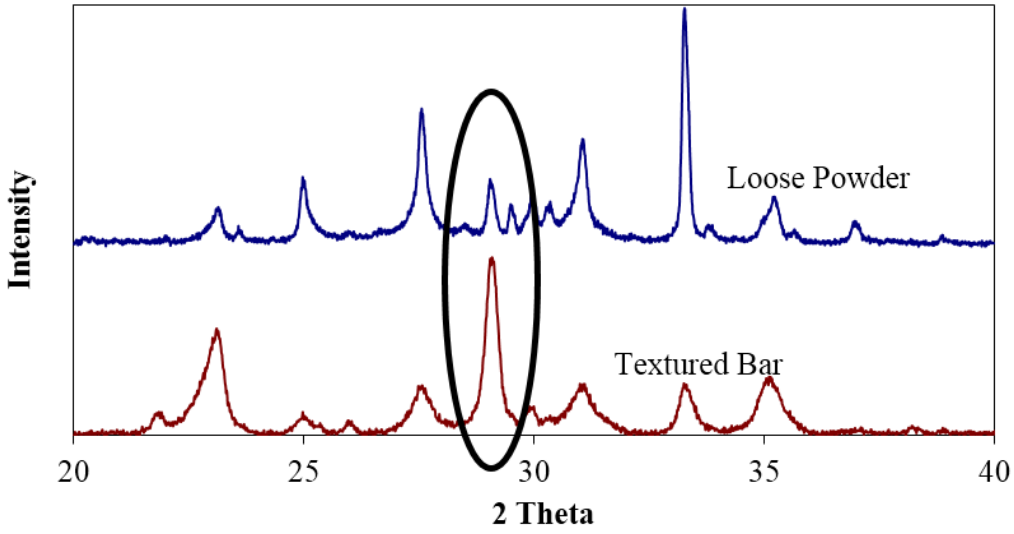

Fig. 23: XRD patterns of untextured loose powder and a coined bar. The circled peak is the (0010) peak. The dominance of this peak in the coined bar indicates the enhancement of out of plane c-axis texture.

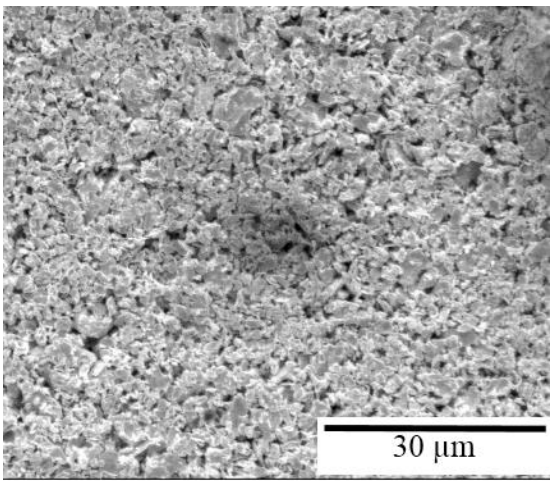

Fig. 24: Surface (hammer side) of coined Bi-2212 1 mm x 1 mm bar showing the high degree of uniformity and aligned particles.

Texturing for Wire Fabrication

While 1 mm square Bi-2212 bars were acceptable for demonstrating the texturing method and provided a first attempt at achieving a short sample measurement, these bars

were not robust enough to fabricate a billet. Additionally, given their small size, a monocore wire development was ill advised since any monocore development that obtained an appreciable (>20%) area fraction of superconductor would require the use of prohibitively small Ag components. As such, a bar with greater cross sectional area was required for the purpose of manufacturing a monocore wire based on a high density textured powder. To match Ag tubes that were available with dimensions of 7.3 mm OD and internal square section of 4.5 mm flat to flat, the die set from the 1 mm square bar experiments was modified to produce a 4 mm x 4 mm x 150 mm bar of Bi-2212 compacted at 20 ksi. Such a bar is shown in Fig. 25. As in the previous case with the 1 mm square bars, compaction took place in air. Again, texture was confirmed via XRD and microscopy with xray spectra and SEM with identical results to those presented for the 1 mm x 1 mm bars. Density of the 4 mm coined bars was consistent with results from both the 1 mm bars and pellet studies and the 20 ksi compaction pressure yielded a density of roughly 4.2 g/cm^3, or 64% of single crystal density [81].

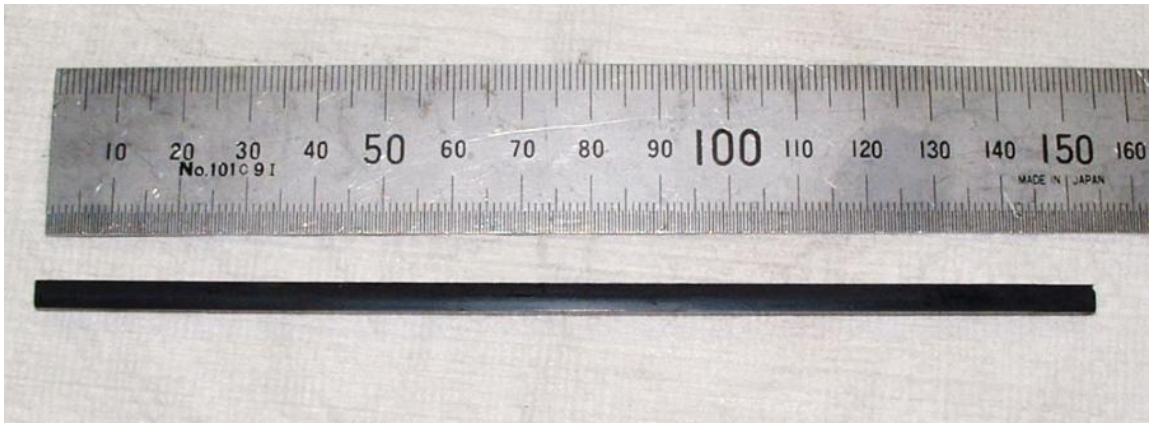

Fig. 25: Coined 4 mm x 4 mm x 150 mm bar as a precursor to TPC fabrication.

2.4 Texturing Conclusions

Two methods for texturing Bi-2212 loose powders were studied through a series of experiments. Both the magnetic orientation and mechanical texturing were demonstrated to align the anisotropic Bi-2212 particles. However, the uniaxial compression technique yielded the highest quality oriented powders and was determined to be the most amenable form of textured powder for wire development and transport current testing as evinced by the pellet studies. While continuous ribbons of high density textured powder were possible through a roll compaction process, the investment to reliably produce high quality ribbons was uneconomical for research scale developments. Instead of continuing the development of these ribbons, high quality square bars were fabricated to provide testable textured powders for both wire fabrication studies and direct short sample measurements.

3. WIRE FABRICATION

3.1 Introduction to Wire Fabrication

Details of the OPIT process and the evolution of Bi-2212 from a novel superconducting material to a round wire form were presented in the introductory chapter of this work. As such, the following chapter focuses specifically on the details of the wire fabrication of a monocore textured powder conductor. The intention of such a wire fabrication process was to both produce a conductor amenable to short sample testing and to investigate the deformation properties of a Bi-2212/Ag composite for further conductor development.

Wire fabrication required four main components that will be discussed in detail. First, billets were fabricated with a textured powder precursor. Following this step, an isostatic extrusion was the first deformation step in the process. Third, deformation continued through a series of wire drawing operations. And finally, wires were stripped of supporting copper from the deformation processes to provide an oxygen transport path during heat treatment.

3.2 Billet Fabrication

The three primary components of the textured powder billets are shown in Fig. 26 [81]. They consist of a textured powder Bi-2212 component compacted uniaxially as described in the texturing chapter, an Ag tube (Tanaka fine Ag provided by SupraMagnetics) drawn with a square inner section, and finally, an alloy 110 Cu extrusion jacket.

Fig. 26: Billet components during assembly including Cu extrusion jacket, Ag tube, and coined Bi-2212 rod partially inserted into the Ag tube.

The dimensions of these components are listed in Table 4 along with their suppliers. The copper extrusion jacket was additionally machined to the form shown in Fig. 27 through multiple steps. Gun drilling of the inner diameter was carried out by HDH instruments Pattison, TX with subsequent machining of the tapered nose cone and evacuation tube port taking place at TAMU. The evacuation tube consisted of a 9.5 mm OD, 8.0 mm ID Cu tube and was brazed in place. Upon the completion of all machining and soldering steps, the interior was cleaned with a series of solvents, first by mechanically scrubbing the interior and ultimately through ultrasonic agitation to remove all internal grease and debris. Notably, no acids were used to remove the surface layer of copper oxide within the extrusion jacket since this would favor the metallurgical bonding of the Ag and Cu

Fig. 27: Cross sectional view of assembled billet showing from interior to exterior the placement of the Bi-2212 rod, Ag tube, and Cu extrusion jacket. The evacuation tube and Cu plugs are ommitted for clarity.

Table 4: Billet Components

Material/Supplier	OD	ID	Fabricated
Cu 110/ McMaster Carr	1.25”	0.297”	HDH Instruments/TAMU
Ag/Tanaka	0.289”	4.5 mm flat to flat	SupraMagnetics
Bi-2212/Nexans	4 mm x 4 mm	--	TAMU

interfaces. Upon termination of the final cleaning step, the extrusion jacket was placed within an Ar glove box to await assembly of the remaining billet components.

Fabrication of the Ag tube was carried out at SupraMagnetics who provided a single 18.5” long tube to TAMU. The tube was EDM cut at TAMU to yield 2, 6.5” long tubes and 1, 6” long tube. The 6” long tube was reserved for future work while the remaining 6.5” tubes were first cleaned with ethanol, then taken to a class 100 clean room and etched to a dull bright with 0.8 M HNO_3. Tubes were sealed within the cleanroom in an ethanol bath which was maintained until the tubes were placed in the vacuum port of the Ar glove box. At this point, the ethanol was evaporated by evacuating the chamber and the Ag tubes were stored in the Ar glove box until billet assembly.Four independent Bi-2212 components were fabricated for the fabrication of two billets. The redundancy was in part due to the fragile nature of the square rods and the difficulty of inserting the rods into the Ag tube by hand without fracturing the Bi-

2212 component. Billets were labeled based upon the Bi-2212 component. Ultimately, bars TAMU IV-2 and TAMU IV-4 were used in the study. The dimensions of these bars are presented in Table 5 along with their initial density and other pertinent parameters. Of specific interest is the fact that bar TAMUIV-2 was calcined at 600 C for 4 h in a 10 mTorr vacuum followed by an 8 h soak at 200 C under 1 atm of O_2 in an attempt to pull off volatiles that had adsorbed on the bar's surface and in interstitial spaces and to remove as much H and C contamination from the powder as possible. This heat treatment was done in concert with examples from the literature [82, 83]. Upon completion of the heat treatment, the bar was removed from the furnace under atmospheric conditions and immediately transferred to the glove box where it was stored under Ar until billet assembly. Once inserted into the glove box, it was evident that a slight brown discoloration had occurred on all sides of billet TAMU IV-2. The billet was scraped to remove any discoloration and assembly proceeded.

Billet assembly took place by hand in the Ar glove box. The Bi-2212 bars were dressed with a razor blade to loosen the powder at their surfaces and facilitate sliding into the Ag tubes. Bars were inserted such that the 2212 bar was recessed into the Ag

Table 5: Textured Rods Used in Billets

Sample	Width/Height/Length (mm)	Mass (g)	Density (g/cm^3)	Compaction Pressure (ksi)	Calcined
TAMU IV-2	3.91/3.90/150	9.92	4.34	20.7	Yes
TAMU IV-4	3.90/3.95/150	9.69	4.19	20.7	No

tube by roughly 0.25” on each side. This void space was filled with a custom Ag plug that was fabricated with Ag wire which had been previously cleaned and entered the glove box in the same manner as the Ag tubing. With the Ag plugs in place, the Ag and 2212 component was inserted into the extrusion jacket. A Cu rod which had previously been degreased in the same fashion as the interior of the extrusion jacket was used to fill 2” of the remaining void space within the extrusion jacket and a Cu mesh was packed into the remaining void. A needle valve was attached to each billet’s evacuation tube. This valve was closed in the Ar environment, sealing the billet with a protective atmosphere. At this point, billet assembly was complete and the billets were removed from the glove box. In an effort to remove trapped gases within the billets and to anneal the metallic components, both billets were attached to a vacuum pump and evacuated while the billets heated to 450 C and were held for 6 h. Vacuum pressure was monitored and a base pressure of 10 mTorr was established within the system. At 100 C and 300 C, momentary spikes in the vacuum pressure were observed, presumably corresponding to the removal of surface water and CO_2 contamination respectively. It was not possible to ascertain which billet served as the originator of these pressure spikes as the billets were co-treated in a common vacuum system.

At the end of the 6 hour anneal, the billets were removed from the furnace and the evacuation tubes were first crimped, then welded shut behind the needle valve. The crimping and welding operations took place with the vacuum pump in operation and acted to seal the vacuum in place during transport of the billets from TAMU to the Applied Superconductivity Center in Tallahassee, FL for extrusion. Images of the

Fig. 28: Fully assembled, sealed billets with carbide die over evacuation tube.

completed billets are shown in Fig. 28. At this point, billet fabrication was complete and the billets were shipped to Tallahassee for extrusion.

3.3 Extrusion

An isostatic extrusion was selected for the first deformation of the assembled billets. This decision was made due to the low modulus of silver, significant void space in the billet between the Ag and 2212 components, and because of the mismatched moduli of the Bi-2212 and Ag components. By choosing an extrusion with a strain sufficient to remove the residual void space, the billet would essentially be locked in place for subsequent drawing operations. Isostatic extrusions apply a hydraulic load about the entirety of the billet which prevents mushrooming effects for soft modulus materials. An additional concern for billets of mixed moduli, such as our billet with soft Ag and hard Bi-2212 is the propensity for the conductor to sausage. This effect occurs

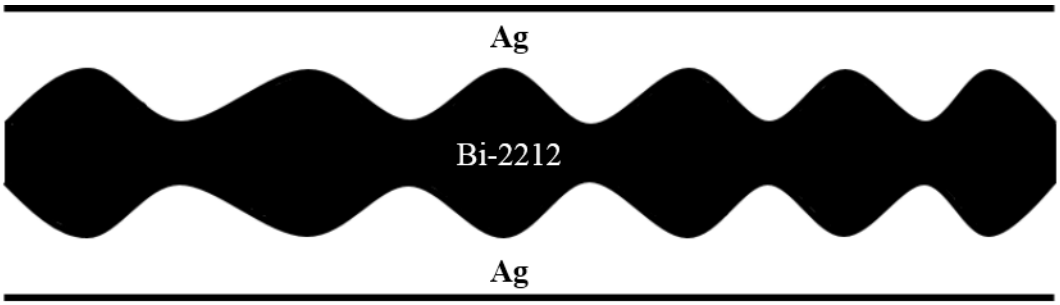

Fig. 29: Sausaging phenomenon caused by over-deforming a mixed composite with a high modulus interior (Bi-2212) and low modulus exterior (Ag).

when the soft modulus material preferentially deforms until a sufficient load is applied to deform the hard component. Motion continues through the die in a stick slip motion resulting in a linked sausage appearance of the filamentary composite, similar to the image shown in Fig. 29. The isostatic loading addresses this issue by preventing the bulging effects that are typical of sausaged composites. Finally, extrusion serves to perform a severe areal reduction which reduces the number of subsequent passes necessary to achieve a fine wire dimension. In this light, it appears most economical to take the largest reduction possible in the extrusion pass without causing a sausaging phenomenon or degradation of the conductor.

With the aforementioned concerns in consideration, a moderate engineering strain of 2.2, corresponding to a reduction in diameter from 1.25” down to 0.5”, was selected for the extrusion. This reduction was calculated to be sufficient to remove any void space within the billet and primarily served to lock the components in place for subsequent drawing. The strain was inherently limited by several concerns. First, a pragmatic issue arose with the necessity to fit the 3/8” diameter evacuation tube through the extrusion die. Second, energy deposited due to the deformation of the billet results in

a significant temperature increase. Given the sensitivity of the Bi-2212 component to excessive heat, and the propensity of Ag and Cu to alloy, the maximum temperature of the billet would preferably stay below 600 C. As the temperature rise would increase with increasing applied strain and the temperature rise is highly dependent on empirical factors such as die condition, lubricant used, strain state of the material extruded, and extrusion rate among others which made this value difficult to calculate, a conservative strain was chosen. Additionally, extrusion at a higher strain would run the risk of breaking the billet or otherwise degrading the conductor.

Due to the specialized equipment necessary to achieve a desirable result, the extrusion was carried out at the Applied Superconductivity Center in Tallahassee, FL under the expert tutelage of William Starch. Fig. 30 shows the extrusion press. Prior to the extrusion, the billets were machined to confirm their precise outer diameter and taper

Fig. 30: Isostatic extrusion press at ASC. Billets are loaded through the opening at left into the extrusion chamber. The chamber is flooded with hydraulic fluid, and pressurized until the billet seals on the die. Continued increase in hydraulic pressure extrudes the billet.

by ASC staff and lubricated a Loctite Nickel Anti-Seize compound. While lubrications can be a significant concern in multifilament Bi-2212 processing, the fact that the outer copper jacket was isolating the billet from the lubricant mitigated any concerns that may have arisen.

Extrusions of both billets were carried out without incident with extrusion rates being controlled by an experienced operator and the hydraulic pressure within the chamber continually monitored. Plots of the hydraulic pressure vs. extrusion distance were charted during the extrusion. The smooth nature of these plots which maintained a nearly constant loading pressure during processing indicated that no significant sausaging or non-homogeneous reduction occurred along the length of the billet.

Upon removal from the press, the billets had extended in length to 1.55 m each. This included a leader and tail of copper that did not contain the Ag/2212 composite. At this stage, sampling of the billets to determine the uniformity of the transverse and

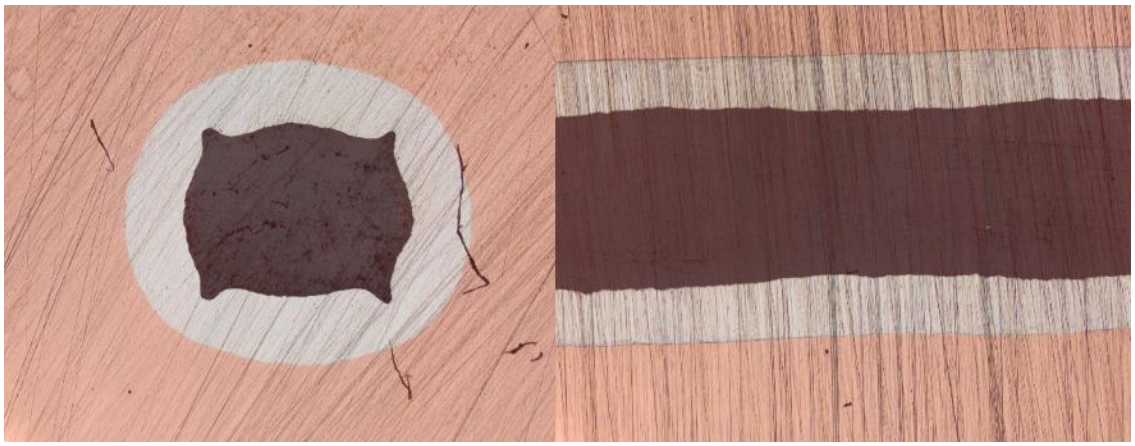

Fig. 31: Polished sections of extruded billet. Left: Transverse section showing the earring phenomenon and anisotropic reduction with preferential reduction in the vertical direction. Right: Longitudinal section showing relatively uniform Ag/Bi-2212 interface.

longitudinal sections. Polished samples at this stage are shown in Fig. 31 [81]. In this early analysis, it was evident that sausaging did not occur in a significant fashion in the extrude conductor. From the transverse section, two effects were also clear: the Bi-2212 reduced anisotropically and the conductor exhibited an "earring" effect. The anisotropic reduction was an anticipated effect and was attributed to the anisotropic modulus of the textured Bi-2212 which preferentially shears along the ab planes. Meanwhile, the earring was not anticipated, but can be explained by the square inner geometry of the Bi-2212 undergoing a round deformation coupled with the difference between the Bi-2212 and Ag moduli.

As the billets had been cut for sampling, and gas contamination of the billets was a significant concern, the back of the billet was pointed using a swaging machine. This effectively re-sealed the billet with a crimped metal seal, preventing significant gaseous diffusion while the billets were shipped for drawing.

3.4 Wire Drawing

Post-extrusion, billets IV-2 and IV-4 were both nominally 0.500" in diameter and of 1.55 m in length. In order to examine multiple parameters in the drawing process, the billets were halved with roughly 18" (taken from the tail of the extruded billet) cut from the back of each billet. These tail billets were labeled as TAMUIV-2b and TAMUIV-4b respectively. Due to the large amount of copper still jacketing the Ag/2212 component, the "b" series billets were machined down from the ½" diameter to a ¼" diameter in an effort to reduce the amount of copper that would later be removed and to determine if

changing the copper wall thickness would alter the deformation properties. Drawing took place at SupraMagnetics, a firm experienced with drawing Bi-2212 wires.

Table 6: Drawing Schedule for "A" Billets

Die Size	Reduction %	Total Strain (eng.)
0.5000"	Starting Size	2.2
0.4600"	15.36	2.4
0.4100"	20.56	2.6
0.3650"	20.75	2.8
0.3250"	20.72	3.1
0.2893"	20.76	3.3
0.2573"	20.90	3.5
0.2294"	20.51	3.8
0.2053"	19.91	4.0
0.1819"	21.50	4.2
0.1620"	20.68	4.5

Carbide dies with an 8.5 degree entrance angle and long landing were selected based on previous experience of the SupraMagnetics staff. Since copper was still jacketing the Ag/2212 component so a mixture of lubricating oils were used to assist in the drawing process. The reduction schedule used on the "A" schedule billets is shown in Table 6, while the "B" reduction schedule is shown in Table 7.

The drawing process consisted of iteratively pointing (swaging) the front end of the wire, lubricating the sample, passing the point through the die, then pulling the wire through the die via a hydraulically pulled jaw. A picture of the draw bench with a billet is shown in Fig. 32. Periodically, samples of various lengths were cut from the back of the billet to analyze the cross section and for future studies of the core densities, cross section, and transport properties of the conductor.

Table 7: Drawing Schedule for "B" Billets

Die Size	Reduction %	Total Strain (eng.)
0.250”	Starting Size	2.2
0.2294”	15.80	2.4
0.2053”	19.91	2.6
0.1819”	21.50	2.8
0.1620”	20.68	3.1
0.1440”	20.99	3.3
0.1285”	20.37	3.5
0.1144”	20.74	3.8
0.1019”	20.66	4.0
0.0907”	20.77	4.2
0.0808”	20.64	4.5

Wire fabrication continued without breaks until the wire diameters and lengths listed in Table 8 were achieved. Ends were pointed in a similar manner to the post extruded samples in an effort to prevent gaseous diffusion into the cores. At this point, the wire

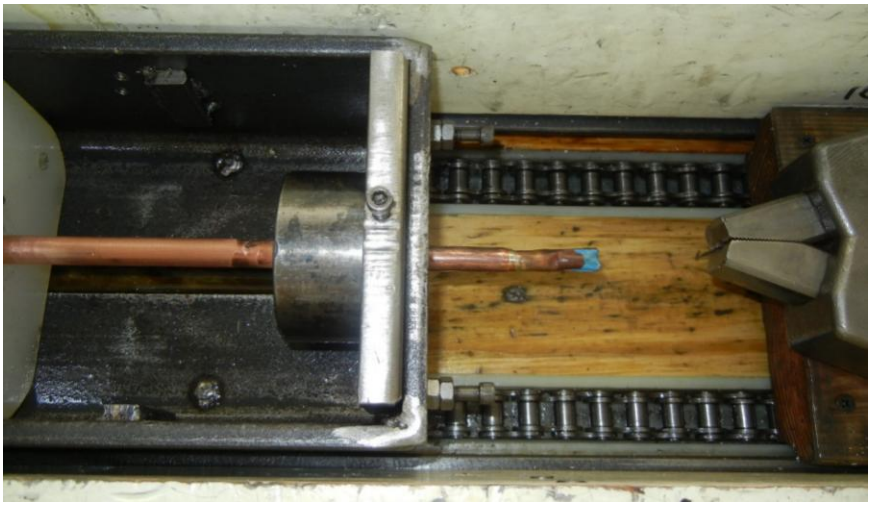

Fig. 32: Billet during drawing process. The sample at left is pointed and inserted through the die. The pointed end is then grabbed by the jaws at right and the rod/wire is pulled through the die mounted in the bull block.

fabrication was considered complete and the products of the effort were stored until the copper could be removed and the Ag/Bi-2212 wires heat treated.

Table 8: Dimensions of Drawn Conductors

Billet	Cu Diameter (mm)	Ag width (mm)	Quantity (m)
2A	4	1	3
2B	2	1	4
4A	4	1	0.2
4A	0.5	0.125	>5
4A	1	0.25	>5
4B	0.5	0.25	>5

3.5 Copper Removal

After all deformation processes had been completed, heat treatment of the Ag/Bi-2212 wires could not take place until the Cu jacket was removed from the conductors. This was a requisite as the Cu jacket would likely alloy with the Ag and diffuse into the Bi-2212 as a potential poison as well as the more significant issue of preventing oxygen transport into the superconducting cores. As many common etchants for Cu, such as HNO_3 also aggressively attack Ag and are imminently harmful to the Bi-2212 cores, much care was required to select an etchant that would preferentially etch Cu. A mixture of Ferric Chloride ($FeCl_3$), HCl, and ethanol was selected for this task. Samples were cut into ~2” lengths for transport measurements. Multiple sealants were tested to prevent the etchant from entering the Bi-2212 cores through the cut ends and a waterproof commercial silicone based sealant was the highest performing material.

While the etchant proved to be effective at removing only the copper component, it was a painfully slow process, requiring several days to clean the largest diameter

samples. As such, it was often beneficial to employ a pre-etch with HNO_3 to expose some component of the Ag. This etch was then immediately followed by the Cu only etchant until all Cu was removed.

After all Cu was visibly seen to be removed, samples were cleaned using a light etch of NH_4OH, H_2O_2, and ethanol. This etch removed a surface layer of Ag and any Cu residue that may have remained. Samples were rinsed and stored in ethanol until they could be transported to a vacuum chamber where they were stored until ready for further processing.

3.6 Wire Fabrication Conclusions

The wire fabrication effort was largely a success with the monocore extrusion and drawing process proceeding without breaks in the conductor or dramatic sausaging. Anisotropic reduction of the Ag/Bi-2212 composite was observed as a result of the differential modulus of the textured Bi-2212 powder. Even with this preferential deformation, a minimum filament of 175 μm x 100 μm was achieved. No difference was observed in the deformation properties of the "A" and "B" schedule billets, suggesting that more copper may have been removed without detriment to the process. Sufficient lengths of conductor were produced for heat treatment optimization studies of the wire to take place with multiple diameters and billet preparations available for investigation.

4. HEAT TREATMENTS

4.1 Introduction to Bi-2212 Heat Treatments

The previous chapters have described Bi-2212 wire fabrication and powder properties which comprise 2 of the 3 basic processing steps for Bi-2212/Ag conductors. The final step to achieving high current densities in Bi-2212/Ag wires is a heat treatment which grows, connects, and densifies the superconducting cores. Typically, this is achieved by taking the Bi-2212 past its melt temperature followed by recrystallizing the superconducting phase out of the melt [68, 82, 84-86]. While seemingly similar to melting ice chips then freezing them into a solid mass, Bi-2212 melt processing is anything but simple: the melt temperature depends on the oxygen partial pressure [84], melting occurs incongruently with decomposition into a Bi rich liquid and solid phases [44, 49, 50, 87], the presence of Ag alters the melt temperature, and oxygen escapes from the melt which has a lower oxygen solubility than the stoichiometry of the solid phase. Additionally, poisoning of the superconductor can occur when either a diffusing element (such as Cr or Cu) is able to move through the Ag or the Ag itself is attacked (such as with Si), leading to significant leakage of the superconducting cores [26, 27, 88].

Because of the complications associated with consolidating and texturing the superconducting cores within a Bi-2212/Ag wire, significant effort has been put into the development of an optimum heat treatment procedure for Bi-2212 wires. Due to the prolific, broad spreading nature of this research, a comprehensive discussion of the

various heat treatments that have been reported within the literature is neither practical nor informative as the majority of the efforts led to unsuccessful results.

4.1.1 Partial Melt Processing

Out of the myriad of processing options reported in the literature, one route has dominated the development and become the standard of comparison for all other processing routes: Partial Melt Processing (PMP). In PMP, a wire sample or coil is placed in a controlled atmosphere (typically 100% O_2 or alternatively, dry air) and heated to a temperature typically between 5 and 15 C above melt. The conductor is briefly held at this temperature, usually between 5 and 30 minutes, then slowly cooled to an intermediate annealing temperature between 830 and 840 C where the conductor is held for a period of about 48 hours before finally cooling to room temperature. A typical time/temperature profile of PMP is shown in Fig. 33 [81]. Details of the temperatures,

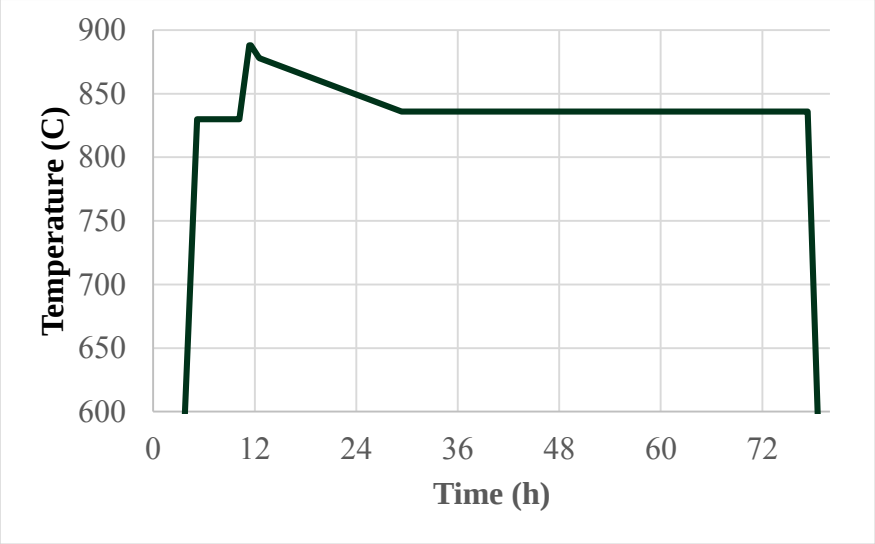

Fig. 33: Time vs. temperature profile for a standard partial melt processing heat treatment.

intermediate steps, ramp rates, and holding times vary wildly between studies but the following effects have been generally demonstrated to influence Bi-2212 processing:

1. J_c is highly dependent on the peak melt temperature and time at peak temperature [89].
2. Oxygen uptake during the slow cooling and anneal are critical to the recrystallization process and the re-formation of the Bi-2212 phase [82, 84, 90, 91].
3. Upon melting, the filamentary structure of Bi-2212/Ag multifilament wires is significantly altered [92].
4. The Bi-2212 recrystallized along the Ag interface in a well textured manner, yet the bulk within the filaments do not exhibit strong texture [85].

To elaborate upon this first point, the growth kinetics of the solid phases within the melt dictate which phases will be left after recrystallization. If the temperature remains too low, alkaline earth cuprates favorably form large solid phases which can grow to a similar scale of the filament diameter. During the recrystallization, these phases are not consumed and can occlude the entire filament, blocking transport currents. These growth dynamics are exacerbated by extending the time in melt. Additionally, if the temperature is raised too high, an alternative set of parasitic phases form, again blocking current transport in the re-crystallized conductor. In the end, a balance must be struck between the two extremes and a narrow processing window of ~4 C must be maintained for optimum performance to be achieved [93]. Immediately, this raises concerns that a large scale coil for either accelerator magnets or significant

research applications (NMR spectroscopy) would be capable of being effectively processed as typical thermal diffusion times for coils of this scale and temperature range are of the same time scale as the optimum time at peak temperature [94]. As a result, coils of Bi-2212 have the propensity to have regions that are either over or under-reacted [95, 96]. Furthermore, maintaining a temperature within 4 C on a large volume of conductor is a difficult engineering task. Both effects pose significant challenges to making Bi-2212 an engineering ready conductor.

Likewise, the slow cooling which allows O_2 to over-dope the Bi-2212 conductor reaching its optimum performance is difficult to translate from short sample windings into coil form. This is primarily due to the fact that oxygen must diffuse through insulation materials and several layers of the coil. Additionally, controlling the thermal behavior of a large coil to achieve the slow cooling rates required for PMP can be difficult as described before.

Finally, the fact that filaments merge and grow into one another during PMP is a result of several factors including the ability of liquid Bi-2212 to dissolve a small amount of Ag, the ability of Bi-2212 grains to grow through the Ag matrix, connecting filaments, and the effects of residual gas pressures within the initially isolated filaments causing the Ag matrix to creep and filaments to merge. Regardless of the mechanism, these bridged filaments have three distinct effects. In a positive sense, the merged filaments allow transport currents to flow around occlusions in a single filament. This shared transport allows Bi-2212 wires to carry high currents even though transport current is blocked in every filament by either a parasitic phase, high angle grain

boundary, or void space. Indeed, without these bridges, transport in Bi-2212 conductors would be limited to a fraction of the achieved transport to date. While this first effect is positive in nature, the remaining two effects are detractions from the potential performance of Bi-2212 conductors. The second effect of note is the fact that if superconductor is in the interstitial space of the matrix, density within the filaments has been sacrificed, reducing the current carrying capacity of the filament [92]. The final effect is that the coupled filaments increase the effective filament size of the conductor which has serious implications for ramped magnets which depend on low magnetization losses within the superconducting wires [92, 97].

Despite the challenges and possible limitations of PMP, it remains the dominant processing route for Bi-2212 conductors. Several variants to PMP have been investigated and those pertinent to enhancing texture or improving density are reported in the sections that follow.

4.1.2 Isothermal Melt Processing

Isothermal Melt Processing (IMP) is a variation of PMP in which the temperature of a wire or coil is held constant and the partial pressure of O_2 is varied, thereby changing the melting temperature of the Bi-2212 to below that of the furnace. The melt is continued for an appropriate time, then the O_2 partial pressure is again changed in order to pull the conductor out of the melt. While comparable results to PMP were achieved through this process, controlling the local atmosphere of O_2 with sufficient precision to achieve the melt was a limitation to scaling IMP to coils [98-102].

4.1.3 Magnetic Melt Processing

Magnetic Melt Processing (MMP) is a direct variant of the PMP described in detail above. However, while the PMP is taking place, coils or wires are subjected to a significant background magnetic field. By orienting the magnetic field normal to the axis of the conductor (in either short straight samples or coil geometries), the presumption was that during recrystallization, the anisotropic Bi-2212 particles would preferentially orient themselves with their conducting planes orthogonal to the applied field. By aligning the bulk of these particles within the filament, HAGB may be reduced and transport properties improved. In actuality, the enhancements seen through this process were on the order of a 10% increase in J_c. Given the immense overhead and difficulty scaling the process for coil applications, this method of processing was not further investigated [66, 67].

4.1.4 Split Melt Processing/React Wind Sinter

Unlike the previous processing approaches, split melt processing (SMP) and react wind sinter (RWS) were conceived solely to simplify coil processing. In RWS, conductors were partially melted as described previously while still on the spool or in short straight lengths. Instead of continuing the full heat treatment, RWS conductors are quenched before the typical 836 C sintering step at an intermediate temperature. The coil or final geometry is then wound. Invariably, this led to fractures in the brittle superconducting filaments. However, after winding, the coils were subjected to the remainder of the heat treatment, resuming at the same temperature at which they were previously quenched. The results of such processing were more promising than one may

initially presume, actually exceeding the PMP results by up to 40% in some experiments [86]. Results from this heat treatment method indicated that there is a mechanism for "healing" micro fractured Bi-2212 interconnections after the peak melt temperature. This is most likely due to the re-melting of the mixture that results from quenching/cooling the reaction prior to recrystallization of the Bi-2212 phase.

4.2 Sintering Heat Treatment

As previously stated, the melt processing of Bi-2212 is carried out to connect and texture the Bi-2212 grains within a filamentary structure. In OPIT conductors where core densities typically exhibit ~70% theoretical density in the as drawn condition and near random texture, it is highly important to densify and align the particle grains [103]. However, if Bi-2212 were already textured for maximum transport properties and at near full density, the requirement to fully melt the superconducting cores appears to be relaxed as the only obstacle to transport current flow is the lack of connection between the superconducting grains. If one were able to grow the grains within a core in a manner that increased their contact area and locally merged adjoining grains, there would theoretically be no distinction between this method and a melt processing method.

Indeed, single crystal studies [104] demonstrated that transport properties might be recovered when a crystal of Bi-2212 was cleaved along its ab planes, then subsequently sintered below melt temperature whereby the grains might grow and connect through solid phase diffusion. This approach is both unique to the textured powder conductor process and could potentially lessen the stringent requirements on Bi-2212 conductor processing. The benefit of this final statement may be seen by

comparing the Bi-2212 and Nb_3Sn internal Sn reaction formation heat treatments [105]. Nb_3Sn coils fabricated with internal Sn conductor are subjected to a long time, multistep diffusion based process which results in the high performance of state of the art RRP internal Sn conductors. While these heat treatments are long, often requiring up to 2 weeks for the completion of meter scale research coils, they are by no means cumbersome enough or expensive enough to limit production of full length accelerator magnets. Additionally, these heat treatments are sensitive to fluctuations on the order of 10 – 15 C, not the 2 - 4 C temperature ranges required by Bi-2212 conductors [106-108].

Due to the specific benefits of the textured powder conductor, namely the high density and pre-achieved texture, a study of the effects of sintering on high density, textured bulks of Bi-2212 was not prevalent within the literature. An independent study of sintering parameters on textured Bi-2212 bulks (pellets) and wires made by the textured powder process were carried out in this work. Three measureable parameters were of interest in this investigation, achieved density, achieved grain size, and transport current density. The results of the density and grain size investigations of pellets, stamped bars, and wires subjected to sintering heat treatments will be presented here while the transport properties will be discussed in a following chapter.

4.2.1 Texture and Density Evolution in Pellets

As pellets were chronologically the first samples to be investigated for texture and provided a simple test bed for x-ray diffraction studies, they were also the first samples subjected to a systematic study of density and texture evolution during sintering. Pellets were prepared in the same manner as described in the previous chapters and were

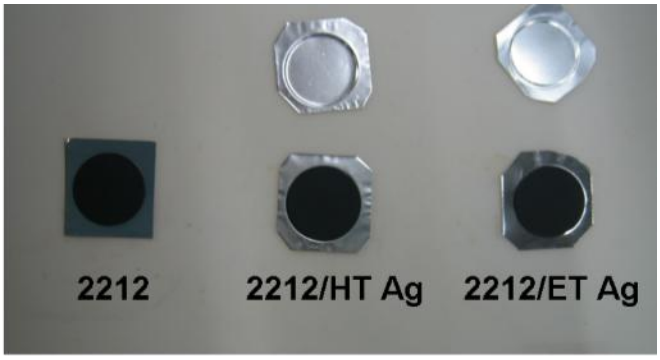

Fig. 34: Pressed pellets on Ag boats with different Ag preparations. From left to right these are as received Ag, Annealed Ag, and Etched + Annealed Ag.

characterized for texture by SEM imaging and XRD. Samples were heat treated on alumina boats with an Ag foil base to prevent interaction between the boat and Bi-2212 and provide an ease of handling during processing. Fig. 34 [80] shows these pellets prior to being loaded into the furnace. A general heat treatment profile was used and shown in Fig. 35 [81] with the peak temperature and time at peak temperature as the variables in different studies. All samples were heat treated in 1 atm of flowing O_2.

Table 9 [80] provides a synopsis of the pellets studied in this work with the time, temperature, initial density, final density, typical grain sizes after heat treatment and texture parameter of the heat treated pellets presented. Dimensional measurements were carried out by averaging several measurements from a set of calipers. This was the most precise measurement technique available that did not risk significantly damaging the pellets before or after heat treatment. Mass measurements were carried out on a Mettler P1200 scale with a resolution of 10 mg.

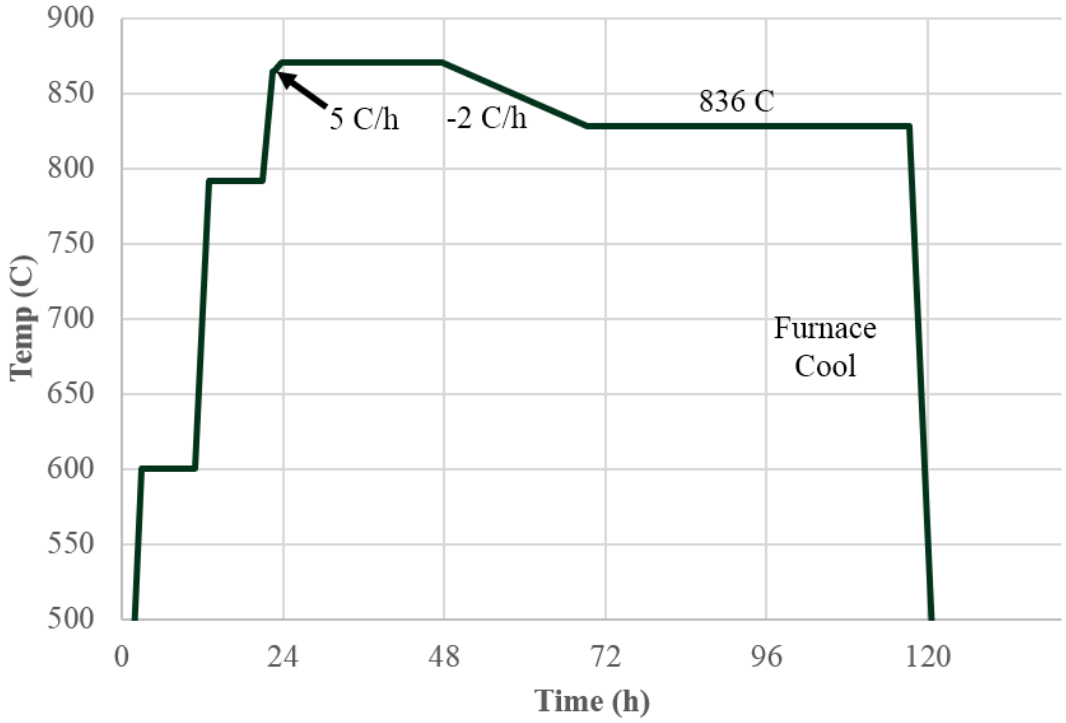

Fig. 35: Time vs. Temperature profile of Sintering HT's. Peak temperature and time at Peak temperature were both variables.

From the results presented in Table 9, it is evident that increasing time and temperature resulted in higher densities and a greater degree of texture. An optimum sintering time of ~24 h was found to maximize the grain sizes. Continuing beyond this threshold resulted in little or no additional densification or texture enhancement. The overall behavior of the sintered samples agreed with initial predictions that solid phase diffusion would be the dominant mechanism for solidifying and densifying the Bi-2212 pellets and this process would strictly behave as an exponential dependent on time and temperature.

Table 9: 20 Ksi Compacted Pellets With Texture Evolution Due to Sintering Heat Treatments [52, 80].

Heat Treatment		Density	Avg. Grain Size in ab plane	Texture Parameter
Temp (C)	Time (h)	g/cm^3	μm	τ
Green Pellet	0	3.98	1.20	0.68
800	2	--	1.39	0.69
835	2	4.24	1.55	0.74
835	24	4.37	1.79	0.75
865	24	5.13	3.55	0.80
875	2	5.24	2.69	0.84
875	24	6.32	4.31	0.89

While the macroscopic measurements shed light on the overall behavior of the sintering process, it was worthwhile to examine the microsctructure of the pellets through a series of SEM investigations of their surfaces. Fig. 36a through Fig. 36d [80] show samples sintered at increasing times and temperatures and demonstrate the grain growth achieved during the sintering process. Additionally, EDS data associated with these images did not show significant growth of parasitic alkaline earth cuprates, Bi-2201 or other parasitic phases and the grain boundaries of the samples appeared to remain free of occluding phases. Finally, these data also showed a necking and apparent connection between grains which were interpreted as a strong indication of inter grain connectivity.

4.2.2 Texture and Density Evolution in Coined Bars

Following the successful demonstration of grain grown in the pellet heat treatment studies, a series of coined rods were fabricated in an effort to produce a geometry that was amenable to measuring transport properties of the bulk Bi-2212 in the

as sintered condition. These rods were coined in the 1 x 1 x 150 mm^3 die set previously described. Initially, these samples were attempted to be encased in Ag foils to provide a normal conductor that could serve as an interface for soldering attempts as well as a stabilizer and boat material during heat treatment. Fig. 37 shows one of these "cigarette" style conductors after transport measurement testing.

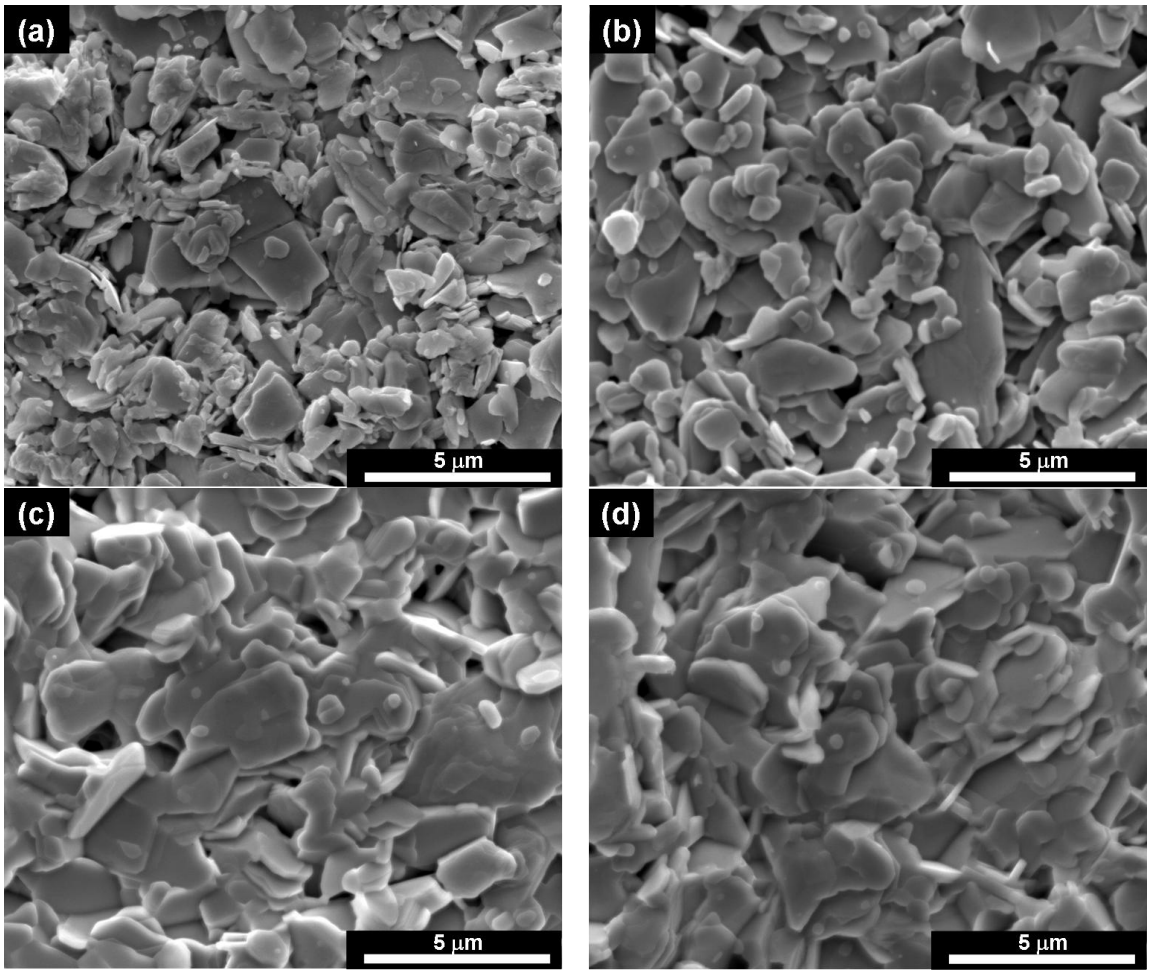

Fig. 36: Surface of textured pellets after various heat treatments of a.) 800 C/2 h b.) 835 C/24 h c.) 865 C/24 h and d.) 875 C/2 h.

Fig. 37: Encased sample from early transport measurement attempts with sintered 1 mm x 1 mm bar encased in a coined Ag foil.

Ultimately, these samples were intended to be characterized with critical current measurements at the NHMFL in Tallahassee, FL. However, some pieces of the samples either broke away from the larger, testable pieces or were sacrificed for microsctructure examination. A sample heat treated at a peak temperature of 870 C for 24 h is shown in transverse section in Fig. 38. From this image, it is clear that significant grain growth has taken place and that parasitic phases, while present, are not growing without limit during the sintering process. Through image analysis, it was also possible to estimate the porosity of the sample and thereby the density of the coined bar. It was found that the density of the rod increased from 4.2 g/cm^3 to 5.6 g/cm^3 during heat treatment. It was evident that the density enhancement came primarily from a thinning of the sample in the vertical direction which also coincided with the imparted c-axis texture. Transport properties and critical temperature data of similar samples will be presented later.

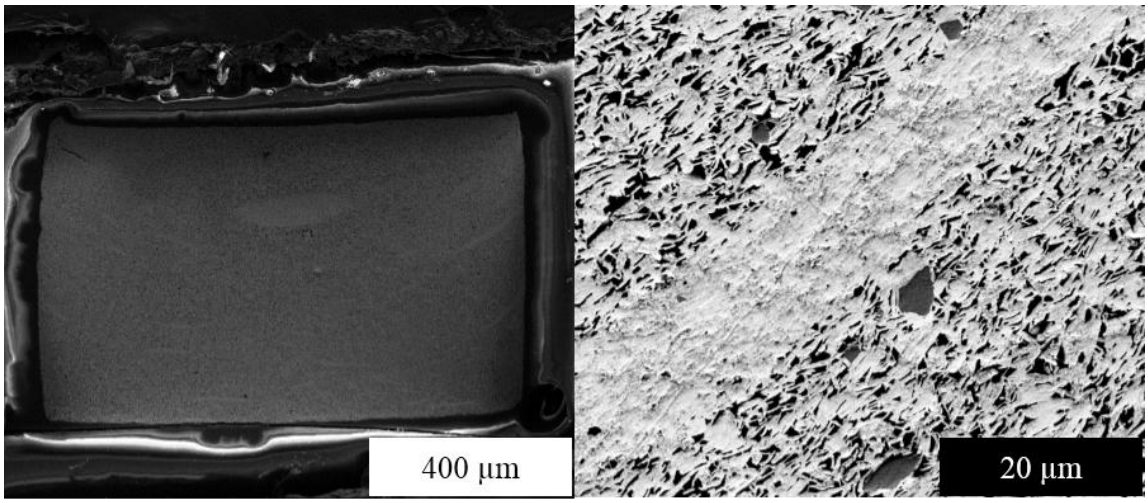

Fig. 38: Transverse section of a 1 mm x 1 mm Bi-2212 bar coined at 20 ksi and sintered for 24 h at 870 C. In image at right, white is Bi-2212, light grey are AEC's, and black is porosity. For the entire sample, the maximum AEC observed was 49 μm^2 and AEC's only accounted for 2% of the transverse area.

4.2.3 Texture and Density Evolution in Wires

Monocore wires fabricated by the method outlined in Chapter 2 were also evaluated for their texture and density evolution during heat treatment. As mentioned previously, samples were drawn on two schedules from two different billets.to multiple sizes.

After copper removal, sintering and partial melt processing of these conductors was carried out as previously described. Samples were prepared as 2" (5 cm) long straight samples that were tested at TAMU. The results of those tests will be the focus of the following chapter and will not be elaborated upon here. All samples were co-heat treated with an OPIT conductor previously acquired from Oxford Superconductor Technologies as a control.

Results from the sintering heat treatment studies were consistent with the previously discussed pellet studies and coined rod studies and a representative image is shown in Fig. 39 [81] which displays the lack of parasitic phase growth and high density of the textured powder cores.

4.2.4 Fine Gauge Wires

As previously described in Chapter 2, a large quantity of very fine 0.52 and 1.10 mm diameter wires were also produced in the study. Chronologically, these samples were heat treated after the larger samples had undergone a rigorous sintering/partial

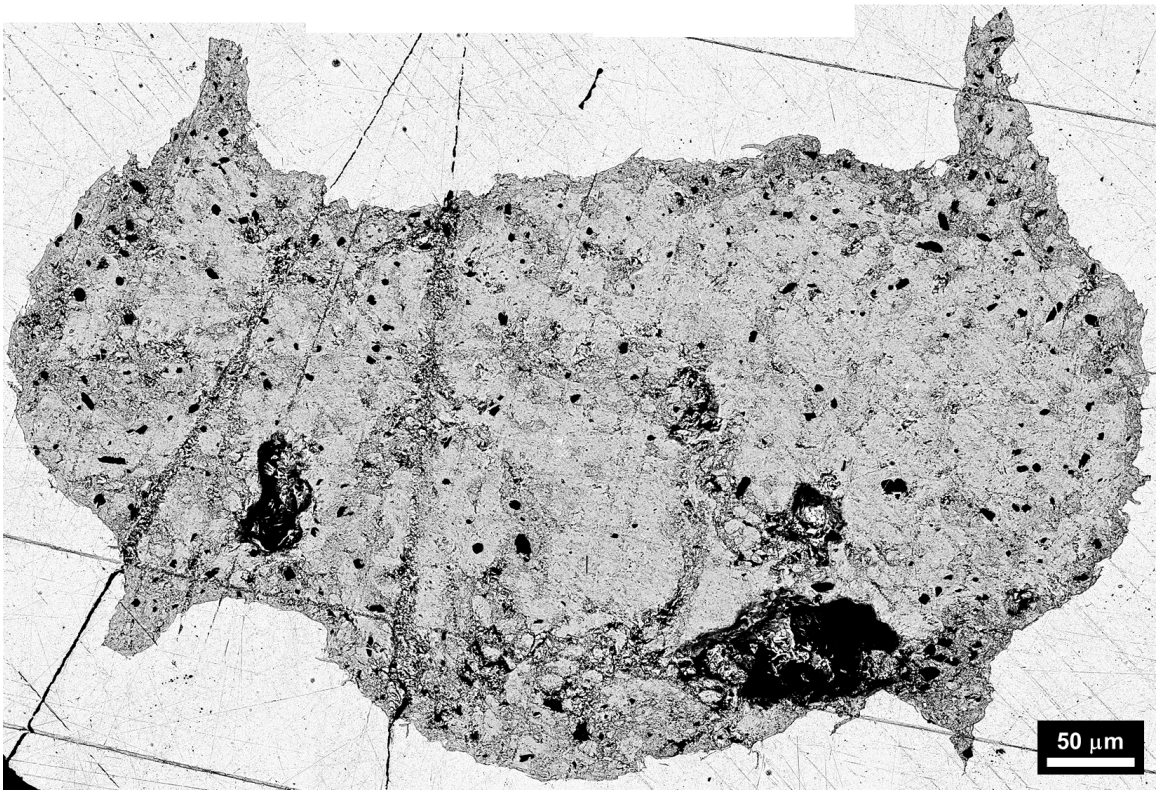

Fig. 39: Transverse section of TPC sintered for 24 h at 875 C. Due to the density and hardness of the Bi-2212 tearaouts were common during the polishing process. No large AEC's are present in the sample and void space is attributed solely to tearouts during sample preparation.

melting heat treatment study. In the first round of heat treatments on these samples, sintering heat treatments were used in an attempt to achieve exceptional transport properties. While temperature control was achieved in an identical manner to the previous sintering work, these samples demonstrated a remarkable and discouraging phenomenon: Bi-2212 crystals appeared to grow out of the Ag sheath. Additionally, seams were found in the Ag matrix which had apparently split due to trapped gases within the monocore element. Both of these effects can be seen in Fig. 40 and Fig. 41

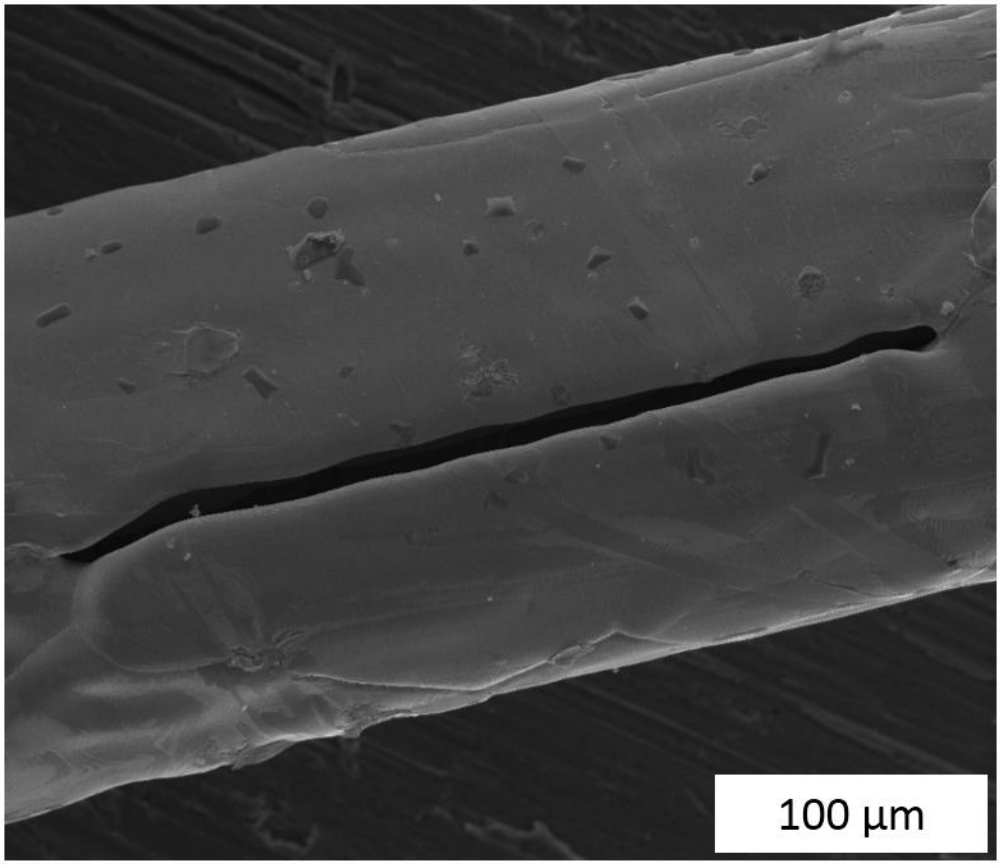

Fig. 40: Seam splitting Ag matrix during sintering HT of a fine wire conductor. This effect is presumably due to trapped gases within the monocore that build up pressure during heat treatment and cause the Ag to rupture.

[81]. Despite the higher starting density, the remaining Ag in these conductors was too thin for subsequent heat treating of the monocores and these conductors were of no additional scientific interest with no samples remaining preserved for what would most likely be a futile and expensive transport property measurement.

4.3 Partial Melt Heat Treatment

As the Bi-2212 was expected to melt at ~880 C, samples heat treated at 881 C, and 888 C were expected to be partially melted. All samples partially melted in this study were subjected to the heat treatment time vs. temperature profile shown in Fig. 33.

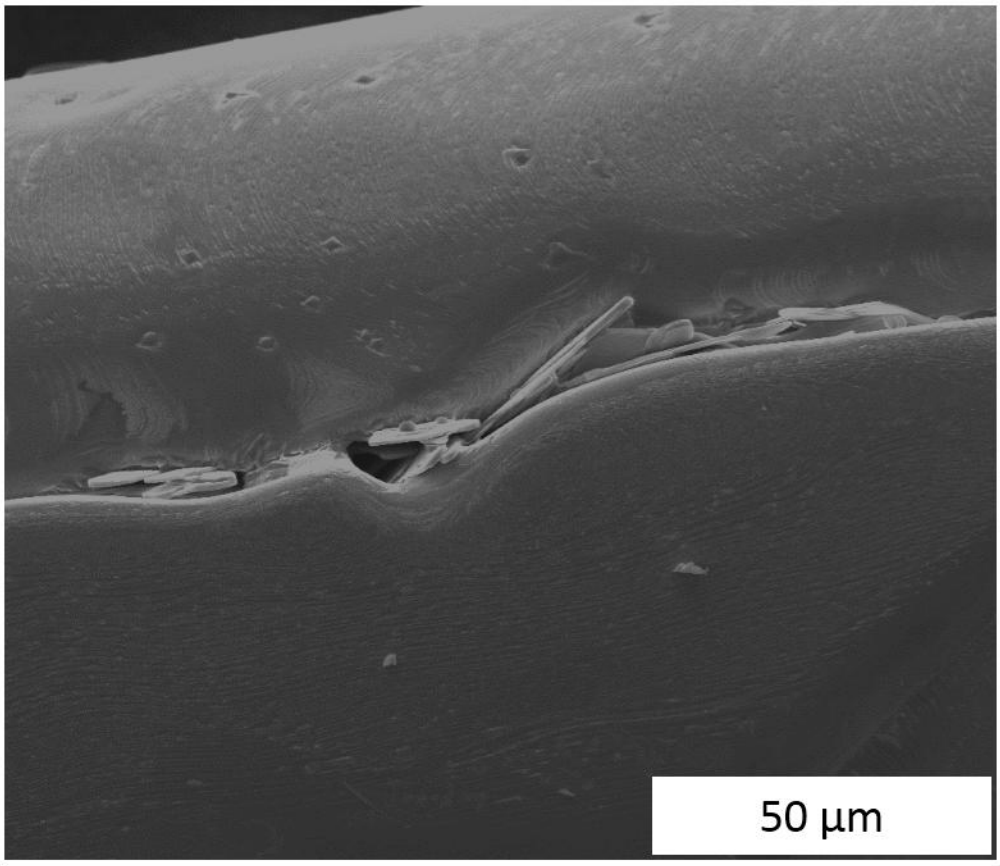

Fig. 41: Bi-2212 growing through a very fine Ag wire.

Fig. 42: Lindberg furnace with quartz tube for heat treatment processing.

One of two Lindberg furnaces were used to perform the partial melt heat treatments. These furnaces were fitted with 1" OD quartz process tubes that were custom made at the TAMU Chemistry glass shop. Vacuum tight seals were employed to provide complete atmosphere control, and the setup is shown in Fig. 42. Thermocouples were placed as close to the samples as possible to ensure a very precise control of the furnace temperature and excellent data logging during heat treatment. When combined with a Ni 200 boat, the temperature profile was flat within 1 C over the entire Ni boat, creating a sufficient isotherm. Baffles were also utilized to limit radiative losses in the small bore furnaces.

Regarding peak temperature selection, the 881 C sample was investigated as a potential "liquid assisted sinter" with hopes that some level of texture may be preserved

through this processing while the 888 C processed samples were anticipated to conform with the well developed concepts present in the literature [51, 86, 92, 93]. Samples with roughly 1mm OD (Ag) were selected in this initial study from Billet IV-2b, which had a Bi-2212 core roughly 650 μm x 300 μm.

Samples from this billet subjected to the partial melt heat treatments exhibited an extremely destructive behavior. Primarily, the powder cores were found to leak out of the Ag crimped ends of the conductor. This effect was much more pronounced in the TPC conductors than in the OPIT wires, as can be seen in Fig. 43 which compares a pre and post reacted sample. Aside from the apparent end leakage, a seam splitting

Fig. 43: Left: Pre-heat treated samples on Ni 200 boat. The central sample is an OPIT control. Right: Samples after heat treatment showing core leakage of TPC samples.

phenomenon also appeared. Both of these effects were a combination of two issues. The first and dominant concern was the buildup of gases within the conductor which was alluded to in part in Section 4.2.4. In those samples, it was apparent that the Ag was splitting along longitudinal seams which subsequently destroyed the integrity of the wire. A second, less obvious cause of the void coalescence was the relatively large size of the Bi-2212 filament. Due to the surface tension of the liquid, it was preferential for large voids to agglomerate in the melted samples. A subsequent search of the literature found that these effects were common for >150 um filaments, even in a multifilament, low core density conductor [109]

Despite the evident leakage from the TPC monocores, samples were preserved for transport measurements that were subsequently carried out and are described in the following chapter.

5. CONDUCTOR CHARACTERIZATION

5.1 Introduction

The ultimate figure of merit for any superconducting wire is the critical current it carries under operational field and temperature conditions. While the current in amperes that a wire carries is of significant importance, it is an insufficient parameter to compare superconducting wires and tapes for magnet applications where space is at a premium. Instead, the transport current per unit of cross sectional area, or engineering current density (J_e) is the figure of merit for magnet conductors. While J_e is the most critical parameter for applications, it does a poor job of relating the fundamental properties of the superconducting material. For this purpose, the critical current density of the superconductor, J_c, is often chosen as the figure of merit for fundamental work on superconducting materials. J_c is specifically defined here as the critical current of a superconducting composite per unit of superconductor cross sectional area. The comparison of J_c in different composite conductors provides insight into whether the superconductor is optimized in the composite relative to some benchmarked standard, typically a best of class sample <1 m long or bulk material properties.

Bi-2212 has its greatest merit as a low temperature, high field conductor, and the characterization of the TPC's fabricated and processed as described in the preceding chapters was focused on the properties of the conductors immersed in boiling liquid helium (4.2 K) and in background magnetic fields up to 5 T. Aside from transport

current measurements, critical temperature measurements were also carried out on select TPC samples.

5.1.1 Basics of Short Sample Measurement

Transport current measurements typically take place in one of two fashions for superconducting wires. The first are short straight samples (short samples) which are typically less than about 8 cm in length. These samples are short enough to fit within the bore of widely available superconducting magnets which are used to apply the background fields used in testing, yet they are long enough to allow for adequate voltage tap spacing which is usually a minimum of 1 cm. Barrel samples which accommodate up to 1 m lengths of conductor are also used, however these are usually applied to materials with straightforward heat treatments (Nb_3Sn, MgB_2) or wires that require no heat treatment at all (NbTi). Additionally, the geometry of these coils induces significant self -field corrections and requires significant tooling to be accomplished reliably. Due to limited availability of conductors as listed in Chapter 3, straight, 5 cm long samples were the focus of the present work.

If one is evaluating either fundamental properties of the superconducting material by comparing J_c's or engineering properties by determining J_e, the pertinent measurement always begins with the evaluation of a wire's critical current. A transport critical current is evaluated by monitoring the voltage across a known length of a representative portion of the wire sample while ramping a current source. While superconducting, the wire will generate no appreciable voltage away from the current supplying joints (these joints inevitably generate some losses as current is required to

transfer from a normal lead, typically Cu, through the normal conductor of the superconducting composite wire). As the current ramps, the J_c of the superconducting components is approached and subsequently surpassed, pushing the superconducting material into its normal state. This is accompanied by an immediate current share between the surrounding matrix material and the now quite resistive superconductor which induces a voltage across the sample. This transition between superconducting and normal states may also be induced by holding a fixed current and increasing either the temperature or magnetic field to induce a similar transition, although these methods are less prevalent as they require much more complicated equipment to achieve the same level of precision as a ramped current measurement. Naively, one would expect the transition to take place in a stepwise function, like that shown in Fig. 44, with an instantaneous transition from a zero voltage state to that of a finite voltage from the transition to a resistive medium. In this simple view, the critical current would be found from the vertical line that defines the step. However, nature is rarely as ideal as one would naively hope, and the superconducting transition is no exception. Due to slightly different material properties, varying cross sectional areas of individual filaments, and random temperature or magnetic field fluctuations, the onset of voltage in the superconducting to normal transition is significantly broader than one would expect. Instead of a step function, the transition from superconducting to normal phases appears as a power law rise in voltage characterized by $V \alpha (I/Ic)^n$, where I_c is the critical current, I is a current near I_c (typically within 10%), and n is the index of the transition. The V vs. I behavior of such a transition is shown in Fig. 45. In this case, the critical parameter,

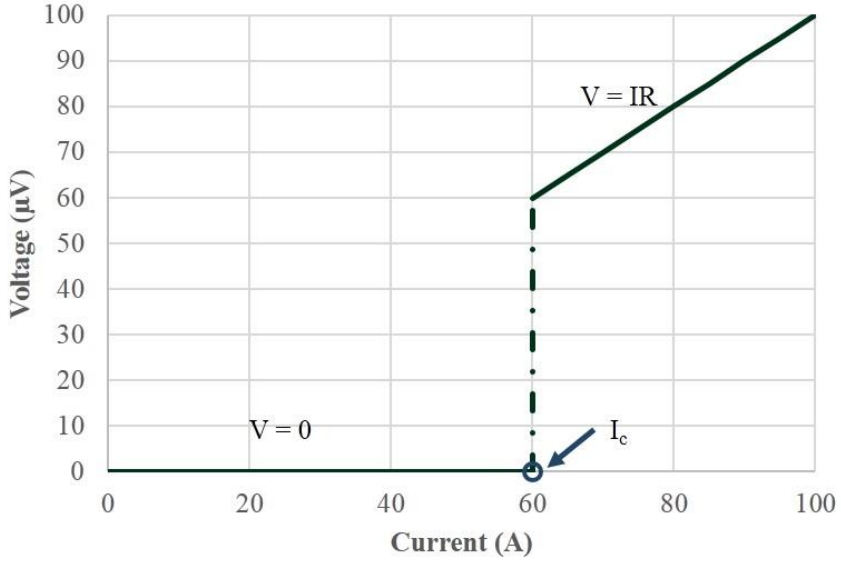

Fig. 44: Stepwise V vs. I curve for a superconductor that uniformly and instantly transitions to the resistive state.

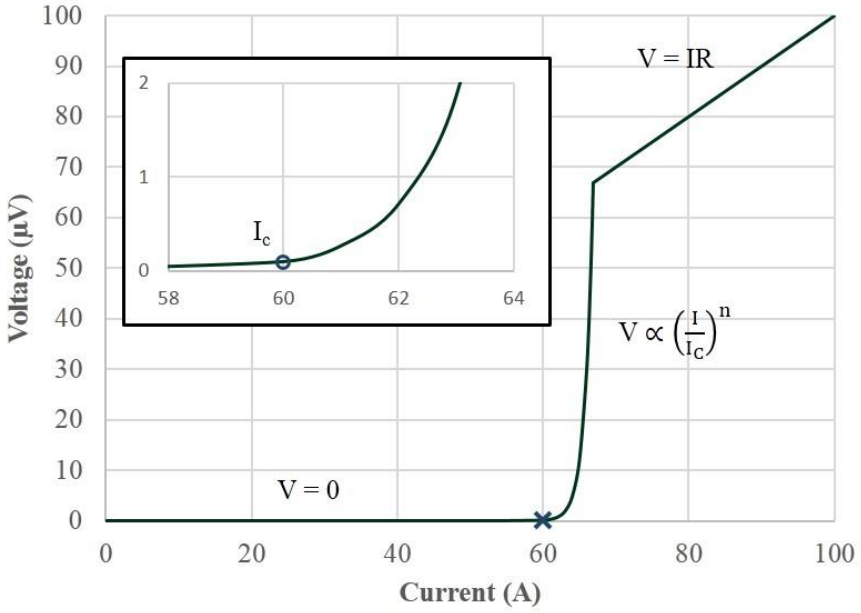

Fig. 45: Idealized V vs. I curve with a finite n value.

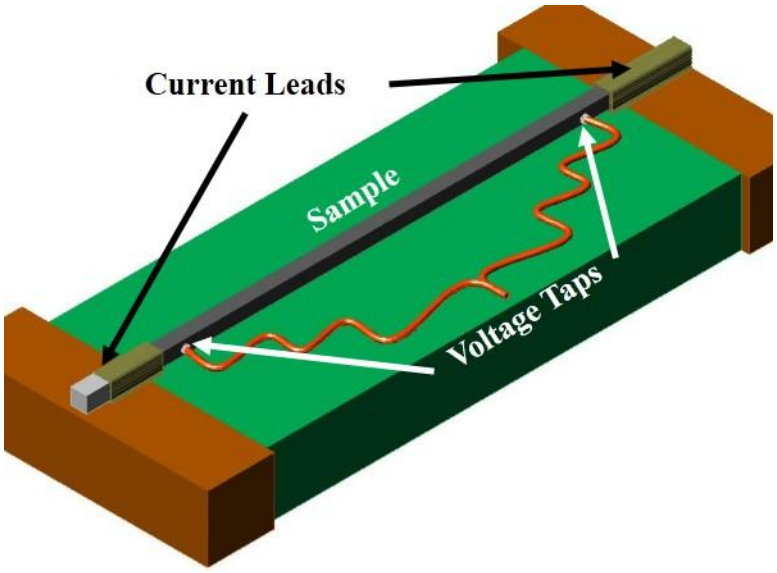

Fig. 46: Principle of a 4 point voltage measurement demonstrated on a 1 mm x 1 mm Bi-2212 coined bar.

I_c, is no longer clear and could be indicated at any arbitrary point along the transition as a mixed superconducting/normal state exists within the wire. Due to the arbitrary nature of assigning a practical value for I_c, a series of conventions have been adopted within the field. Typically, Bi-2212 critical currents are reported at a 1.0 μV/cm threshold. This value is also used in MgB_2, YBCO, and other emerging, high temperature materials. However, magnet engineers have previously used a 0.1 μV/cm criterion for LTS materials. The difference in heat generation between the two criterion (at constant current) is an order of magnitude greater for the HTS materials and great care must be taken when specifying HTS conductors and designing compatible cryogenic systems for magnets based on these conductors. The 1.0 μV/cm criterion is also driven by pragmatic concerns, as short straight samples of the HTS conductors typically allow for voltage tap

spacing on the order of 1 cm and typical fast voltage meters are accurate to the nV level, setting a minimum threshold for quench detection at 1 μV/cm levels.

Experimentally determining I_c is accomplished through a 4 point voltage measurement as sketched in Fig. 46 [40]. Current is applied through a pair of leads at either end of a sample and the voltage is simultaneously measured across the middle pair of voltage taps. By measuring the distance between the taps, the electric field between the taps may be readily calculated, making for a fair comparison between samples with inevitably differing tap lengths. Currents are typically monitored by measuring the voltage across a calibrated shunt and calculating the delivered current. This decouples the measurement somewhat from variations in the delivery of the current from the power supply and is particularly important when a digital supply is used.

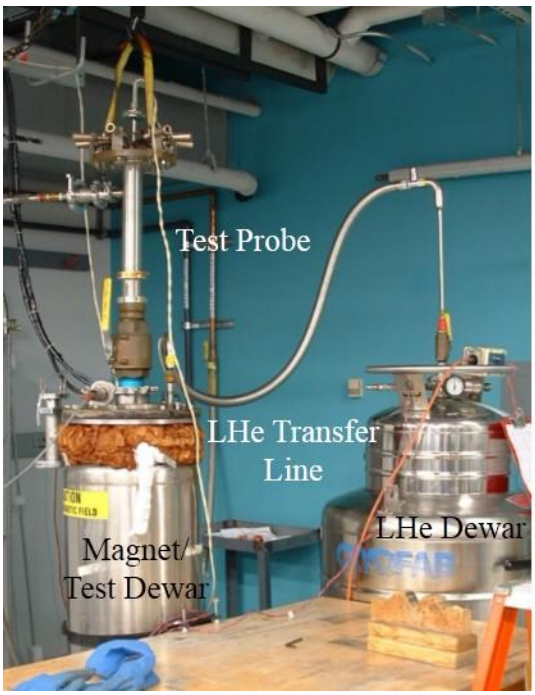

Fig. 47: Test facility at the NHMFL.

Fig. 48: Test facilities at TAMU under test conditions.

5.2 Experimental Setup

Transport measurements were carried out at both the NHMFL and TAMU with different experimental configurations, although capabilities of the two facilities are very similar (0 – 5 T variable magnetic field, 4.2 K pool boiling LHe, and 1 kA current supply). The apparatus at the NHMFL is shown in Fig. 47 while the TAMU facility, kindly provided by Dr. Naugle's laboratory, is shown in Fig. 48. In both cases, samples were limited to 5 cm lengths.

Generally, testing was broken into two distinct phases. The first phase was carried out on the coined and sintered 1 mm x 1mm Bi-2212 bars. Transport measurements took place at NHMFL while a very limited study of the critical

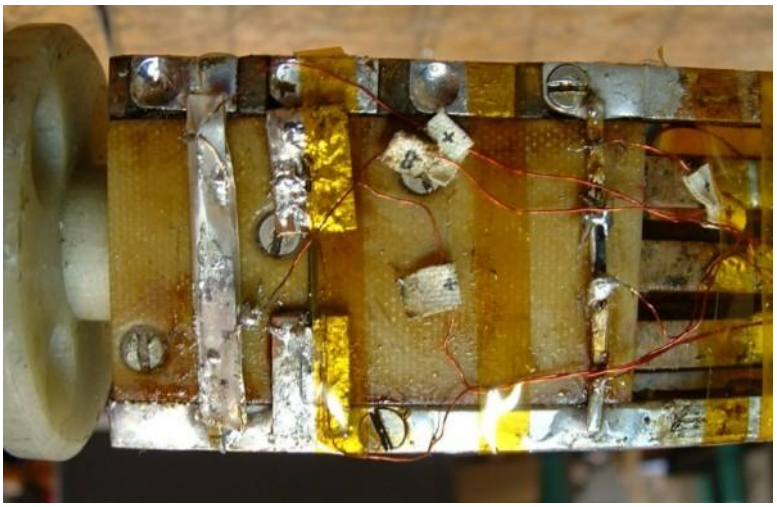

Fig. 49: NHMFL short sample testing probe with a cigarette style sample at left, bare bridge center, and open faced sample at right.

temperature was performed on a PPMS at TAMU. A second phase of transport measurement testing took place at TAMU and focused on wire samples.

5.2.1 Transport Properties of Coined Bars

As previously mentioned, sintered 1 mm x 1 mm square bars were tested at the NHMFL on the probe shown in Fig. 49. These tests were conducted in collaboration with ASC/NHMFL staff. Two specific sample geometries were used in the study. The first is shown in Fig. 49 which depicts a "cigarette" rolled Bi-2212/Ag composite which was fabricated by first coining the Bi-2212 bar, then stamping an Ag foil into a "U"-shaped cup, followed by crimping the top of the foil around the Bi-2212 bar. These crude wires were then sintered as described in previous chapters.

The second sample geometry was a bare bridge of Bi-2212. These samples were supported on either side during reaction bake by a pair of Ag foils that isolated the Bi-

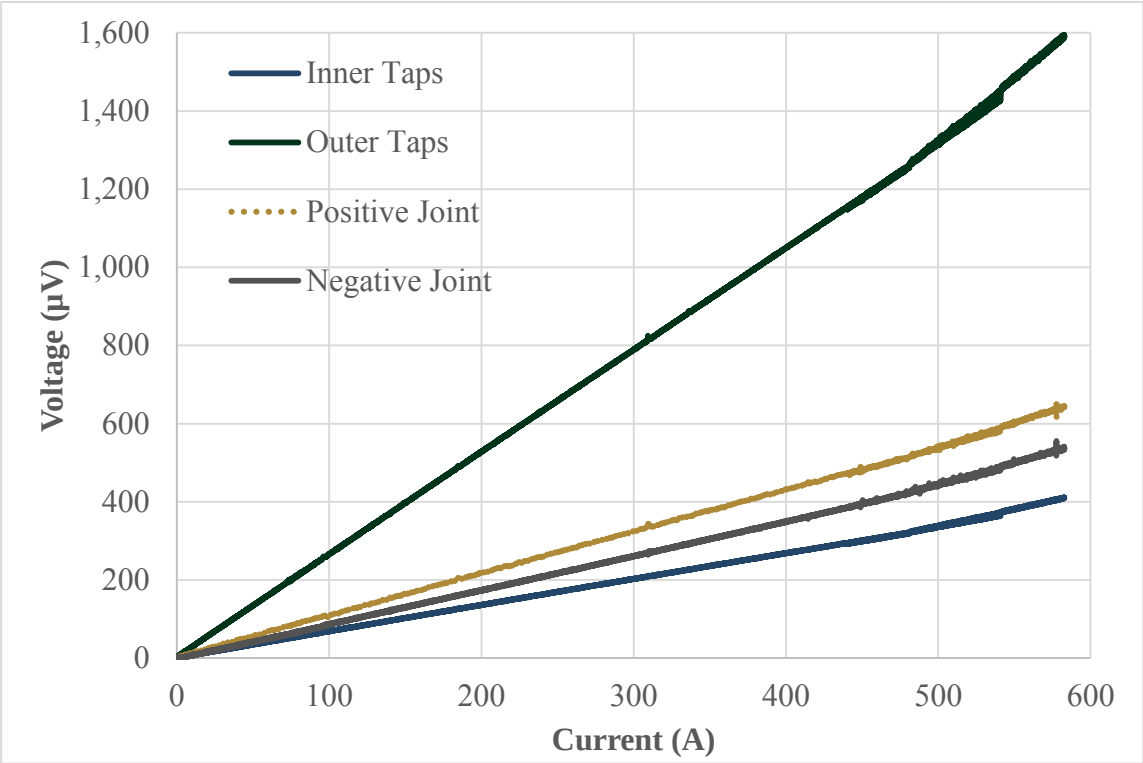

Fig. 50: V vs. I curve for a "cigarette" rolled sample. The linear nature of the curve indicates no appreciable current is being carried through the superconductor. Inner taps are across the interior of the sample for a traditional 4 point measurement. Outer taps are across the entire sample, and the joint taps are the voltages across the positive and negative joints respectively.

2212 from the alumina furnace boat. Additionally, the Ag was intended to fuse to the Bi-2212, allowing a current connection to be made.

Two rounds of testing took place. In the first round, only the “cigarette” rolled samples were tested. A typical V – I curve for one of these conductors is shown in Fig. 50 and the results of the first round of testing are summarized in Table 10. The linear nature at all currents of the V – I curve was a strong indication that the superconductor was not acting as a zero resistance current path. While discouraging, these data were not conclusive indications of a poor performance of the superconductor as a poor interface

between the Bi-2212 and Ag components could have resulted in a large resistance between the superconductor and Ag.

Table 10: Results of First Round of Short Sample Measurements. All Bi-2212 was Coined at a Pressure of 20 ksi.

Sample	Sintering T_{max}/Time	Measured Resistance (μΩ)
I-8	870 C, 24 h	0.11
I-13	860 C, 24 h	0.76
I-14	860 C, 24 h	0.18
I-15	860 C,24 h	1.00

To clarify whether the underlying effect was the result of poor superconducting properties or an inadequate transfer of current to the superconductor, a new series of samples were fabricated. Again, "cigarette" rolled samples were created with an open top geometry and additional, open bridge samples were also heat treated. The open top samples were subsequently filled with an Indium based solder which wetted well to the Ag. By pooling the solder around the Bi-2212 component, the superconductor was surrounded on four sides. As indium contracts more than Bi-2212 upon cooling, this guaranteed at least a mechanical "clamping" joint between the Bi-2212 and Ag current leads. This geometry also allowed for voltage taps to be placed in contact with the Bi-2212 components. However, solders do not wet to Bi-2212 well, so voltage taps could not be directly attached to the oxide component in this geometry.

The second sample are the open bridge samples shown mounted to the probe in Fig. 49. Samples were sandwiched between Cu blocks pre-tinned with an In rich solder. The total encapsulation of the Bi-2212 rod was again intended to act as a clamped

current joint. Unlike the previous cigarette rolled samples, the topography of these samples allowed for voltage taps to be twisted around the bars, providing a contact for voltage measurements without relying on solder. As an aside, these samples were incredibly delicate, often fracturing irreparably during handling, soldering, or due to pressure applied during cool down by the voltage taps.

Unfortunately, the bare bridge samples were unable to be adequately tested upon cool down as the In was found to release from the Bi-2212, resulting in kΩ resistances across the bridge. No samples of the bare bridge were able to be reliable tested, and this most robust attempt at measuring the transport properties of the bare superconductor were unfruitful. Results of the indium filled "cigarette" rolled samples are presented in Table 11. Again, these data indicated that the samples exhibited a finite resistance even at very low currents. While much more robust than the previous efforts, these samples still had less than convincing current connections to the Bi-2212 component as evinced by the propensity of the In to release from the bare bridge samples.

Table 11: Second Round of Short Sample Testing. All Bars Were Coined at 20 ksi and Heat Treated at 870 C for 24 h.

Sample	Applied Field (T)	Measured Resistance (μΩ)
I-8	5	0.96
II-5	0	1.66
II-5	5	4.42
I-4	0	0.36
I-4	5	0.68

5.2.2 Critical Temperature of Sintered, Coined Rods

After the previous failures to adequately characterize the transport properties of the Bi-2212 coined rods, a small sample was submitted for characterization on a physical properties measurement system (PPMS) housed within Dr. Naugle's laboratory. This device has a fully instrumented suite with a variable temperature cryostat, 9 T magnet, and mA current supply. As only μA currents were required for T_c measurements, a robust low current lead was developed. The sintered rods of Bi-2212 were coated with ~10 nm of a Pt/Pd alloy through a sputtering process usually applied to SEM samples. This alloy interface was intimately adhered to the sample surface and In solders wetted

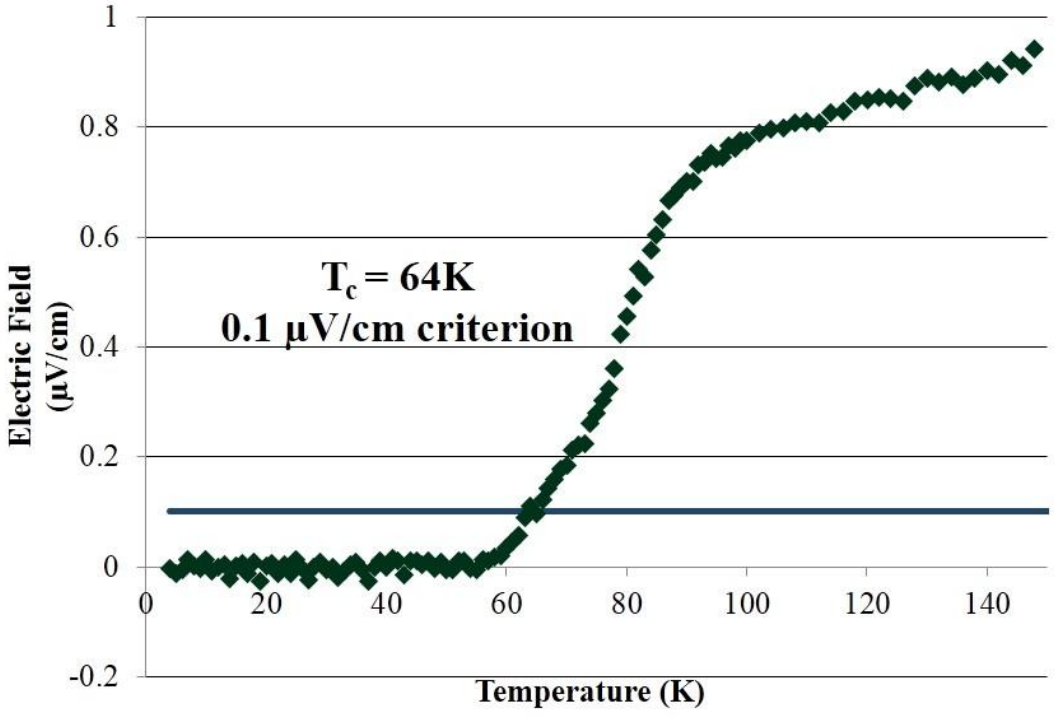

Fig. 51: V vs. T data for a sintered 1 mm x 1 mm coined bar. 1 uA of current was applied to the sample.

readily to the alloy. In this manner, 4 leads, 2 for current input, 2 for voltage measurement, were applied to the sample.

Results of the T_c measurement are shown in Fig. 51 and show a very broad transition from the zero resistance state to normal behavior. These data conclusively showed that the sintered samples were acting as a superconductor, albeit the broad transition indicated a lack of phase homogeneity across the sample. Caution should be taken before reading more into this T_c data, as only a single sample was analyzed and the use of transport currents in a macroscopic sample can be unreliable as only the lowest resistance path is sampled which is in stark contrast to magnetization measurements that sample the properties of the conductor on a much finer scale (typically on the order of a coherence length). Further analysis of this sample via microscopy showed an apparent density of only around 90% after sintering. The residual porosity in the conductor was taken as an indication that connectivity between grains needed to be improved for significant transport currents to be achieved. As such the paradigm of sintering a 60% dense sample was abandoned in favor of developing a wire-like conductor based upon the textured powder process that would exhibit a high quality Bi-2212/Ag interface for reliable transport current measurements.

5.2.3 Transport Properties of Monocore TPC's and OPIT Wires

Testing of the monocore TPC wires and control OPIT conductors took place exclusively at TAMU. To enable these tests, a new sample holder was fabricated to provide consistent testing of the samples at currents up to 1 kA in background magnetic fields of 5 T. The assembled probe and mounted sample are shown in Fig. 52. To

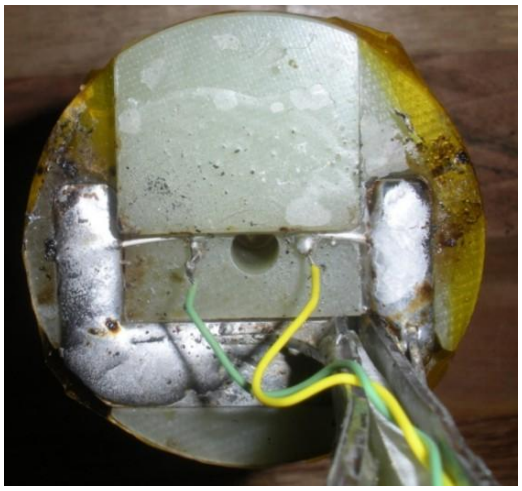

Fig. 52: G10 short sample holder for testing at TAMU. The magnetic field was applied such that the Lorentz forces acting on the sample were directed toward the supporting ledge.

prevent Lorentz forces from degrading the wires, the direction of the magnetic field in the probe was applied in such a way that it was guaranteed to always push the sample toward the supporting ledge shown on the probe. For curved samples, wax was used to fill the void space and prevent high stress points from forming during testing.

While the facilities at TAMU were comparable to those at NHMFL, the sampling rate of the data acquisition system at TAMU was considerably lower (~3 Hz) than the NHMFL data acquisition system. This difference did not affect the veracity of the tests, but accounts for the aesthetic change in the data between the TAMU and NHMFL tests. The only scientific difference between the two facilities was the slower rate of quench detection at TAMU which ultimately resulted in the destructive loss of some samples after they had already contributed to the volume of data.

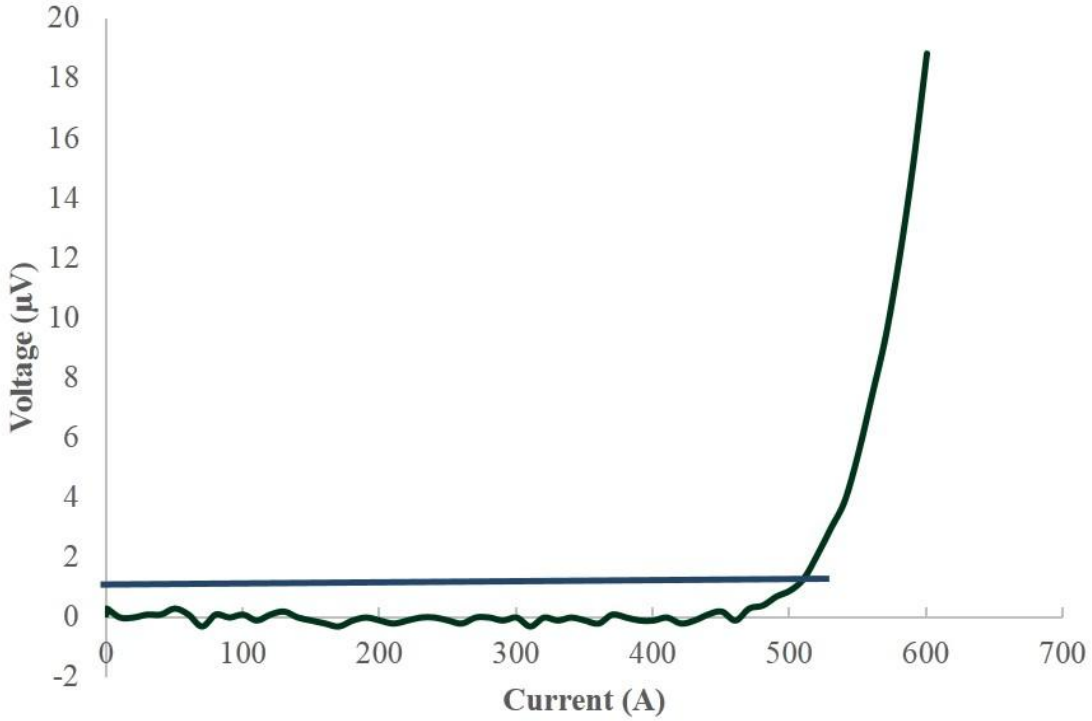

Fig. 53: V vs. I of OPIT conductor from Table 12.

Table 12: Transport Properties of 1 mm Class TPC's With Various Heat Treatments. All Samples Were From Billet 2b.[81]

Sample/HT	875 C, 24 h	877 C, 24 h	881 C, PM	888 C, PM	OST 888 C, PM
I_c	6	2	10	13	500

Table 12 shows the results of the critical current measurements of the OPIT and TPC samples tested, while Fig. 53 and Fig. 54 [81] show the V – I curves for the highest performing TPC and OPIT control.

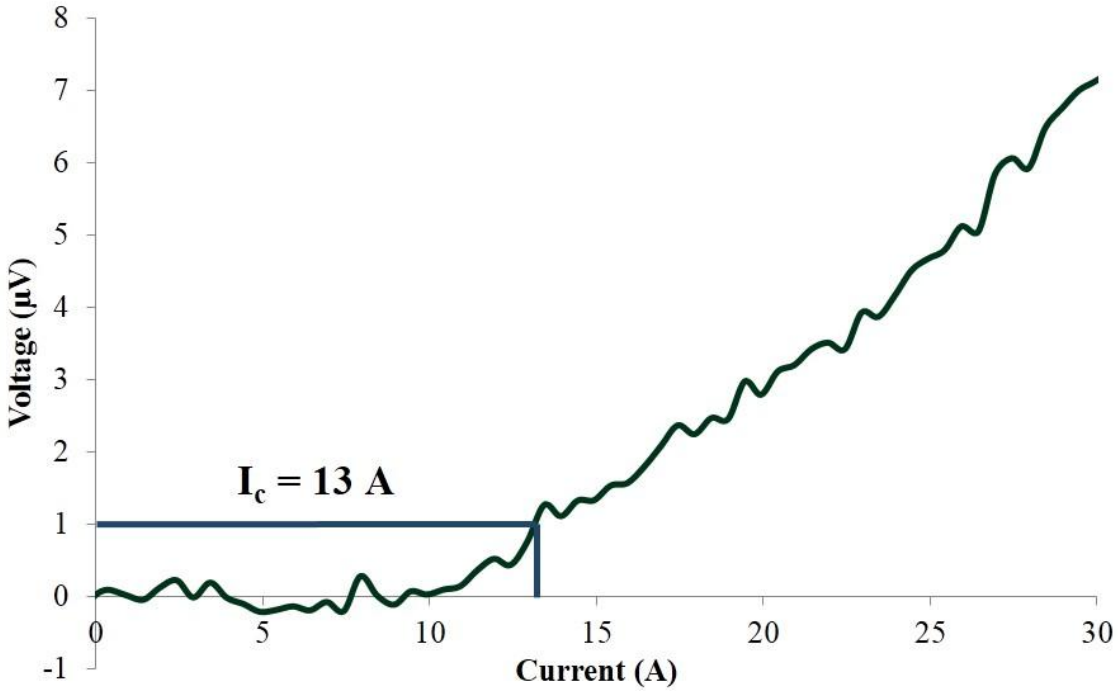

Fig. 54: V vs. I curve of highest performing TPC.

5.3 Analysis

The results presented in the previous section indicated that the TPC's were indeed superconducting albeit with dismally low transport current densities with a maximum I_c of only 13 A from a partially melted sample. Given the amount of superconductor within each monocore, the expected transport current for a comparable J_c to OPIT conductors, would have been 640 A (Assumed J_c 3000 A/mm^2 [19, 25, 47]. By contrast, the 500 A achieved in the OPIT conductor are perfectly in-line with expectations for this conductor for PMP heat treatments [19, 92, 110].

Since the OPIT conductor matched expectations and was commonly heat treated within the same furnace, with the same calibrated thermocouples, and with the same

handling procedure as the TPC's, it was evident that the underperformance of the TPC's was not due to any external variables, but rather to the conductors themselves.

To illuminate the cause of this underperformance, microscopy investigations were carried out on the tested samples. Examining the sintered samples, shown in Fig. 39 did show a very low void space fraction (ie. High density). With the confirmation of a very high density conductor, no apparent occlusions from parasitic phases, and knowledge of the imparted texture, the only possible degradation mechanism was a lack of connectivity between grains, or a weak linked structure.

Since previous studies had already demonstrated that grains were indeed growing and connecting to one another in the sintered samples and subsequent TEM studies showed apparently clear grain boundaries, the question appeared to be how much of an interface is required to carry transport currents in Bi-2212 conductors. As previously described, the J_c of Bi-2212 particles is highly anisotropic with a factor of ~1000 x more current flowing in the ab planes than along the c-axis [31, 111]. Using this ratio, one may calculate for two overlapped grains which have wetted to one another as shown in Fig. 55 the minimum allowable overlap of the Bi-2212 particles that would allow for

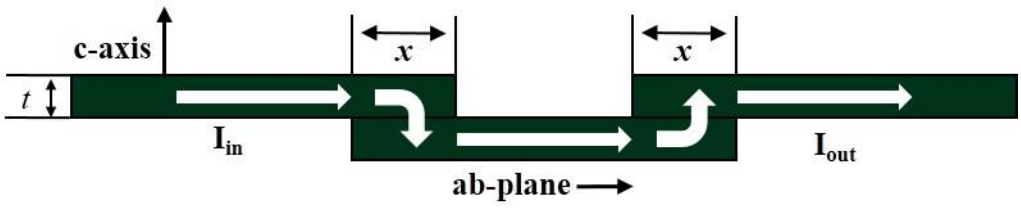

Fig. 55: Brick wall model of transport current flow in a granular Bi-2212 conductor.

intergrain transport currents to be carried without grain boundary limitations. A brief series of equations is sufficient to explain the behavior:

$$A_{overlap} = w_{overlap} * x$$

$$A_{cross} = w_{overlap} * t$$

$$I_{in} = J_c^{ab} * A_{cross} = J_c^c * A_{overlap} = I_{out}$$

Where $A_{overlap}$ is the area of the overlapped joint available for transport, A_{cross} is the cross sectional area of the grain leading into the joint, J_c^{α} is the current density in the plane of α, $w_{overlap}$ is the width of the overlapped joint, x is the length of the overlapped joint, t is the thickness of a grain, and I_{in}/I_{out} are the current into and out of the joint which must be continuous. With the relation that

$$J_c^{ab} = J_c^c \times 10^3$$

One finds

$$x = \frac{t * J_c^{ab}}{J_c^c} = \frac{t * J_c^c \times 10^3}{J_c^c} = t \times 10^3$$

With the characteristic value of t = 100 nm, a 100 μm long overlap must be created between adjacent grains to support c-axis transport current. Since the grains observed in this study were on the order of 5 μm after sintering, it is abundantly clear that there is not a sufficient overlap between the sintered grains to overcome a weak linked behavior. While this is a simplistic calculation that does not take into account any more detail than the geometric properties of the joint, it is sufficient to describe the underperformance of the sintered samples.

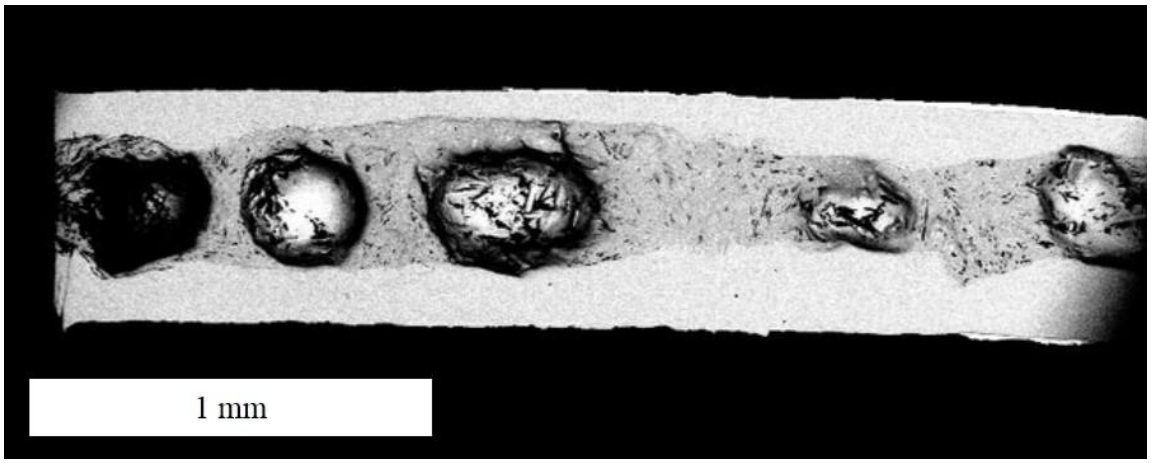

Fig. 56: Longitudinal section of an 888 C partially melted TPC from billet 2b. Note the very large voids that occur in several locations.

Regarding the low I_c's of the partially melted TPC's, a microstructure investigation was sufficient to elucidate the problem. As previously mentioned, these samples were prone to leak out the crimped ends of the conductor during heat treatment. Longitudinal and transverse sections of these samples were examined with the SEM and images are presented in Fig. 56 and Fig. 57 [81] respectively for the TPC's partially melted at a peak temperature of 888 C, corresponding to the 500 A performing OPIT conductor. It is immediately clear that these TPC's are suffering from very large void space that was caused by a combination of capillary action and hydrostatic pressure from trapped gases escaping during the partial melt.

Meanwhile, the 881 C partially melted samples suffered from a different, yet equally traumatic effect. These samples showed a drastic growth of parasitic phases along with void spaces, indicating that melting did take place in these samples. These results also aligned well with examples in the literature which reported that samples of

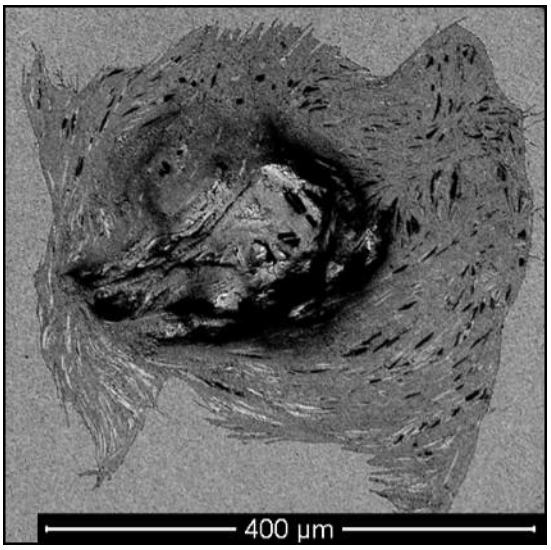

Fig. 57: Transverse section of a TPC partially melted at 888 C. Again, a large bubble is visible while a few parasitic phases (black) are evident.

OPIT wires heat treated at too low of a temperature incurred excessive growth of parasitic phases. This is thought to occur because the growth dynamics at these lower temperatures favor the formation of AEC's and Cu free phases [44, 49, 50, 112, 113].

6. CONCLUSIONS

To summarize the work of the previous chapters, three major conclusions were reached in this study. First, multiple methods demonstrated that Bi-2212 loose powders may be textured. These included magnetic orientation and continuous roll processing, however an optimum method for research level developments was found to be uniaxial die compaction. This process resulted in at least 50% dense precursors with exceptional levels of texture as evaluated by XRD methods and confirmed through microscopy.

Secondly, a monocore wire development successfully proved that texture imparted in a Bi-2212 precursor may be maintained through a deformation process that is conducive to the production of km long lengths of wire. This included extrusion and drawing steps which were not marred by sausaging phenomena or breaks during fabrication. Additionally, the density achieved after these deformation processes indicated that less than 5% void space was present in the monocores.

Finally, the non-melt heat treatment was found to be unsuccessful at providing robust paths for transport current in the TPC monocores. While Bi-2212 grains were observed to grow in the ab planes and no deleterious effects were observed at the grain boundaries, J_c of these sintered conductors were limited to approximately 1% of the levels achieved in partially melted OPIT conductors. This underperformance was primarily attributed to a lack of connectivity within the conductors which was the result of insufficient contact areas of overlapped grains which were limited in their current carrying capacity by the J_c in the ab plane.

Due to the ability of the TPC method to achieve a very high core density and high degree of texture in a fine wire conductor, there is merit to continue development of TPC's. Proximal steps in this effort should focus on the development of a multifilamentary round wire based on a textured precursor. In such a conductor, the anisotropic modulus of the Bi-2212 component could be used to advantage by arraying the c-axis of a multifilamentary composite radially. Additionally, these conductors should utilize an alloy outer sheath to improve their structural integrity and powder handling should take place in a tightly controlled Ar or O_2 atmosphere to prevent the deleterious adsorption of gaseous species on the precursor powder. Finally, overpressure processing should be utilized to realize the full potential of such a conductor. The overall advantage of this TPC would be the potential for a higher engineering density due to the increase in superconducting core density and additionally, the preferential deformation of the textured Bi-2212 could lead to very fine filament sizes. However, these developments are left for a new generation of students and researchers who will hopefully learn in earnest from the successes and failures of this work.

REFERENCES

[1] H. K. Onnes, "Further Experiments with Liquid Helium. C. On the Change of Electric Resistance of Pure Metals at Very Low Temperatures etc. IV. The Resistance of Pure Mercury at Helium Temperatures," in *Through Measurement to Knowledge*. vol. 124, K. Gavroglu and Y. Goudaroulis, Eds., ed Netherlands: Springer, 1991, pp. 261-263.

[2] D. v. Delft and P. Kes, "The Discovery of Superconductivity," *Physics Today,* vol. 63, pp. 38-43, September 2010.

[3] J. Eisenstein, "Superconducting Elements," *Reviews of Modern Physics,* vol. 26, pp. 277-291, July 1954.

[4] J. G. Daunt and J. W. Cobble, "Superconductivity of Technetium," *Physical Review,* vol. 92, pp. 507-508, 1953.

[5] S. J. Williamson, "Bulk Upper Critical Field of Clean Type-II Superconductors: V and Nb," *Physical Review B,* vol. 2, pp. 3545-3556, November 1970.

[6] C. C. Koch, R. H. Kernohan, and S. T. Sekula, "Superconductivity in Technetium-Vanadium Alloy System," *Journal of Applied Physics,* vol. 38, pp. 4359-4364, October 1967.

[7] A. A. Abrikosov, "On the Magnetic Properties of Superconductors of the Second Group," *Soviet Physics Jetp-USSR,* vol. 5, pp. 1174-1183, 1957.

[8] L. Bottura, "A Practical Fit for the Critical Surface of NbTi," *IEEE Transactions on Applied Superconductivity,* vol. 10, pp. 1054-1057, March 2000.

[9] A. Godeke, B. ten Haken, H. H. J. ten Kate, and D. C. Larbalestier, "A General Scaling Relation for the Critical Current Density in Nb3Sn," *Superconductor Science & Technology,* vol. 19, pp. R100-R116, October 2006.

[10] P. H. Kes, "Flux Pinning," in *Handbook of Superconducting Materials*. vol. 1, D. A. Cardwell and D. S. Ginley, Eds., ed Bristol, UK: Institute of Physics, 2003, pp. 195-206.

[11] M. Wilson, *Superconducting Magnets*. New York, USA: Oxford University Press, 1983.

[12] K.-H. Mess, P. Schmuser, and S. Wolf, "Basics of Superconductivity," in *Superconducting Accelerator Magnets*, ed Singapore: World Scientific Publishing Co., 1996, pp. 7-28.

[13] M. N. Wilson, "100 Years of Superconductivity and 50 Years of Superconducting Magnets," *IEEE Transactions on Applied Superconductivity,* vol. 22, 2012.

[14] L. D. Cooley, A. K. Ghosh, and R. M. Scanlan, "Costs of High-Field Superconducting Strands for Particle Accelerator Magnets," *Superconductor Science & Technology,* vol. 18, pp. R51-R65, April 2005.

[15] M. A. Green, "Economic Factors Involved in the Design of a Proton Synchrotron or Storage Ring With a Superconducting Guide Field," in *Proceedings of the 1968 Summer Study on Superconducting Devices and Accelerators*, Brookhaven National Laboratory, 1968, pp. 981-997.

[16] M. F. Murphy, "Superconducting Magnets For Whole-Body Magnetic-Resonance Imaging," *IEEE Transactions on Magnetics,* vol. 25, pp. 1755-1758, March 1989.

[17] H. Liebel, "High-Field Superconducting Magnets," in *High-Field MR Imaging*, J. Henning and O. Speck, Eds., ed Heidelberg: Springer-Verlag, 2011, p. 7.

[18] H. W. Weijers, U. P. Trociewitz, W. D. Markiewicz, J. Jiang, D. Myers, E. E. Hellstrom*, et al.*, "High Field Magnets With HTS Conductors," *IEEE Transactions on Applied Superconductivity,* vol. 20, pp. 576-582, June 2010.

[19] H. Miao, K. R. Marken, M. Meinesz, B. Czabaj, S. Hong, A. Twin*, et al.*, "High Field Insert Coils from Bi-2212/Ag Round Wires," *IEEE Transactions on Applied Superconductivity,* vol. 17, pp. 2262-2265, 2007.

[20] CERN, "LHC Design Report Chapter 7: Main Magnets in the Arcs," CERN, Geneva, Switzerland CERN-2004-003-V-1, 2004.

[21] L. M. Lederman, F. T. Cole, M. R. Donaldson, D. A. Edwards, H. T. Edwards, and P. F. M. Koehler, "A Report on the Design of the Fermi National Accelerator Laboratory Superconducting Accelerator," Fermi National Accelerator Laboratory1979.

[22] "Design Report Tevatron 1 Project," Fermi National Accelerator Laboratory FERMILAB-DESIGN-1982-01, 1982.

[23] "RHIC Configuration Manual," Brookhaven National Laboratory, http://www.bnl.gov/cad/accelerator/docs/pdf/RHICConfManual.pdf2006.

[24] A. Godeke, D. Cheng, D. R. Dietderich, P. Ferracin, S. O. Prestemon, G. Sabbi, *et al.*, "Limits of NbTi and Nb3Sn, and Development of W&R Bi-2212 High Field Accelerator Magnets," *IEEE Transactions on Applied Superconductivity,* vol. 17, pp. 1149-1152, June 2007.

[25] P. J. Lee. (2013, 8/29/2013). *Engineering Critical Current Density vs. Applied Field*. Available: http://fs.magnet.fsu.edu/~lee/plot/Jeprog-070813-1358x974-256pal.png

[26] A. Godeke, "Findings from the use of Bi-2212 in Wind-and-React Sub-Scale Racetrack Coils," presented at the MAP HTS Magnets Workshop, Fermilab, Batavia, IL, 2012.

[27] A. Godeke, D. Cheng, D. R. Dietderich, C. D. English, H. Felice, C. R. Hannaford, *et al.*, "Development of Wind-and-React Bi-2212 Accelerator Magnet Technology," *IEEE Transactions on Applied Superconductivity,* vol. 18, pp. 516-519, June 2008.

[28] A. McInturff, P. McIntyre, and A. Sattarov, "50 Tesla superconducting solenoid for fast muon cooling ring," in *2007 IEEE Particle Accelerator Conference, Vols 1-11*, New York, 2007, pp. 2978-2980.

[29] R. M. Scanlan, D. R. Dietderich, and H. C. Higley, "Conductor Development for High Field Dipole Magnets," *IEEE Transactions on Applied Superconductivity,* vol. 10, pp. 288-293, March 2000.

[30] R. M. Scanlan, A. P. Malozemoff, and D. C. Larbalestier, "Superconducting Materials for Large Scale Applications," *Proceedings of the IEEE,* vol. 92, pp. 1639-1654, October 2004.

[31] R. Sieburger, P. Muller, and J. S. Schilling, "Pressure Dependence of the Superconducting Transition Temperature in $Bi_2Sr_2CaCu_2O_{8+Y}$ as a Function of Oxygen Content," *Physica C-Superconductivity and Its Applications,* vol. 181, pp. 335-339, October 1991.

[32] U. P. Trociewitz, "Bi2212 Superconductors in High Field Applications," *NHMFL Reports 2006,* vol. 13, 2006.

[33] J. Akimitsu, A. Yamazaki, H. Sawa, and H. Fujiki, "Superconductivity in the Bi-Sr-Cu-O System," *Japanese Journal of Applied Physics,* vol. 26, pp. L2080-L2081, 1987.

[34] Y. C. Lan, G. C. Che, S. L. Jia, F. Wu, C. Dong, H. Chen, *et al.*, "The Effects of Composition, Synthesis, Conditions, Oxygen Content and F Doping on

Superconductivity and Structure for R-Substituted Bi-2201," *Superconductor Science & Technology,* vol. 9, 1996.

[35] C. Michel, M. Hervieu, M. M. Borel, A. Grandin, F. Deslandes, J. Provost*, et al.*, "Superconductivity in the Bi-Sr-Cu-O System," *Z. Phys. B.,* vol. 68, pp. 421-423, 1987.

[36] I. Matsubara, H. Tanigawa, T. Ogura, H. Yamashita, M. Kinoshita, and T. Kawai, "Upper Critical Field and Anisotropy of the High-T_c $Bi_2Sr_2Ca_2Cu_3O_X$ Phase," *Physical Review B,* vol. 45, pp. 7414-7417, April 1992.

[37] S. Salem-Sugui Jr., A. D. Alvarenga, J. Mosqueira, J. D. Dancausa, C. Salazar Mejia, E. Sinnecker*, et al.*, "Magnetic Phase Diagram of the Layered Superconductor $Bi_{2+x}Sr_{2-x}CuO_{6+\delta}$ (Bi2201) with $T_c \approx 7$ K," *Superconductor Science & Technology,* vol. 25, 2012.

[38] F. Chang, P. J. Ford, G. A. Saunders, L. Jiaqiang, D. P. Almond, B. Chapman*, et al.*, "Anisotropic Elastic and Nonlinear Acoustic Properties of Very Dense Textured $Bi_2Sr_2CaCu_2O_{8+y}$," *Superconductor Science & Technology,* vol. 6, 1993.

[39] J. A. Campa, E. Gutierrez-Puebla, M. A. Monge, I. Rasines, and C. Ruiz-Valero, "Single-Crystal Growth of Superconducting $Bi_2Sr_2CaCu_2O_8$ Using Rotary Crucibles," *Journal of Crystal Growth,* vol. 125, pp. 17-26, 1992.

[40] K. Damborsky, F. Lu, A. McInturff, P. McIntyre, N. Pogue, and E. Sooby, "Development and Characterization of a Highly Textured Bi-2212 Superconducting Ribbon " presented at the Texas Section of the American Physical Society, 2011.

[41] G. B. Galinski, G. Ozeryansky, and L. R. Motowidlo, "The Dependence of J(C) on Bending Strain in Round Multifilament Bi2sr2cac2ox Wires Sheathed in Ag and Ag Alloys," *Applied Superconductivity,* vol. 3, pp. 117-121, Jan-Mar 1995.

[42] J. Jiang, X. Y. Cai, A. Polyanskii, L. A. Schwartzkopf, D. C. Larbalestier, R. D. Parrella*, et al.*, "Through-Process Study of Factors Controlling the Critical Current Density of Ag-Sheathed $(Bi,Pb)_2Sr_2Ca_2Cu_3O_x$ Tapes," *Superconductor Science & Technology,* vol. 14, pp. 548-556, 2001.

[43] D. C. Larbalestier, A. Gurevich, D. M. Feldmann, and A. Polyanskii, "High-T_c Superconducting Materials for Electric Power Applications," *Nature,* vol. 414, pp. 368-377, 2001.

[44] T. G. Holesinger, "Investigation of the Phase Equilibria and Phase Transformations Associated with the $Bi_2Sr_2CaCu_2O_y$ Superconductor," Ph. D., Physics and Astronomy, Iowa State University, 1993.

[45] T. Lang, D. Buhl, and L. J. Gauckler, "Sample–Substrate Interactions During Melting of Bi-2212 on Ag," *Superconductor Science & Technology,* vol. 10, pp. 311-317, 1997.

[46] D. E. Wesolowski, M. O. Rikel, J. Jiang, S. Arsac, and E. E. Hellstrom, "Reactions Between Oxides and Ag-Sheathed Bi2Sr2CaCu2Ox Conductors," *Superconductor Science & Technology,* vol. 18, pp. 934-943, July 2005.

[47] J. Jiang, W. L. Starch, M. Hannion, F. Kametani, U. P. Trociewitz, E. E. Hellstrom*, et al.*, "Doubled Critical Current Density in Bi-2212 Round Wires by Reduction of the Residual Bubble Density," *Superconductor Science & Technology,* vol. 24, August 2011.

[48] W. Zhang, M. Polak, A. Polyanskii, E. E. Hellstrom, and D. C. Larbalestier, "Formation of Porosity and Its Effects on the Uniformity of J(c) in Bi-2212/Ag Tapes," in *Advances in Cryogenic Engineering Materials, Vol 44, Pts A and B*. vol. 44, U. B. Balachandran, D. G. Gubser, K. T. Hartwig, R. P. Reed, W. H. Warnes, and V. A. Bardos, Eds., ed New York: Plenum Press Div Plenum Publishing Corp, 1998, pp. 509-516.

[49] M. O. Rikel, D. Wesolowski, Y. Yuan, and E. E. Hellstrom, "Competitiveness of Porosity and Phase Purity in Melt Processed Bi2212/Ag Conductors," *Physica C-Superconductivity and Its Applications,* vol. 354, pp. 321-326, May 2001.

[50] M. O. Rikel, D. Wesolowskii, A. A. Polyanskii, X. Y. Cai, K. Marken, H. Miao*, et al.*, "Effect of Solidification Conditions on Microstructure of Melt Processed Bi2212/Ag Conductors," *Physica C-Superconductivity and Its Applications,* vol. 372, pp. 1839-1842, August 2002.

[51] C. Scheuerlein, M. Di Michiel, M. Scheel, J. Jiang, F. Kametani, A. Malagoli*, et al.*, "Void and Phase Evolution During the Processing of Bi-2212 Superconducting Wires Monitored by Combined Fast Synchrotron Micro-Tomography and X-ray Diffraction," *Superconductor Science & Technology,* vol. 24, November 2011.

[52] K. Damborsky, F. Lu, P. McIntyre, and N. Pogue, "Texturing of Micaceous Superconductor Powder and Fabrication of Wire to Preserve the Texture," *IEEE Transactions on Applied Superconductivity,* vol. 21, pp. 2783-2786, June 2011.

[53] K. Damborsky, P. McIntyre, and N. Pogue, "Magnetic Orientation of Bi-2212 Powder," in *Cryogenic Engineering Conference - International Cryogenic Materials Conference*, Tucson, Arizona, 2010, pp. 321-328.

[54] Y. Aoki, N. Ohtani, T. Hasegawa, L. Motowidlo, R. S. Sokolowski, R. M. Scanlan*, et al.*, "A High-Tc Superconducting Rutherford Cable Using Bi-2212 Oxide Superconducting Round Wire," *Advances in Superconductivity XII,* pp. 827-829, 2000.

[55] D. Sager, L. P. Meier, L. J. Gauckler, and M. Chen, "Influence of Precursor Calcination Parameters on the Critical Current Density of Bi-2212 Superconductors," *Physica C-Superconductivity and Its Applications,* vol. 434, pp. 125-134, February 2006.

[56] Y. Qi, W. S. Chen, C. B. Zhang, and H. Z. Yang, *Rapid Synthesis of Bi-Sr-Ca-Cu-O Ceramics by Sol-Gel*. Liaconing: Liaoning Science & Technology Publ House, 2005.

[57] T. Kanai and T. Kamo, "Control of Oxygen Release from Bi-2212 Phase in a Partial Melt Process," *Superconductor Science & Technology,* vol. 6, pp. 510-513, July 1993.

[58] R. L. Meng, C. Garcia, Y. Q. Wang, W. N. Kang, I. Rusakova, and C. W. Chu, "Processing of Low Cost Bi-2212 Tapes," *Physica C-Superconductivity and Its Applications,* vol. 306, pp. 223-227, September 1998.

[59] M. Rikel, personal communication ed: Nexans GmbH, 2010.

[60] G. Grasso, "Processing of High T_c Conductors: The Compound Bi,Pb(2223)," in *Handbook of Superconducting Materials*. vol. 1, D. A. Cardwell and D. S. Ginley, Eds., ed Bristol, UK: Institute of Physics, 2003, pp. 479-537.

[61] I. S. Oh and K. Mukherjee, "Texture Formation in Superconducting BSCCO-2212/Ag Composite Tapes - Effect of Cold-Rolling and Laser Float-Zone Melting Technique," *Physica C-Superconductivity and Its Applications,* vol. 227, pp. 197-204, June 1994.

[62] H. Miao, H. Kitaguchi, H. Kumakura, K. Togano, T. Hasegawa, and T. Koizumi, "Bi2Sr2CaCu2Ox/Ag Multilayer Tapes with J(c)> 500000A/cm(2) at 4.2 K and 10 T by Using Pre-Annealing and Intermediate Rolling Process," *Physica C-Superconductivity and Its Applications,* vol. 303, pp. 81-90, July 1998.

[63] T. D. Aksenova, P. V. Bratukhin, S. V. Shavkin, V. L. Melnikov, E. V. Antipova, N. E. Khlebova*, et al.*, "Texture Formation in Bi2Sr2Ca1Cu2Ox/Ag Tapes

Prepared by Partial Melt Process," *Physica C-Superconductivity and Its Applications,* vol. 205, pp. 271-279, February 1993.

[64] J. Reeves, D. Adolphs, A. Arndt, D. Zwicky, M. Rikel, and E. Hellstrom, "Effect of PAIR Process on Microstructure of Ag-Sheathed Bi-2212 Tapes," *Physica C-Superconductivity and Its Applications,* vol. 341, pp. 2021-2022, November 2000.

[65] H. Maeda, P. Sastry, U. P. Trociewitz, J. Schwartz, K. Ohya, M. Sato*, et al.*, "Effect of Magnetic Field Strength in Melt-Processing on Texture Development and Critical Current Density of Bi-Oxide Superconductors," *Physica C-Superconductivity and Its Applications,* vol. 386, pp. 115-121, 2003.

[66] H. B. Liu, P. J. Ferreira, J. B. Vander Sande, and A. Otto, "Bi-2212/Ag Tapes Melt-Grown Under an Elevated Magnetic Field (0-10 T)," *Physica C-Superconductivity and Its Applications,* vol. 316, pp. 234-238, May 1999.

[67] H. Maeda, K. Ohya, M. Sato, W. P. Chen, K. Watanabe, M. Motokawa*, et al.*, "Microstructure and Critical Current Density of Bi2212 Tapes Grown by Magnetic Melt-Processing," *Physica C-Superconductivity and Its Applications,* vol. 382, pp. 33-37, October 2002.

[68] A. Matsumoto, H. Kitaguchi, H. Kumakura, and K. Togano, "Microstructure and Superconducting Properties of Bi-2212/Ag Tapes Fabricated Using Melt-Solidification Under a Temperature Gradient," *Physica C-Superconductivity and Its Applications,* vol. 350, pp. 147-151, February 2001.

[69] M. Ionescu, S. X. Dou, M. Apperley, and E. W. Collings, "Phase and Texture Formation in Bi-2212/Ag Tapes Processed in Oxygen," *Superconductor Science & Technology,* vol. 11, pp. 1095-1097, October 1998.

[70] J. B. Shi, B. S. Chiou, J. C. Ho, and H. C. Ku, "Anisotropic Magnetic-Properties of Bi2Sr2CuO6+Delta Single-Crystal," *Physica C-Superconductivity and Its Applications,* vol. 197, pp. 157-160, July 1992.

[71] W. C. Lee, J. H. Cho, and D. C. Johnston, "Magnetic-Properties and Superconducting-Fluctuation Diamagnetism Above Tc in Bi2-xPbxSr2CaCu2O8+Delta(x=0.0,0.1,0.2,0.3,0.5) and Bi2-xPbxSr2Ca2Cu3O10+Delta(x=0.2,0.25)," *Physical Review B,* vol. 43, pp. 457-462, January 1991.

[72] D. C. Johnston and J. H. Cho, "Magnetic-Susceptibility Anisotropy of Single-Crystal Bi2Sr2CaCu2O8," *Physical Review B,* vol. 42, pp. 8710-8713, November 1990.

[73] Buehler. (2/28/2014). *Castable Mounting Systems*. Available: http://www.buehler.com/consumables/mounting/castable-mounting-systems

[74] K. Damborsky, P. McIntyre, and N. Pogue, "Magnetic Texturing of Bi-2212 Powder," presented at the 14th US-Japan Workshop on Advanced Superconductors, Tallahassee, FL, 2009.

[75] J. I. Shimoyama, K. Kadowaki, H. Kitaguchi, H. Kumakura, K. Togano, H. Maeda*, et al.*, "Processing and Fabrication of Bi2Sr2CaCu2Oy/Ag Tapes and Small-Scale Coils," *Applied Superconductivity,* vol. 1, pp. 43-51, Jan-Feb 1993.

[76] H. Kumakura, "Bi-2212/Ag Composite Tapes Processed by Doctor-Blade or Dip-Coating Process," in *Bismuth-Based High-Temperature Superconductors*, H. Maeda and K. Togano, Eds., ed New York, New York: Marcel Dekker, 1996, pp. 451-476.

[77] D. U. Gubser, T. L. Francavilla, C. S. Pande, B. B. Rath, and W. K. McDonald, "V3Ga Wire Fabricated by the Modified Jelly Roll Technique," *Journal of Applied Physics,* vol. 56, pp. 1051-1054, 1984.

[78] M. Bajko, F. Bertinelli, N. C. Lasheras, S. Claudet, P. Cruikshank, K. Dahlerup-Petersen*, et al.*, "Report of the Task Force on the Incident of 19 September 2008 at the LHC," European Organization for Nuclear Research, CERN, Geneva, Switzerland LHC Project Report 1168, 2009.

[79] D. W. Ha, S. C. Kim, I. Y. Han, J. G. Oh, J. H. Lee, S. S. Oh*, et al.*, "Study on Bi-2212 Rutherford Cabling Process for SMES," *IEEE Transactions on Applied Superconductivity,* vol. 18, pp. 1192-1195, June 2008.

[80] F. Lu, K. Damborsky, P. McIntyre, A. Mcinturff, N. Pogue, K. Smit*, et al.*, "Studies of Porosity, Connectivity, and Parasitic Phases in Textured Bi-2212/Ag After Non-Melt Heat Treatments," in *International Cryogenics Materials Conference*, Spokane, WA, 2011.

[81] K. Damborsky, F. Lu, P. McIntyre, L. Motowidlo, N. Pogue, and W. L. Starch, "Transport Properties of High Green Core Density Bi-2212 Textured-Powder Conductors," in *CEC-ICMC*, Anchorage, AK, 2013, p. Accepted.

[82] E. E. Hellstrom and W. Zhang, "Formation and Prevention of Bubbles when Melt Processing Ag-Sheathed Bi2Sr2CaCu2Ox (2212) Conductors," *Superconductor Science & Technology,* vol. 8, pp. 317-323, May 1995.

[83] G. Duperray and P. Herrmann, "Processing of High T_c Conductors: The Compound Bi(2212)," in *Handbook of Superconducting Materials*. vol. 1, D. A.

Cardwell and D. S. Ginley, Eds., ed Bristol, UK: Institute of Physics, 2003, pp. 449-477.

[84] E. E. Hellstrom and W. Zhang, "Melt Processing Bi(2212) Conductors, the Influence of Oxygen on Phase Relations in the Melt," in *Bismuth-Based High-Temperature Superconductors*, H. Maeda and K. Togano, Eds., ed New York, New York,: Marcel Dekker, 1996.

[85] M. O. Rikel, J. L. Reeves, N. A. Scarbrough, and E. E. Hellstrom, "Effect of Various Processing Variables on Grain Alignment at Bi-2212/Ag Interface," *Physica C-Superconductivity and Its Applications,* vol. 341, pp. 2573-2574, November 2000.

[86] T. M. Shen, X. T. Liu, U. P. Trociewitz, and J. Schwartz, "Electromechanical Behavior of Bi2Sr2CaCu2Ox Conductor Using a Split Melt Process for React-Wind-Sinter Magnet Fabrication," *IEEE Transactions on Applied Superconductivity,* vol. 18, pp. 520-524, June 2008.

[87] T. G. Holesinger, D. J. Miller, H. K. Viswanathan, and L. S. Chumbley, "Solidification of Bi2Sr2CaCu2Oy and Bi2Sr1.75Ca0.25CuOy," *Journal of Materials Research,* vol. 8, pp. 2149-2161, September 1993.

[88] A. Godeke, D. W. Cheng, D. R. Dietderich, C. R. Hannaford, S. O. Prestemon, G. Sabbi*, et al.*, "Progress in Wind-and-React Bi-2212 Accelerator Magnet Technology," *IEEE Transactions on Applied Superconductivity,* vol. 19, pp. 2228-2231, June 2009.

[89] R. Nast, B. Ringsdorf, B. Runtsch, K. P. Weiss, and W. Goldacker, "The Influence of the Maximum Heat Treatment Temperature on the Performance of Thin Reinforced Multifilament Bi-2212 Wires for Cables," in *9th European Conference on Applied Superconductivity*, Dresden, Germany, 2009.

[90] H. Fujii, H. Kumakura, H. Kitaguchi, K. Togano, W. Zhang, Y. Feng*, et al.*, "The Effect of Oxygen Partial Pressure During Heat Treatment on the Microstructure of Dip-Coated Bi-2212/Ag and Ag Alloy Tapes," *IEEE Transactions on Applied Superconductivity,* vol. 7, pp. 1707-1710, June 1997.

[91] A. Tollestrup, "Temperature Profile Measurements During Heat Treatment of BSCCO 2212 Coils," FERMILAB-TM-2505-APC, 2011.

[92] T. Shen, J. Jiang, F. Kametani, U. P. Trociewitz, D. C. Larbalestier, J. Schwartz*, et al.*, "Filament to Filament Bridging and its Influence on Developing High Critical Current Density in Multifilamentary Bi2Sr2CaCu2Ox Round Wires," *Superconductor Science & Technology,* vol. 23, February 2010.

[93] T. M. Shen, J. Y. Jiang, F. Kametani, U. P. Trociewitz, D. C. Larbalestier, and E. E. Hellstrom, "Heat Treatment Control of Ag-Bi2Sr2CaCu2Ox Multifilamentary Round Wire: Investigation of Time in the Melt," *Superconductor Science & Technology,* vol. 24, November 2011.

[94] A. Godeke, D. W. Cheng, D. R. Dietderich, M. G. T. Mentink, S. O. Prestemon, and G. L. Sabbi, "Heat Treatment Optimizations for Wind-and-React Bi-2212 Racetrack Coils," in *Superconductivity Centennial Conference 2011*. vol. 36, P. H. Kes and H. Rogalla, Eds., ed Amsterdam: Elsevier Science Bv, 2012, pp. 812-817.

[95] A. Malagoli, F. Kametani, J. Jiang, U. P. Trociewitz, E. E. Hellstrom, and D. C. Larbalestier, "Evidence for Long Range Movement of Bi-2212 Within the Filament Bundle on Melting and Its Significant Effect on J(c)," *Superconductor Science & Technology,* vol. 24, July 2011.

[96] M. Dalban-Canassy, D. A. Myers, U. P. Trociewitz, J. Jiang, E. E. Hellstrom, Y. Viouchkov*, et al.*, "A Study of the Local Variation of the Critical Current in Ag-Alloy Clad, Round Wire Bi2Sr2CaCu2O8+x Multi-Layer Solenoids," *Superconductor Science & Technology,* vol. 25, pp. 1-10, November 2012.

[97] M. D. Sumption, L. R. Motowidlo, and E. W. Collings, "Determination of the True (or Potential) Transport-J(c) of a Multifilamentary Bi : HTSC/Ag Strand in the Presence of Bridging and Generalized Sausaging," *Physica C-Superconductivity and Its Applications,* vol. 291, pp. 267-273, December 1997.

[98] T. G. Holesinger, D. J. Miller, H. K. Viswanathan, K. W. Dennis, L. S. Chumbley, P. W. Winandy*, et al.*, "Directional Isothermal Growth of Highly Textured Bi2Sr2CaCu2Oy," *Applied Physics Letters,* vol. 63, pp. 982-984, August 1993.

[99] T. G. Holesinger, J. M. Johnson, J. Y. Coulter, H. Safar, D. S. Phillips, J. F. Bingert*, et al.*, "Isothermal Melt Processing of Bi2Sr2CaCu2O-Gamma Round Wire," *Physica C-Superconductivity and Its Applications,* vol. 253, pp. 182-190, October 1995.

[100] T. G. Holesinger, D. S. Phillips, J. Y. Coulter, J. O. Willis, and D. E. Peterson, "Isothermal Melt Processing of Bi-2212 Thick-Films," *Physica C-Superconductivity and Its Applications,* vol. 243, pp. 93-102, February 1995.

[101] T. G. Holesinger, W. L. Hults, and W. M. Dai, "Isothermal Melt Processing of Bi-2212 Wires and Tapes," in *Impact of Recent Advances in Processing of Ceramic Superconductors*. vol. 84, W. WongNg, U. Balachandran, and A. S. Bhalla, Eds., ed Westerville: Amer Ceramic Soc, 1998, pp. 175-184.

[102] T. G. Holesinger, P. S. Baldonado, N. Van Vo, W. M. Dai, K. R. Marken, and S. Hong, "Isothermal Melt Processing of Bi-2212 Tapes," *IEEE Transactions on Applied Superconductivity,* vol. 9, pp. 1800-1803, June 1999.

[103] J. Y. Jiang, H. P. Miao, Y. B. Huang, S. Hong, J. A. Parrell, C. Scheuerlein, *et al.*, "Reduction of Gas Bubbles and Improved Critical Current Density in Bi-2212 Round Wire by Swaging," *IEEE Transactions on Applied Superconductivity,* vol. 23, June 2013.

[104] J. L. Wang, X. Y. Cai, R. J. Kelley, M. D. Vaudin, S. E. Babcock, and D. C. Larbalestier, "Electromagnetic Coupling Character of 001 -Twist Boundaries in Sintered Bi2Sr2CaCu2O8+X Bicrystals," *Physica C-Superconductivity and Its Applications,* vol. 230, pp. 189-198, September 1994.

[105] A. Godeke, "Performance Boundaries in Nb_3Sn Superconductors," Ph.D., University of Twente, 2005.

[106] E. F. Holik, C. P. Benson, R. Blackburn, N. Diaczenko, T. Elliott, A. Jaisle, *et al.*, "Construction and Component Testing of TAMU3, a 14 Tesla Stress-Managed Nb3Sn Model Dipole," in *Advances in Cryogenic Engineering, Vols 57a and 57b*. vol. 1434, J. G. Weisend, J. Barclay, S. Breon, J. Demko, M. DiPirro, P. Kittel, *et al.*, Eds., ed Melville: Amer Inst Physics, 2012, pp. 649-655.

[107] P. Ferracin, D. W. Cheng, D. R. Dietderich, H. Felice, A. Godeke, A. R. Hafalia, *et al.*, "Design of LD1, a Large-Aperture High-Field Nb3Sn Dipole Magnet," *IEEE Transactions on Applied Superconductivity,* vol. 22, June 2012.

[108] A. McInturff, R. Blackburn, N. Diaczenko, T. Elliott, T. Holik, A. Jaisle, *et al.*, "Current Status of the Texas A&M Magnet R&D Program," *IEEE Transactions on Applied Superconductivity,* vol. 21, pp. 1620-1623, June 2011.

[109] H. Maeda, P. Sastry, U. P. Trociewitz, J. Schwartz, K. Ohya, and M. Sato, "Critical Current Density and Microstructures of Thick Monocore Bi2212 Tapes Grown in High Magnetic Fields," *IEEE Transactions on Applied Superconductivity,* vol. 13, pp. 3339-3342, June 2003.

[110] D. W. Ha, S. C. Kim, J. G. Oh, H. S. Ha, N. J. Lee, K. J. Song, *et al.*, "Influence of Filament Number on Workability and Critical Current Density of Bi-2212/Ag Superconducting Wires," *IEEE Transactions on Applied Superconductivity,* vol. 17, pp. 3099-3102, June 2007.

[111] T. W. Li, A. A. Menovsky, J. J. M. Franse, and P. H. Kes, "Flux Pinning in Bi-2212 Single Crystals with Various Oxygen Contents," *Physica C-Superconductivity and Its Applications,* vol. 257, pp. 179-186, January 1996.

[112] M. O. Rikel and E. E. Hellstrom, "Development of 2201 Intergrowths During Melt Processing Bi2212/Ag Conductors," *Physica C-Superconductivity and Its Applications,* vol. 357, pp. 1081-1090, August 2001.

[113] P. Majewski, "Phase Equilibria and Crystal Chemistry of the High-Temperature Superconducting Compounds of the System Bi2O3-SrO-CaO-CuO," in *Bismuth-Based High-Temperature Superconductors*, H. Maeda and K. Togano, Eds., ed New York, New York: Marcel Dekker, 1996.